AFOSR-TR. 81-0611

AeroChem TP-413

LEVEL

AD A102411

IONIC MECHANISMS OF CARBON FORMATION IN FLAMES

DTIC
ELECTE
AUG 4 1981
C

H.F. Calcote and D.B. Olson

AeroChem Research Laboratories, Inc.
P.O Box 12
PRINCETON, NEW JERSEY 08540

May 1981

Final Report for the period 1 January 1977 - 31 December 1980

Approved for Public Release
Distribution Unlimited

Prepared for

AIR FORCE OFFICE OF SCIENTIFIC RESEARCH
Bolling Air Force Base
Washington, DC 20332

FOREWORD AND ACKNOWLEDGMENTS

REPORT DOCUMENTATION PAGE	READ INSTRUCTIONS BEFORE COMPLETING FORM

1. REPORT NUMBER	2. GOVT ACCESSION NO.	3. RECIPIENT'S CATALOG NUMBER
AFOSR-TR- 81 - 0611	AD-A103477	

4. TITLE (and Subtitle)	5. TYPE OF REPORT & PERIOD COVERED
IONIC MECHANISMS OF Carbon FORMATION IN FLAMES.	Final Report, 1 January 1977- 31 December 1980
	6. PERFORMING ORG. REPORT NUMBER AeroChem-TP-413

7. AUTHOR(s)	8. CONTRACT OR GRANT NUMBER(s)
H.F. Calcote and D.B. Olson	F49620-77-C-0029

9. PERFORMING ORGANIZATION NAME AND ADDRESS	10. PROGRAM ELEMENT, PROJECT, TASK AREA & WORK UNIT NUMBERS
AeroChem Research Laboratories, Inc. P.O. Box 12 Princeton, NJ 08540	2308/A2 61102F

11. CONTROLLING OFFICE NAME AND ADDRESS	12. REPORT DATE
Air Force Office of Scientific Research/NA Building 410 Bolling AFB, DC 20332	11 May 1981
	13. NUMBER OF PAGES 216

14. MONITORING AGENCY NAME & ADDRESS(If different from Controlling Office)	15. SECURITY CLASS. (of this report)
	Unclassified
	15a. DECLASSIFICATION DOWNGRADING SCHEDULE

16. DISTRIBUTION STATEMENT (of this Report)

Approved for public release; distribution unlimited.

17. DISTRIBUTION STATEMENT (of the abstract entered in Block 20, if different from Report)

18. SUPPLEMENTARY NOTES

19. KEY WORDS (Continue on reverse side if necessary and identify by block number)

Soot Formation
Hydrocarbon Flames
Ion-Molecule Reactions

20. ABSTRACT (Continue on reverse side if necessary and identify by block number)

A critical survey of the literature and experimental mass spectrometric studies of ion profiles in low pressure acetylene and benzene flames support an ionic mechanism of soot nucleation. The initial precursor ion, $C_3H_3^+$, is produced by chemi-ionization and this ion grows by very rapid ion-molecule reactions with acetylene and other C_xH_y species to produce larger ions which eventually become incipient soot particles. Preliminary computer simulations using the proposed mechanism qualitatively describe many of the observed

DD FORM 1473 EDITION OF 1 NOV 65 IS OBSOLETE
1 JAN 73

experimental features including the rapid growth of large ions.

A new definition of the Threshold Soot Index, TSI, as a relative number varying from 0 to 100 (from least to greatest tendency to soot) makes it possible to organize all literature data on both premixed flames and diffusion flames into two rational sets so that the effect of molecular structure on sooting determined by different techniques can be compared. The results show some major differences from accepted trends.

Selected available data on soot formation in gas turbine combustors for various fuel compositions have been compared with laboratory data on soot formation for various fuels in a search for a simple correlation. For some sets of data such a correlation was found for TSI, or the reciprocal of the fuel smoke point (related to TSI), but for other sets of data the correlation was poor. The reasons for the differences are not understood.

Accession For

NTIS GRA&I
DTIC TAB
Unannounced
Justification

By
Distribution/
Availability Codes
Dist | Avail and/or
| Special

A

TABLE OF CONTENTS

I. INTRODUCTION AND STATEMENT OF WORK

During the decade preceding the initiation of this program on 1 January 1977 extensive evidence had accumulated indicating a relationship existed between soot formation and flame ionization. The objective of this program was to explore that relationship, especially as it relates to the nucleation step in soot formation. The working hypothesis was that soot precursors are hydrocarbon ions which grow via very rapid ion-molecule reactions to become incipient soot particles.

The work was further motivated by the anticipated future use by the Air Force of synfuels derived from coal, tar sands, and shale oil. These fuels are expected to have higher molecular weights, more aromatic and poly-cyclic aromatic compounds, and thus greater C/H ratios than current petroleum derived fuels. These fuel characteristics all increase the soot forming tendencies in combustion systems. Soot formation in aircraft jet engines degrades component lifetime and creates tactically undesirable visible smoke. Thus, the program was specifically directed to both long term understanding of the mechanism of soot formation and immediate empirical relationships which would be useful to the Air Force in evaluating the use of synfuels in jet aircraft.

The statement of work from the contract reads:

1. Determine the effect of fuel type (representative of coal and petroleum derived fuels) on carbon and ion formation processes in both premixed and diffusion flames. An ion mass spectrometer will be used for ion profile identification; and other techniques, using e.g., electrostatic probes, microwave cavities, gas sampling probes, thermocouple probes, and emission and absorption spectrometers will used as required during the progress of the work. Included will be mass spectrometric identification of the ions present in the soot nucleation and particle growth zones of flames of a number of fuels, at equivalence ratios near and in excess of those necessary for smoke formation.

2. Determine the effect of pressure on carbon and ion production processes in the combustion of some representative fuels.

3. Determine the effect of chemical additives on carbon and ion production processes in the combustion of some representative fuels. Included will be determination of the effects of alkali and alkaline

1

earth additives on soot formation parameters and a study of their influence on flame ion chemistry.

4. Study of the sooting characteristics of flames of mixed hydrocarbons for the purpose of ascertaining synergistic effects and developing a means for predicting the smoke tendency of real fuel systems.

5. Interpret, as the work progresses, the results from the above experiments, and data already in the literature, in terms of an ionic mechanism of carbon formation in flames.

6. Interpret the above data and mechanisms in terms of the potential effects of new fuels on soot formation in air breathing engines, and possible means of minimizing soot formation in air breathing engines.

7. Perform the following tasks to demonstrate the applicability of laboratory studies of the effects of fuel molecular structure on soot emissions to practical airbreathing jet engines:

    a. Survey and critically analyze the available experimental measurements on soot emissions and flame radiation from turbojet engines and larger scale combustors simulating practical engine conditions.

    b. Interpret and correlate the above results with small scale laboratory measurements of sooting properties of various fuel components with the objective of defining which laboratory testing procedures best relate fuel composition to engine performance.

    c. Recommend specific laboratory scale and/or engine scale tests needed to support tentative conclusions derived from analysis of currently available data.

II. STATUS OF RESEARCH EFFORT

The results of this program have been submitted for publication or pre-
sented in a detailed report so they will only be summarized here; the publica-
tions and relevant report are incorporated as appendices.

Soot formation in flames has been studied extensively and a voluminous
literature exists. At times the literature is confusing because of the fail-
ure to recognize the complexity of the problem--or to overestimate it--and
more specifically because of failure to recognize that a number of reasonably
distinct steps are involved in proceeding the six or seven decades in molecu-
lar weight from molecular species to relatively large soot particles. A clear
definition of these steps has not been found, yet the most experienced workers
seem to accept the following:

1. Formation of Precursors - the generation of those free radicals or
   ions which are necessary for the initial stages of production of
   nuclei. Precursors grow by combining with more generally available
   flame species, often acetylenes, which are called building blocks.

2. Nucleation - the transformation from a molecular system to a particu-
   late system, e.g., incipient soot particle, where the growing species
   take on the properties of particles as opposed to large molecules.
   In soot formation this probably occurs over a range of diameters
   whereas in usual nucleation phenomena this can be an abrupt crossing
   of two controlling rates.

3. Growth - the growth of incipient soot particles by molecular addition.

4. Coagulation - the collision and coalescence of two particles, of the
   same or different size, into one individual particle in which the
   identities of the two particles are completely lost.

5. Agglomeration - a process where a series of particles collide, one
   at a time, and adhere to each other to form a chain of individual
   particles, which are still distinguishable.

6. Aggregation - a process where a series of particles collide, one at
   a time, to form a cluster of individual particles which are still
   distinguishable.

7. Oxidation - oxidative reaction of the particles in any of the above-
   mentioned forms to reduce the particle size.

At the present stages of our work we believe step 1 involves chemi-ionization to produce $C_3H_3^+$; step 2--on which we concentrated in this program--involves rapid ion-molecule reactions to produce very large ions and incipient soot particles which are then electrically neutralized by recombination with free electrons or negative ions. These species grow further and are subsequently thermally ionized to produce charged soot particles. Step 3 may occur on neutral or charged particles. The probable molecules controlling the growth are acetylenes or aromatic radicals or molecules. Next to nucleation this step is probably the least understood. Steps 4, 5, and 6 are all influenced by the electronic charge on the individual soot particles; in fact, charged particles must agglomerate and neutral particles must aggregate. The oxidation step (step 7) competes with the growth steps (i.e., steps 2-6) in determining the ultimate particle size or the existence or nonexistence of particles. The present indication is that the oxidation step is dominated by OH reactions with the growing particle.

The extensive literature on soot formation in flames required some of our initial efforts to be directed to critically interpreting the available information on the nucleation step. This resulted in the paper which is incorporated as Appendix A. Data in the literature were organized to give a detailed description of the chemical sequences leading to soot formation in premixed laminar flames. It was concluded that neutral free radical, polyacetylene, and polycyclic aromatic hydrocarbon mechanisms are not consistent with this description, e.g., the rates are too small to account for the observed rate of soot formation. However, if chemi-ions are assumed to be the precursor onto which free radicals, polyacetylenes, or polycyclic aromatic hydrocarbons add in a series of fast ion-molecule reactions, a mechanism could be developed which was consistent with experiments. Recommendations for testing these mechanisms were made and have served to guide this program.

The experimental effort performed under the contract was principally directed to obtaining flame ion profiles (concentration vs distance) through near sooting and sooting flames by use of a mass spectrometer. This work resulted in two publications which are incorporated as Appendices B and C. A major change in ion identity occurs in both acetylene and benzene flames as the equivalence ratio is increased through the critical equivalence ratio for soot formation. The major ion, $C_3H_3^+$, is replaced by large positively charged aromatic ions with mass greater than 300 and increasing C/H ratio. The profiles of

these heavy ions through flames correspond with a group of unidentified species previously associated by Homann and Wagner* with precursors of soot formation. A mechanism to rationalize the identity of these observed ions can be created very simply by a series of ion-molecule reactions which continually build larger ions. We extrapolate this reaction sequence to form incipient soot particles. Future work will be directed at following the reaction series through to larger ion species. A computer program using realistic rate constants was used to demonstrate that reaction rates at the observed ion concentrations are sufficiently fast to account for our conclusions. The actual individual ion concentrations can be measured more accurately by correlating electrostatic probe measurements of absolute ion concentrations with mass spectrometric profiles. Dual concentration maxima are observed for many of the individual ions near the critical equivalence ratio for soot formation. The reasons for this phenomenon are not understood.

Our experimental observations and our interpretation of the data are consistent with an ionic mechanism of soot formation although we have not demonstrated that this is the only logical explanation. Several observations remain unexplained such as changes in ion identity and concentration at the critical equivalence ratio for soot formation.

Since a primary motivation for this program was the prospect of the Air Force using synfuels, some consideration was given to how changes in molecular structure might affect the propensity of a fuel to soot. It became clear that the available literature data on the subject were poorly organized and that unwarranted generalizations had been repeated over and over until they had become dogma. We thus set about reorganizing the available data and making some measurements ourselves. This led to the definitions of the "threshold soot index," TSI, for both premixed and diffusion flames as a measure of the tendency of a fuel to soot. For premixed flames TSI is related to the critical equivalence ratio (i.e., composition) at which soot first occurs. For diffusion flames TSI was defined using the well established smoke point measurement of the maximum smoke free height of a laboratory diffusion flame. A similar analysis should now be done to organize the available information on the quantity of soot produced as a function of molecular structure—a completely different problem. The definition of TSI, varying from 0 to 100

---

* See Appendices A-C for details

for the least to the greatest tendency to soot, permitted the oganization of all the available measurements into two self-consistent groups. All the premixed flame data regardless of source or technique were consistent and all of the diffusion flame data were consistent. In fact, there seems to be a greater correlation between premixed and diffusion flame behavior than previously recognized. The paper summarizing this work is incorporated as Appendix D.

The main objective, of course, in this program was to contribute to a solution to the Air Force's problems associated with soot formation in turbojet engines. The success of the above work on TSI encouraged us to look for correlations between soot formation in turbojet engines and in laboratory flames. This effort is important for two reasons: to confirm that laboratory studies are relevant to what occurs in a turbojet engine and, if successful empirical correlations can be found, to greatly reduce expensive full-scale turbojet engine tests. This work was supported by the AF Environics Division, Engineering and Service Laboratory, Tyndall AFB. The special report resulting from this work is incorporated as Appendix E. Data from aviation gas turbine combustors were examined to determine the effects of fuel properties on soot related measurements such as engine smoke number, combustor flame radiation, and/or combustor liner temperature. It was clearly demonstrated that soot production depends strongly on fuel composition. Correlation of some sets of combustor data with laboratory measurements was very good; in other cases the correlations were rather poor. A major problem in making such correlations was the inadequate identity of the composition of the aviation fuel used. This was a preliminary study and more work is definitely warranted.

III. PUBLICATIONS

The major publications resulting from this work are listed below in chronological order of submission and are incorporated as Appendices A-E as indicated:

A. Calcote, H.F., "Mechanisms of Soot Nucleation in Flames - A Critical Review," March 1980. AeroChem TP-400a.

   Accepted for publication in Combustion and Flame--it should appear soon.

B. Olson, D.B. and Calcote, H.F., "Ions in Fuel-Rich and Sooting Acetylene and Benzene Flames," May 1980. AeroChem TP-397a.

   Accepted for publication in the Eighteenth Symposium (International) on Combustion (The Combustion Institute, Pittsburgh, in press).

C. Olson, D.B. and Calcote, H.F., "Ionic Mechanisms of Soot Nucleation in Premixed Flames," November 1980. AeroChem TP-405a.

   Accepted for publication in Particulate Carbon: Formation During Combustion, Proceedings of the General Motors Symposium, Warren, MI, October 1980 (Plenum Press, New York, in press).

D. Calcote, H.F. and Manos, D.M., "Effect of Molecular Structure on Incipient Soot Formation," January 1981. AeroChem TP-406.

   Submitted to Combustion and Flame.

E. Gould, R.K., Olson, D.B., and Calcote, H.F., "Correlation of Soot Formation in Turbojet Engines and in Laboratory Flames," February 1981. AeroChem TP-407, ESL-TR-81-09.

   This has been accepted for distribution by the AF Environics Division, Engineering and Service Laboratory, Tyndall AFB. It should be available in final form.

IV. PERSONNEL

The key personnel in this program have been the authors but others contributed from time to time as their special talents were required. The participation of the following technical personnel is thus gratefully acknowledged:

> R.M. Bowser, Research Technician
>
> R.K. Gould, PhD, Physics
>
> L.R. Koenig, Research Technician
>
> D.M. Manos, PhD, Physical Chemist
>
> W.J. Miller, PhD, Physical Chemist
>
> H.N. Volltrauer, PhD, Physical Chemist

V. TECHNICAL INTERACTIONS

Technical interactions with the scientific community have been more frequent than usual for a fundamental scientific program because of the great interest in soot stimulated by the prospect of synfuels. This interaction has taken several forms: formal presentations (mostly invited) and individual contacts or participation in workshops.

A. FORMAL PRESENTATIONS*

1. "Fundamental Mechanisms of Carbon Formation in Hydrocarbon and Synthetic Fuel Combustion," H.F. Calcote, 1977 AFOSR Meeting on Air-Breathing Combustion Dynamics, West Lafayette, IN, 12-16 September 1977.

2. "Ionic Mechanism of Carbon Formation in Flames," W.J. Miller and H.F. Calcote, Fall Technical Meeting, Eastern Section: The Combustion Institute, United Technologies Research Center, East Hartford, CT, 10-11 November 1977.

3. "Ionic Mechanisms of Carbon Formation in Flames," H.F. Calcote, School of Engineering and Applied Science, Princeton University, Princeton, NJ, 6 December 1977.

---

*The name of the author who presented the lecture is underlined where there was more than one author.

4. "Ionic Mechanism of Carbon Formation in Flames," H.F. Calcote, National Bureau of Standards, Washington, DC, 13 December 1977.

5. "Ionic Mechanisms of Carbon Formation in Flames," H.F. Calcote, AFOSR Contractors Meeting on Air-Breathing Combustion Dynamics, Dayton, OH, 10-13 October 1978.

6. "Ionic Mechanisms of Soot Formation in Flames, An Invited Review," H.F. Calcote, Fall Technical Meeting, Eastern Section: The Combustion Institute, Miami, FL, 29 November-1 December 1978.

7. "An Ionic Mechanism of Soot Formation in Flames," H.F. Calcote, Army Ballistic Research Laboratories, Aberdeen, MD, 10 January 1979.

8. "Mechanisms of Soot Formation in Flames - An Invited Review," H.F. Calcote, AIAA 17th Aerospace Sciences Meeting, New Orleans, LA, 15-17 January 1979.

9. "Ionic Mechanisms of Carbon Formation in Flames," H.F. Calcote and D.B. Olson, AFOSR Contractors Meeting on Air-Breathing Combustion Dynamics and Kinetics, Alexandria, VA, 28 January-1 February 1980.

10. "Soot Formation in Combustion Systems," H.F. Calcote, Tyndall AF Base, FL, 27 March 1980.

11. "Ions in Fuel-Rich and Sooting Acetylene and Benzene Flames," D.B. Olson and H.F. Calcote, Eighteenth Symposium (International) on Combustion, Waterloo, Canada, 17-22 August 1980.

12. "Ionic Mechanism of Soot Nucleation in Premixed Flames," D.B. Olson and H.F. Calcote, Invited Paper, General Motors Symposium "Particulate Carbon: Formation During Combustion," Warren, MI, 15-16 October 1980.

13. "The Effect of Molecular Structure on the Tendency to Soot," H.F. Calcote and D.M. Manos, Fall Technical Meeting, Eastern Section: The Combustion Institute, Princeton, NJ, 12-14 November 1980.

B. **WORKSHOP AND INDIVIDUAL CONTACTS (EXAMPLES)**

1. Project SQUID Workshop on Alternate Hydrocarbon Fuels for Engines, Columbia, MD, 7-9 September 1977; H.F. Calcote was a panel member.

2. Project SQUID Workshop on Gas Turbine Combustion Design Problems, Purdue University, West Lafayette, IN, 31 May-1 June 1978; Attended by H.F. Calcote.

3. Roguemore, W.M., AF Aeropropulsion Laboratory, Wright-Patterson Air Force Base, OH, several personal conversations and phone calls.

4. Personnel at NASA (Lewis) whom H.F. Calcote visited on 20 June 1979.

5. Attendees at the Annual Conference on Fire Research sponsored by the Center for Fire Research, National Bureau of Standards, August 22-25 1979; Attended by D.B. Olson.

6. Gann, R.G. and attendees at an invited discussion on Soot Formation Chemistry, National Bureau of Standards, 18-19 December 1979; Attended by H.F. Calcote.

7. Farmer, R.C., Louisiana State University, Baton Rouge, LA, several conversations and phone calls.

8. Glassman, I., and attendees at the Princeton University Weekly Seminars in Fluid Mechanics and Combustion.

9. D'Alessio, A., at the Universita P. le V. Tecchio, Napoli, Italy, correspondence and discussions at meetings.

10. Michaud, P. and Barassin, A. of the Centre de Recherches sur la Chemie de la Combustion et des Hautes Temperatures at Universite d'Orleans, Orleans, France. Several personal conversations, exchange of pre-published papers.

11. Homann, K., Institute fur Physikalische Chemie der Technischen Hochschule, Darmstadt, Germany, conversations at meetings, exchange of letters, and he visited AeroChem in August 1980.

12. Naval Air Propulsion Center in Trenton, NJ, especially Donald Brunda; we have visited their facility on several ocassions and Brunda visited AeroChem in September 1980.

13. Kern, R.D., University of New Orleans, conversations at several meetings.

14. Howard, J. and Bittner, J., MIT. Frequent personal discussions and phone calls.

15. Blazowski, W., Exxon. Frequent personal discussions and phone calls.

16. Tyndall AF Base, especially Capt. Clewell--see above.

VI. INVENTIONS AND PATENT DISCLOSURES

There are no inventions or patent disclosures to report.

Mechanisms of Soot Nucleation in Flames*

– A Critical Review –

H.F. CALCOTE

AeroChem Research Laboratories, Inc.

P.O. Box 12, Princeton, New Jersey 08540

ABSTRACT

Data in the literature have been organized to give a detailed description of the chemical sequences leading to soot formation in a premixed laminar flame. Neutral free radical, polyacetylene, and polycyclic aromatic hydrocarbon mechanisms are not consistent with this description. However, when chemi-ions are assumed to be the precursor on which the free radicals, polyacetylenes, and polycyclic aromatic hydrocarbons repeatedly add in fast ion-molecule reactions, a mechanism can be developed which is consistent with experiment. This mechanism should be tested further by careful observations of both ion and neutral species (including free radical) profiles in flames and by developing a computer model of the process to compare with experiment.

INTRODUCTION

There has been much excellent work on the mechanism of soot formation in combustion systems and the field has been periodically reviewed [1-9] in various degrees of depth. Yet an understanding of the process has eluded us, mainly because it is so complex. The objective of this paper is to interpret some of the available data in terms of the various mechanisms that have been suggested and to point out the problems associated with specific mechanisms. To reduce the effort to a manageable magnitude the main concern will be with premixed homogeneous flames. Certainly some of the results will be applicable to diffusion flames or flames in heterogeneous systems such as spray burning or surface fires, but the chemistry in these systems is often masked by diffusive processes. It is therefore logical to start with what is hopefully the more simple chemical system and then evaluate the usefulness of the results in more complex systems.

Soot collected from flames consists of chainlike aggregates of spherical units having diameters of 10 to 50 nm. These spherical units have a hexagonal structure similar to graphite and have a carbon-to-hydrogen, C/H, atomic ratio of about 8:1 to 12:1. Observations of the end product, however, tell very little about the details of the process of soot formation--many individual steps are involved in progressing from a fuel molecule to a soot particle. Incidently, the word "soot" is preferred for the end product although it is often referred to as "carbon." Calling the end product carbon can be misleading because, in addition to the hydrogen content mentioned above, soot can also contain other elements, especially oxygen.

Three rather distinct steps are generally recognized in soot formation:

1. Nucleation - the transformation from a molecular system to a particulate system, or the formation of embryonic species which grow faster than they decompose or otherwise disappear by reaction.

2

2. Growth to spherical particles of 10 to 50 nm (100 to 500 Å) diam.

3. Aggregation or agglomeration of the spherical units to form chains.
The nucleation step is the least understood, so the discussion will be confined
to that step.

The overall process from primary molecular species (including free radi-
cals and/or ions) to soot aggregates is displayed in Fig. 1. The molecular
species are indicated as ions in the figure in anticipation of the conclusions
to be reached in this study. The basic problem, clearly demonstrated by this
figure, is how does the process proceed from molecular size to particles with
diameters three orders of magnitude greater, or equivalent molecular weights
ten orders of magnitude greater than the starting material in times on the
order of milliseconds? For comparison a large molecule such as m-octylphenyl,
$C_{48}H_{34}$, has a molecular weight of 610 amu and ovalene, $C_{32}H_{14}$, consisting of
ten six-membered rings has a molecular weight of 398 amu. Another problem is
how does the C/H ratio of the growing species increase from that typical of
molecular systems to that of soot?

The study of soot forming species has been approached experimentally from
both extremes; from the large particle side the electron microscope has been
used to look at smaller and smaller particles, down to about 15 nm diam [10]
and from the molecular species side, mass spectrometry (both neutral and ionic)
and gas chromatography have been used to look at large molecules and ions, up
to molecular weights of about 500 amu [11-17]. Some of the molecular species
and ions which have been observed in flames are listed in Tables 1 and 2.
Some of these large molecules have also been shown to be associated with soot
particles by driving them off by heating the soot particles [16,19-24].

That soot formation in premixed flames is a nonequilibrium process has
been recognized for many years [1,25]. This is demonstrated by the data in
Table 3 which compares the thermodynamic, or equilibrium critical equivalence

3

ratio ϕ_c[1] at which soot is calculated to be produced with the experimental value at which soot is observed in a one atmosphere premixed flame. The calculated adiabatic flame temperatures for thermodynamic equilibrium soot formation are compared with the calculated adiabatic flame temperature for the observed ϕ_c. Soot is produced as the flame is made fuel rich, i.e., by increasing ϕ, which is accompanied by decreasing temperature; the lower ϕ_c and higher flame temperatures observed experimentally indicate the nonequilibrium nature of the process. The greater ratios of these quantities (larger nonequilibrium) for benzene and n-hexane indicate greater tendencies to produce soot for these substances than for acetylene. Translating this observation into a conclusion about the relative chemistry for these substances is difficult because of the large differences in flame temperatures, especially between acetylene and the other two substances; increasing the flame temperature generally decreases the observed tendency to produce soot [26]. Both the rate of production of soot and the rate of burning of soot increase with temperature--but the burning rate increases more rapidly [26]. In fact it has been demonstrated that the mechanism of soot formation in the pyrolysis of aromatic hydrocarbons is different above and below 1800 K [27]. A useful experiment would be to determine the critical equivalence ratio for soot formation for these fuels at the same

---

[1] Equivalence ratio, ϕ, is defined as:

$$\phi = \frac{(Fuel/O_2)_{actual}}{(Fuel/O_2)_{stoichiometric}}$$

where stoichiometric is arbitrarily defined as producing only CO_2 and H_2O as products.

temperature. This could be done by increasing the unburned gas temperature of the cooler flame (benzene) or lowering the temperature of the acetylene flame gases. Pre-cooling the acetylene would be necessary because to raise the temperature of the other two fuels to match the flame temperature of acetylene requires temperatures at which they would pyrolyze.

SOME EXPERIMENTAL OBSERVATIONS

Historically, mechanisms proposed for the nucleation step in soot formation have involved polymerization of acetylene in one manner or another, or in the case of aromatics, the use of the aromatic molecule as a building block. Proposed intermediates in these processes have included the radicals C, C_2, CH, C_2H, CH_2, C_3H_4, C_4H_3 [28-31]; the polyacetylenes C_4H_2, C_6H_2, and $C_{10}H_2$ [16,28, 30,32,33]; polycyclic aromatic hydrocarbons (PCAH) [16,18,34,35]; and conjugated species such as 1,3-butadiene [36] or vinyl acetylene [35]. All of the proposed intermediates have been observed in sooting flames.

Before examining specific mechanisms, some of the data upon which these ideas have been based will be presented. For this presentation the data from several workers have been replotted and in some cases reinterpreted to give as precise as possible a picture of what occurs in the flame front of a sooting flame. Fortunately--or by design--much of the work has been done on flat flame burners with acetylene-oxygen flames at 2.7 kPa (20 Torr) at an equivalence ratio of about 3.5 (well into the soot producing concentration region which begins at about $\phi = 2.4$) and with an unburned linear flow velocity, of 50 cm s^{-1}. Where there are deviations from these conditions the results cannot, unfortunately, be adjusted to these conditions because the structure of a flat flame is more intimately related to interaction with the burner, e.g., by heat transfer and free radical losses, than we would like to admit [37]. Thus increasing the linear flow velocity may make the flame move closer to the burner [11,37,38] rather than further away as would be expected and may increase

the flame temperature [30]. Nevertheless, a good semiquantitative picture of what occurs can be obtained by combining data from various sources on the same graph even though the conditions deviate somewhat from ideal. This also demonstrates the accuracy which might be attached to the various sets of data. The basic experimental flame is described in Fig. 2.

The flame temperature through the basic flame along with emission profiles of C_2, CH, and OH which characterize the location of the luminous zone, often referred to as the flame front, are displayed in Fig. 3. The theoretical adiabatic flame temperature is 2490 K.

The increase in particle diameter through the flame for both neutral and charged species is given in Fig. 4. The Prado and Howard (PH) data [5] are for $\phi = 3.0$ and the particle diameters would be expected to be smaller than the Bonne, Homann and Wagner (BHW) data [28]; the fact that they are larger is an indication of the absolute accuracy of the results. It is significant that the slopes of the neutral and charged particle diameters are different and that the two diameters are about the same at small distances from the flame front. This seems to indicate that once small neutral particles are formed they continue to grow faster than the charged particles. This will be discussed in the section on thermal ionization.

The growth of soot through a flame is also measured as an increase in soot volume concentration (volume of soot per unit volume in the flame) or mass concentration of soot; such data are presented in Fig. 5. The variation in "large molecules" through the flame has also been measured and is summarized in Fig. 5. The concentration of "large molecules" is determined by subtracting the volume [11] or mass [28] concentration of soot determined by electron microscopy from that observed by light absorption which is sensitive to both large and very small particles. The lower limits of measurement by the electron microscope were 1.5 nm and 4 nm (Refs. 11 and 28, respectively) so the large molecules are

6

thus arbitrarily defined as "particles" with a diameter of less than a few nm.
For a point of reference a 2 nm diam particle with density 1.5 g cm^{-3} would
have a molecular weight of 4000.

Certainly the most useful data, from the standpoint of developing a
quantitative mechanism are concentration profiles through a flame. Such data
are presented in Fig. 6. The main products are CO, H_2, H_2O, CO_2, and C_2H_2
[33] (profiles for H_2 and CO_2 were not given). Homann and Wagner [16] di-
vide the hydrocarbon species observed into three groups: (1) acetylenes and
polyacetylenes, mass range 26 to 146 amu; (2) polycyclic aromatic hydrocarbons,
mass range 78 to ≈ 300 amu, typified on the figure as $C_{14}H_8$ (176 amu); and
(3) a group of "reactive polycyclic aromatic hydrocarbons," probably with side
chains, containing more hydrogen than (group 2) aromatics, mass range ≈ 150 to
550 amu (limit of mass range of mass spectrometer used). This last group is
identified on Fig. 6 as "precursors" of soot particles following Homann and
Wagner [33]. The polyacetylenes reach steady-state values and are apparently
in equilibrium with acetylene and hydrogen so Bonne et al. [28] have used the
concentration data to calculate the heats of formation for C_4H_2 and C_6H_2. The
polycyclic aromatics are formed later than the polyacetylenes but their con-
centrations continue to increase downstream of the flame.

Bittner and Howard [18] observed in a $C_2H_2/O_2/3\%$ Ar flame ($\phi = 3.0$) the
same slow increase in polycyclic aromatics, $C_{10}H_8$, $C_{12}H_8$, $C_{14}H_8$, as well as
C_6H_6 downstream from about 1.5 cm but they also observed these same substances
to peak in the flame front at about 0.5 cm. The major species identified as
polycyclic aromatic hydrocarbons [28] are, naphthalene (128 amu), acenaphtha-
lene (152), phenanthrene (178), pyrene (202), and coronene (300), with pyrene
and acenaphthalene being the most important. Intermediate hydrocarbons with an
even number of carbon atoms were much more frequent than those with an odd
number, regardless of the fuel [28].

The total concentration of polycyclics is about 10^{13} molecule cm^{-3}. Because these continue to rise after the rate of carbon particle formation has gone to zero it is concluded [16] that they cannot be important intermediates or nuclei for soot formation in acetylene flames; they could, of course, be building blocks. A continuous formation of larger and larger polyacetylenes cannot lead to soot formation because carbon particles are not giant linear molecules [7]. The group of molecules identified as precursors in Fig. 6 has not been identified; they all peak at 1.4 cm and differ in mass by 12 mass units, i.e., one carbon atom, and the number of carbon atoms ranges from 15 to > 40.

Other species of importance to mechanisms of soot formation have been observed in acetylene oxygen flames but at a different equivalence ratio from the data of Fig. 6. This information for a flame at the same linear unburned flow velocity, 50 cm s^{-1}, and the same pressure, 2.7 kPa (20 Torr), as for Fig. 6 is presented in Fig. 7 for an equivalence ratio of 2.4, just at the visual limit of soot formation. Some of these species are considered important intermediates in mechanisms of soot formation.

In benzene flames [16,34] polycyclic aromatics are also formed at about 100 times the concentration in acetylene flames and their concentration profiles differ from those in acetylene flames. They reach a maximum concentration within the oxidation zone and decrease at the end of it where most of the soot is formed. The relative concentrations are similar, however, to an acetylene flame. Polyacetylenes rise in the oxidation zone and then decrease in concentration after molecular oxygen is consumed, similar to acetylene flames [40]. In contrast to acetylene flames, soot is already formed at the position in the flame where molecular oxygen has not yet disappeared. The rate of soot formation is higher and the nucleation process seems to be completed earlier.
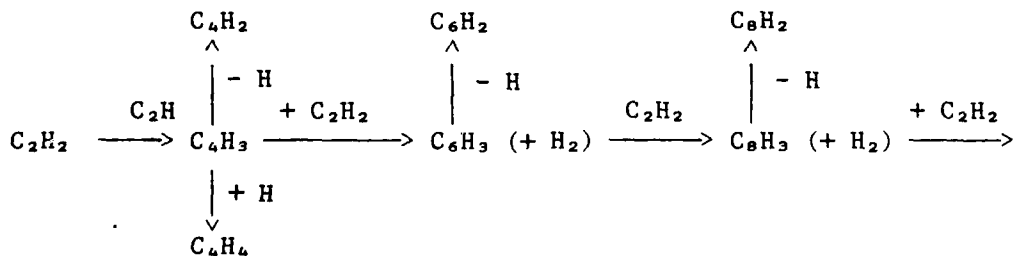
Returning now to Fig. 6, note the concentration profiles for soot parti-
cle number density, large positive ions, ions identified as 300 to 1000 amu,
and charged soot particles. Probably the most striking observation is that the
ion concentration is orders of magnitude less than the polyacetylene or free
radical concentrations. This originally led to the conclusion that ions were
unimportant because they were present in such low concentrations [41]. Further
examination of the data shows that the concentration of large positive ions
exceeds that of soot particles so that there are sufficient ions to serve as
nuclei for particle growth [11]. Another significant observation is that only
some of the soot particles are charged. The location of the peaks for the
various components making up Fig. 6 is also of interest. They move through the
flame front from smaller to larger polyacetylenes, to precursors, identical in
location with ions of mass 300-1000 amu, to charged soot particles, to neutral
soot particles. This order would be consistent with that sequence of reactions.
It is not meant to imply that this order indicates the order of participation of
these species in the mechanism--many things can distort the relative location of
concentration maxima with respect to the order in which reactions occur.

Another set of data which demonstrates how the diameters of small charged
soot particles and of larger neutral soot particles increase on moving through
the flame is displayed in Fig. 8. (see also Ref. 43). A bimodal size
distribution, representing, e.g., two distinguishable systems, one of large
molecular ions and one of ionized soot particles was not observed within an
estimated accuracy of the experiment of 10% [11]. However, in the comments to
the paper, Weinberg stated that in a similar system he observed two separate
peaks, due to small ions and larger particles. The authors confirmed that in
subsequent work they too observed two separate peaks but the work was not yet
completed. In a more recent study Homann [43] has identified two groups of
positively charged species, one group he identifies as the normal hydrocarbon
flame ions and the other with positively charged soot particles.

9

NEUTRAL SPECIES MECHANISMS

Many mechanisms involving many different species have been proposed for soot formation. They have been given such names as: 1. the atomic carbon theory; 2. the C_2 theory; 3. the C_3 theory; 4. the acetylene theory; 5. hydrocarbon polymerization theories; 6. the surface decomposition theory; 7. the Boudouard reaction theory; 8. the polyacetylene theory; 9. poly-aromatics, etc. These cannot all be discussed here. Instead see previous reviews [1-3], especially the excellent one of Palmer and Cullis [1] which discusses these various theories in some detail. Palmer and Cullis were led to comment, "It may be that the nuclei responsible for carbon formation will never be directly identified." The large number of theories which have been propounded indicates the magnitude of the problem. Most discussions culminate with complex diagrams showing a multitude of paths from the fuel via acety-lene(s) to soot. This again is an indication of frustration; one single path which might, of course, vary from system to system would be more intellectually satisfying.
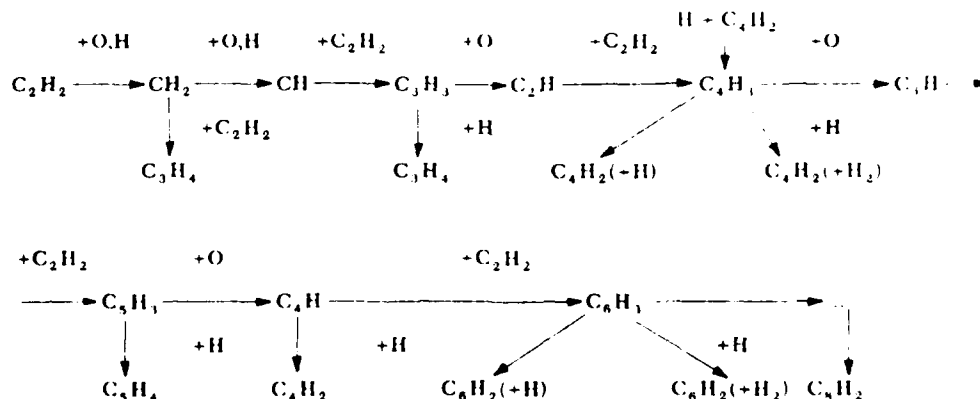
Because of the experimental results of Homann et al. (see, e.g., Fig. 6), paths through polyacetylenes seem attractive and these have been pursued by Bonne et al. [28] as well as by many others [44]. It is not difficult to account for the formation of the large fraction of polyacetylenes observed, e.g., Refs. 7 and 28 (see also subsequent discussion).

$$
C_2H_2 \xrightarrow{\ C_2H\ }
\begin{array}{c} C_4H_2 \\ \wedge \\ \Big| -H \\ C_4H_3 \\ \Big| +H \\ \vee \\ C_4H_4 \end{array}
\xrightarrow{\ +C_2H_2\ }
\begin{array}{c} C_6H_2 \\ \wedge \\ \Big| -H \\ \end{array}
C_6H_3 \ (+H_2) \xrightarrow{\ C_2H_2\ }
\begin{array}{c} C_8H_2 \\ \wedge \\ \Big| -H \\ \end{array}
C_8H_3 \ (+H_2) \xrightarrow{\ +C_2H_2\ }
$$

As large molecules form, the average size of the radicals also continues to increase and larger radicals react with each other and with higher poly-acetylenes forming ever larger molecules. However, as pointed out by Homann [7] and others [2,16,45], a continuation of this series cannot lead to soot because soot is not a giant chain molecule but has a polycyclic carbon structure more like ovalene, $C_{32}H_{14}$ [46];
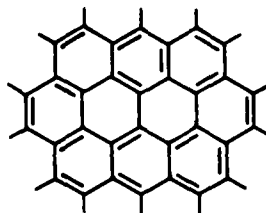
It has been recognized, e.g., by Cullis [44], Thomas [45], and Bonne et al. [28], that rearrangement of a polyacetylene to an aromatic graphite-like structure would be a slow process. In a more recent study of the formation of higher hydrocarbons in the reaction of O atoms with acetylene Homann et al. [47] conclude that polyacetylenes are side products of a fast reaction sequence such as:

$$
\begin{array}{ccccccc}
+O,H & +O,H & +C_2H_2 & +O & -C_2H_2 & H+C_4H_2 & -O \\
C_2H_2 \longrightarrow CH_2 \longrightarrow CH \longrightarrow C_3H_3 \longrightarrow C_2H \longrightarrow C_4H_? \longrightarrow C_?H \longrightarrow \\
\downarrow \quad +C_2H_2 \qquad \downarrow +H \qquad \searrow \qquad \nwarrow +H \\
C_3H_4 \qquad\qquad C_3H_4 \qquad C_4H_2(-H) \qquad C_4H_2(+H_2)
\end{array}
$$

$$
\begin{array}{cccc}
+C_2H_2 & +O & -C_2H_2 & \\
\longrightarrow C_5H_3 \longrightarrow C_4H \longrightarrow C_6H_3 \longrightarrow \\
\downarrow \quad +H \qquad \downarrow +H \qquad \swarrow \quad +H \\
C_5H_4 \qquad C_4H_2 \qquad C_6H_2(+H) \qquad C_6H_2(+H_2) \; C_4H_2
\end{array}
$$

Cullis [44] also concludes that polyacetylenes do not grow sufficiently rapidly to account for the almost instantaneous formation of soot.

Tanzawa and Gardner [48] have approached the problem by studying the shock-heated homogeneous thermal decomposition of C_2H_2/Ar mixtures in the temperature range 1700 to 3400 K. They compared their results as well as

11

those of others, with a computer model including the rates of 13 reactions, which is compatible in principle with the polyacetylene radical mechanism of soot formation developed by Bonne et al. [28].

Reaction	ΔH_0°, kJ	Rate constant, $cm^3 \ mol^{-1} \ s^{-1}$	
$C_2H_2 + M \quad = \quad C_2H + H + M$	519	$4.2 \times 10^{16} \ exp(-448 \ kJ/RT)$	(1)
$C_2H_2 + C_2H_2 = C_4H_3 + H$	192	$1.0 \times 10^{13} \ exp(-192 \ kJ/RT)$	(2)
$C_4H_3 + M \quad = \quad C_4H_2 + H + M$	250	$1.0 \times 10^{16} \ exp(-250 \ kJ/RT)$	(3)
$C_2H_2 + H \quad = \quad C_2H + H_2$	88	$7.8 \times T^{3.2} \ exp(-2 \ kJ/RT)$	(4)
$C_2H_2 + C_2H = C_4H_2 + H$	−75	4.0×10^{13}	(5)
$C_4H_2 + M \quad = \quad C_4H + H + M$	519	$3.5 \times 10^{17} \ exp(-335 \ kJ/RT)$	(6)
$C_6H_2 + M \quad = \quad C_6H + H + M$	519	$5.0 \times 10^{16} \ exp(-335 \ kJ/RT)$	(7)
$C_8H_2 + M \quad = \quad C_8H + H + M$	519	$5.0 \times 10^{16} \ exp(-335 \ kJ/RT)$	(8)
$C_2H_2 + C_4H = C_6H_2 + H$	−75	4.0×10^{13}	(9)
$C_4H_2 + C_2H = C_6H_2 + H$	−75	4.0×10^{13}	(10)
$C_2H_2 + C_6H = C_8H_2 + H$	−80	1.0×10^{12}	(11)
$C_6H_2 + C_2H = C_8H_2 + H$	−80	1.0×10^{12}	(12)
$C_4H_2 + C_4H = C_8H_2 + H$	−80	1.0×10^{12}	(13)

Their modeling results suggest that unfavorable thermochemistry of large C_nH and C_nH_2 species always leads to such a rapid decrease in their concentrations that the above mechanism implies soot nucleation times orders of magnitude larger than observed.

Homann and Wagner [16] suggest the possibility of C_2H or other radicals attacking a polyacetylene molecule to give a branched chain polyacetylene radical

$$C_2H + C_4H_2 \longrightarrow \begin{array}{c} H \\ \diagdown \\ C{=}C{-}C{\equiv}CH \\ | \\ C \\ ||| \\ C \\ H \end{array}$$
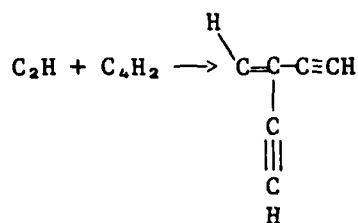
It is then assumed that such branched chain radicals add further poly-acetylenes or hydrocarbons without losing their radical character. "Ring closures are easily imaginable," [16] which would account for the reactive polycyclic aromatic hydrocarbons identified as precursors in Fig. 6. It is assumed that as the radical continues to grow by addition of acetylene and polyacetylene it splits off molecular fragments which account for the formation of byproduct polycyclic aromatics. How this mechanism avoids the problem of slow growth and ring formation is not clear; the mechanism has not been analyzed in detail.
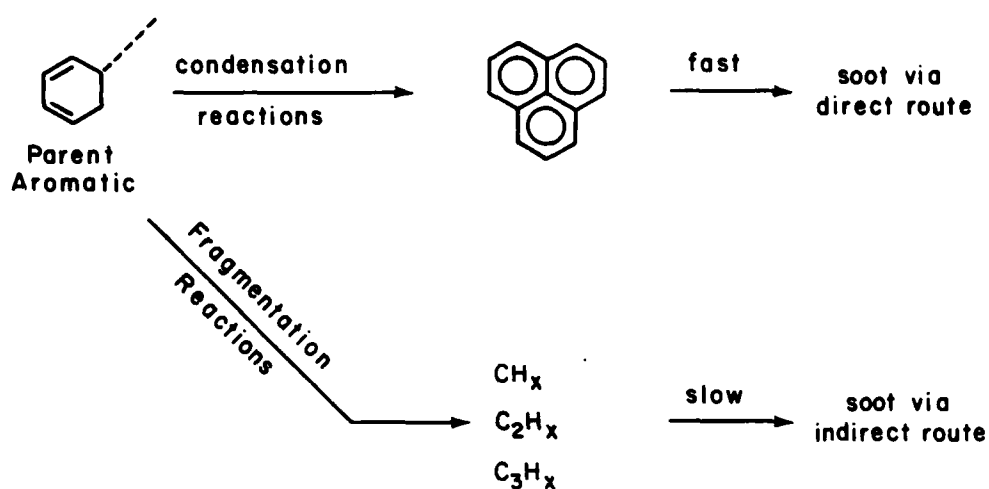
On the basis of the effect of molecular structure on soot formation Glassman [36] argues for the importance of strongly conjugated molecules like 1,2-butadiene combining to form a ring with an ethyl side chain to which butadiene type molecules keep adding. Unfortunately, concentration profiles (Fig. 7) show butadiene to be falling very rapidly even before soot particles are observed. Similarly, Bittner and Howard [35] suggest that in aromatic systems the nucleation process may be initiated by the reaction of vinyl acetylene with a phenyl radical to form naphthalene.

In another computer modeling study Jensen [31] concludes that for the specific case he studied, the production of soot in the exhaust of a rocket engine, the only mechanism consistent with experiment involves C_2, C_2H, and

C_3 as initial nuclei with C_2H_2 as the growth species. This same type of analysis should be performed for the well documented flame of Figs. 3 to 6. Unfortunately, the concentrations of C_2 and C_3 have not been measured in this system. They can be estimated, from 1 atm C_2H_2/O_2 flames [49] as being on the order of roughly 10^{14} and 10^{12} cm^{-3}, respectively.

Mann [50] in a fast flow high temperature carbon-vapor system studied carbon vapor condensation to C_2 and C_3 and then $C_2 + C_3 \rightarrow C_5$ with $k = 6 \pm 2 \times 10^{-10}$ cm^3 s^{-1} which he interpreted as the initial step of coalescence reactions leading to carbon particles. Mechanisms based on C_2 and C_3 condensation reactions were originally proposed by Smith [51] and Cabannes [52], respectively, but have generally been rejected as a general mechanism [3], e.g., because C_2 radiation is very strong in rich cyanogen-oxygen flames which do not form soot. Jessen and Gaydon [49], from absorption spectroscopic studies in an acetylene-oxygen rich flame, concluded that C_2 radicals may serve as the nuclei for soot formation but that C_3 is probably formed by evaporation of incipient soot particles.

In a study of the pyrolysis of aromatic hydrocarbons in shock-heated gases Graham et al. [27] found a decrease in the rate of soot formation above 1800 K although there was a rapid increase in rate with increasing temperature below 1800 K. They interpret their results via a scheme with two pathways:

Parent Aromatic → condensation reactions → fast → soot via direct route

Fragmentation Reactions → CH_x, C_2H_x, C_3H_x → slow → soot via indirect route

Earlier others [29] had proposed direct condensation of aromatic rings to account for the greater tendency of aromatics over aliphatics or acetylene to form soot. As early, however, as 1962 Stehling et al. [53] concluded that polycyclics and aromatics were not the main precursors of soot (see also Ref. 54).

Stein [55] has used well-developed thermodynamic techniques for estimating the energetics of selected polycyclic aromatic hydrocarbons, (PCAH), and with these new data estimated equilibria among several PCAHs and H_2 and C_2H_2. For the first six members of the most thermodynamically favored high temperature PCAH polymerization route he gave:
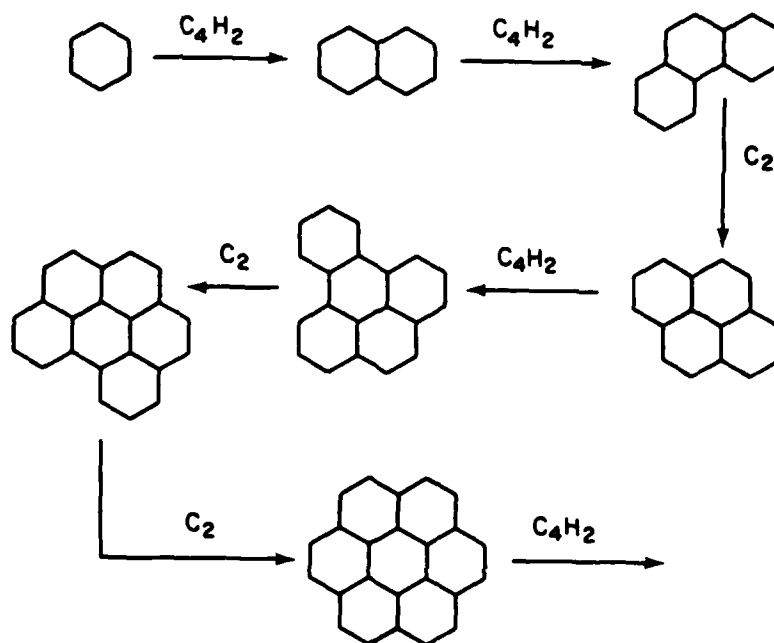
where C_2 and C_4H_2 refer only to the numbers and type of atoms added in each step and do not imply a specific chemical species or mechanism. The significant conclusion of his study was that in a homogeneous equilibrium system above about 1700 K there exists a critical highly condensed polycyclic aromatic species whose concentration is at a minimum with respect to other highly condensed aromatics. He points out that this will constitute a thermodynamic barrier for homogeneous high temperature soot formation. Thus for the proposed pathway in which aromatic units remain intact [55]:
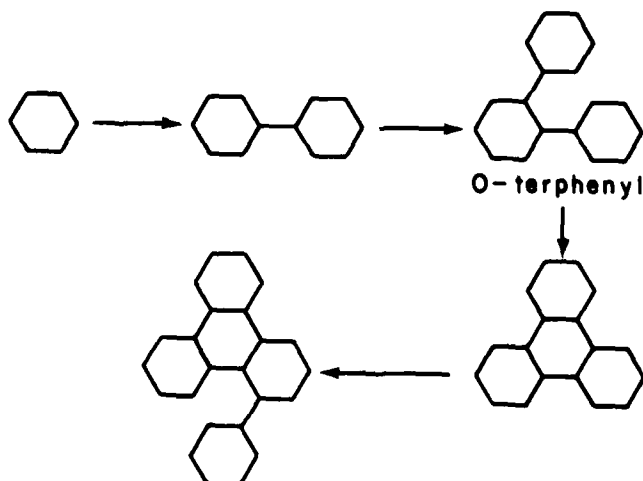
O-terphenyl has the lowest equilibrium concentration over a wide range of conditions. Since the thermal stability of polyacetylenes decreases uniformly with increasing size and PCAHs are the only thermodynamically stable species, he argues that soot formation must occur through PCAHs which represent the most favored thermodynamic path. The species present at the lowest concentration in the path should be involved in the rate limiting step. This thermodynamic data which is now available should be used to evaluate specific reaction schemes to account for soot formation in experimentally studied flames.

Bittner and Howard [18,35] have recently reported detailed neutral species profiles on near sooting, $\phi = 1.8$ ($\phi_c = 1.9$) benzene/oxygen/argon flames at 2.67 kPa. From a detailed analysis of the species concentration profiles and the species flux profiles they conclude that the polycyclic aromatic hydrocarbons observed in sooting flames cannot be formed by condensation reactions of intact aromatic rings, and that much of the carbon that ends up as soot comes from non-aromatic hydrocarbon intermediates. Their flux profiles indicate that the benzene molecule is attacked by OH rather than O and that CO, C_6H_6O and C_5H_6 are early intermediates in the ring destruction process but that C_2H_2 is not. They point out that for rapid growth of aromatic structures by a free radical mechanism the stabilization of the energy rich intermediates formed by the addition of radicals to stable hydrocarbons may be a crucial step and that an aromatic hydrocarbon may do this. From a consideration of the addition of aromatic radicals to non-aromatic molecular species including phenyl and benzyl radicals to acetylene, 1,3-butadiene, vinyl acetylene, methyl acetylene, and allene, only two mechanisms ($C_6H_5 + C_4H_4$) and ($C_7H_7 + C_3H_4$) were found where unimolecular rearrangement of the intermediate to form a six-membered ring is favored over other decomposition channels. The next step is clearly a kinetic model to determine whether the rate through so few

17

of the many possible channels is sufficient to account for the rate of soot formation.

In summarizing the above discussion it seems clear that many neutral species mechanisms for soot formation have been proposed and where they have been examined in detail there are serious problems with the nucleation steps. Polyacetylene mechanisms are rejected as being too slow and having difficulties with rearrangement to a polycyclic structure. Polycyclics have been rejected as the essential nucleating agents because they continue to increase in concentration after the rate of soot formation has gone to zero. Combinations of free radicals which are decaying through the flame front with acetylene, polyacetylenes or polycyclics may be the key to the nucleation mechanism but none of these various concepts have been developed to the point of being convincing. Many of the difficulties arise from the necessity to form cyclic structures without requiring extensive molecular rearrangements and thus large entropy changes. Clearly no completely satisfactory neutral species mechanism currently exists to account for the very rapid formation of soot in flames.

IONIC MECHANISMS

Increasingly authors of papers on soot formation allude to possible ionic mechanisms, often after demonstrating the weakness in neutral free radical mechanisms as demonstrated in the previous section. In fact, a number of specific ionic nucleating mechanisms have been suggested [5,11,37, 56-59]. It will be the purpose in this section, after reviewing some of the observations which have led to considerations of ionic mechanisms, to present a unifying picture of soot formation which utilizes many of the neutral free

radical mechanisms discussed above--to the point where they run into trouble--
with an ionic mechanism which appears to overcome the major problems. There
are, of course, still difficulties remaining, but of a different nature and
requiring a different experimental and theoretical approach than has been
previously pursued. The effect of ions on the growth and agglomeration steps
will not be covered--they have been well documented by Howard and associates
[10,11,42,58,60,61].

Experimental Observations

Some of the experimental observations which have led to the recognition
of the importance of ions will be reviewed. Although in many cases they are
not germane to the nucleation step, they are   relevant as historical
observations which have directed the researcher's attention to ionic mechanisms.

Charged Carbon Particles

Mayo and Weinberg [62] concluded from ion mobility measurements with
electrical potentials across counter-flow diffusion flames that each soot
particle carries unit charge. They interpreted their results as a growth of
soot on flame ions as well as neutral growth followed by charge attachment.
Ball and Howard [61] studied the charge on soot particles by measuring their
mobility after removing them from the flame. They interpreted their results in
terms of thermionic emission and electron capture by the soot particles after
they were formed. This, of course, says very little about the initial mecha-
nism of particle formation but does show that the final particles are elec-
trically charged. Subsequently, Wersborg et al. [11] measured all charged
species larger than about 300 amu in a flat acetylene-oxygen flame at 2.7 kPa
(20 Torr) and demonstrated that only positively charged molecules were present.
The total positive charge concentration showed a distinct peak at a height

19

above the burner just preceding the onset of visible soot formation. The mass distribution of charged species peaked sharply at a mass which increased with increasing height (time) above the burner, Fig. 8. They concluded that nucleation on ions was a feasible mechanism for soot formation under the conditions of their experiment. It is significant that all of the above agree that only positive ions are of importance.

More recently Homann [43] has demonstrated the presence of negative species with concentrations lower than those of positive species. The concentration of negative species peaks for lower molecular weights than for positive ions and then shows a broad range of negative particle masses, still at smaller diameters than the positively charged particles.

Effect of Electric Fields

Weinberg et al. [62-65], in an extensive series of experiments, demonstrated that soot particle growth in a flame can be controlled by means of electric fields. For example, if the electric field is such as to increase the residence time of the positive ions in the flame, larger particles are produced than when the ions are in the flame for a shorter period of time. They also showed that the soot collected on the cathode from a flame deflected by an electric field "is strikingly different from that collected on a cold surface in contact with the flame in the absence of a field." Similar studies and observations have been made by others [66-68].

Identification of Embryo Ion

Miller [69] in a mass spectrometric study of ions in diffusion flames, observed that when soot formation is induced by the addition of small amounts of carbon tetrachloride, the concentration profiles of hydrocarbon-type ions are completely altered, and the concentration of high molecular weight hydrocarbon ions is enhanced by many orders of magnitude. Subsequent mass spectrometric studies by Delfau et al. [13] and Olson and Calcote [17]

20

of ions in premixed flames have demonstrated a strong correlation between the appearance and growth of large positive ions and the onset of soot. The question here is which is the cause and which is the effect?

Electron Addition

Salooja [70] and Bowser and Weinberg [71] have demonstrated that the addition of electrons to flames, from small coated wires placed in the flame, can markedly alter the quantity of soot produced. The effect, enhancement or suppression, is dependent upon the position of the wire in the flame, i.e., where and in what quantity the electrons are introduced.

Chemical Additives

Bartholome and Sachsse [72] in 1949 found that nickel and alkaline earths reduced the quantity of soot formed in a flame. They explained this by picturing the charged additive particles as attaching to the embryo carbon particles and thus repelling each other. More recently, Haynes et al. [73] have demonstrated, by measuring the variation of particle number density and diameter as an almost linear function of ion concentration, that the effect of alkali metal ions is to charge the soot particles thus preventing their growth by collision with each other. Addecott and Nutt [74] showed a correlation between ionization potential and the ability of an additive to reduce soot formation. Similar work was reported by Feugier [75-77] and Bulewicz et al. [78] who demonstrated that ionizable additives, e.g., alkali metals, can either increase or decrease the rate and quantity of soot produced. These latter authors agree that the inhibiting effect of metal additives is related to ionic reactions; their results are interpreted by detailed mechanisms involving the nucleation process. It is also well known [2,58,79,80] that in the production of carbon black, the easily ionized alkali and alkaline earth metals are added to the flame to control both the quantity and the properties of carbon black. On the other hand,

21

Cotton et al. [81] studied the effect of 40 metal additives on propane-air diffusion flames and interpreted their results by a free radical mechanism.

When an easily ionized metal atom is added to a flame, charge transfer from the natural flame ion occurs rapidly producing metal ions [82-84]. Although metal ions could act as nuclei, they would not be expected to be as efficient as normal hydrocarbon flame ions because of less easily formed chemical bonds. It is important to recognize that easily ionizable chemical additives can affect any one of the three steps in particle formation. Interpretation of the observations within a unified framework would be complex and in fact is probably not possible because of limited data. Chemical additive effects will not be treated further in this discussion.

Fuel Structure

Diffusion flames of almost all organic substances except methyl alcohol, formaldehyde, and formic acid produce luminous tips, i.e., form soot particles [3]. Inorganic carbon containing molecules such as carbon monoxide [3], carbon disulfide, and a mixture of carbon disulfide and hydrogen [28], and cyanogen [85] do not produce soot. Of these gases only methyl alcohol [86] and cyanogen [87] produce flame ions. Methyl alcohol produces flame ions inefficiently [88,89] and the ions in cyanogen flames are different from those in hydrocarbon flames [82,87,90]. Carbon monoxide and carbon disulfide do not produce flame ions [91]. Beyond this observation there exists no direct fuel chemistry-related correlation between the tendency to smoke and the tendency to produce ions [92]. This lack of obvious correlation is expected because the means of measuring the trends ignores important parameters such as temperature and neglects any consideration of the complicated kinetics which must be involved.

Ion Concentrations

The concentrations of heavy hydrocarbon ions in an acetylene-oxygen flame at 2.7 kPa were found by Wersborg et al. [11] to be much larger than the peak concentration of soot particles, Fig. 6. From this they conclude that an ionic nucleation of soot particles is feasible. There are problems with these measurements of heavy hydrocarbon ion concentrations as well as with several more recent measurements of ion concentration in sooting flames [11,13,43]. (See discussion following Ref. 17.) More careful measurements of absolute ion concentrations, ranging from small to large ions in nonsooting and sooting flames are highly desirable.

Activation Energy

From the temperature dependence of the critical equivalence ratio for soot formation in ethylene-air flames, Millikan [26] deduced an activation energy for soot formation of 140 ± 40 kJ mol^{-1}. Peeters et al. [93] measured the overall apparent activation energy for chemi-ionization of a series of hydrocarbons added to H_2/O_2 flames and found 140 ± 7 kJ mol^{-1}. The agreement is amazing and is consistent with an ionic mechanism of soot nucleation.

O-Atom Hydrocarbon Reactions

Vinckier et al. [57] found in an acetylene rich system reacting with O atoms that

$$CHO^+ + C_2H_2 \rightarrow C_2H_3^+ + CO \tag{14}$$
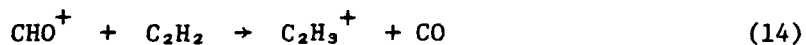
was followed by rapid ionic polymerization with acetylene to form $C_{2n}H_{2n+1}^+$ and $C_{2n}H_{2n-1}^+$. They suggested that such polymer ions are the nucleation centers for soot formation in fuel rich flames.

Ionization During Pyrolysis

Soot is produced under purely pyrolytic conditions, i.e., without the presence of oxygen, so that for an ionic nucleation theory to be generally applicable to both flames and pyrolysis it must be demonstrated, as a minimum, that ions are present in pyrolytic reactions. Abrahamson and Kennedy [94] measured the current between two electrical probes in both argon diluted methane and propane flows through a tube heated to 1300 to 1400 K at 1 atm pressure. For a 42% propane in argon mixture they measured 14 μA current with 25 V applied between two tungsten probes 6.2 mm diam, 26 mm long, and 10 mm apart. Assuming one probe is operating as a Langmuir probe with an ion sheath these results would indicate a positive ion concentration of about 10^{12} ions cm^{-3}.

Bowser and Weinberg [95] have demonstrated the occurrence of chemi-ionization in the pyrolysis of ethylene in the absence of oxygen, behind reflected shock waves. Experiments were carried out with 100% ethylene pyrolysis produced by a reflected shock. The end of the shock tube contained an axial electrode protruding a few mm back into the tube and an electric field was applied between this probe and the tube wall; the current to the probe was displayed on an oscilloscope. Saturation currents were measured with voltages of about 20 kV m^{-1} and ranged from about 0-1 mA at 900 K to 10 mA at 1800 K (calculated shock temperature). They interpret their results as yielding ion concentrations between 10^{11} and 10^{15} ions cm^{-3} at test pressures close to atmospheric.

Both of these sets of experiments indicate very high ion concentrations in hydrocarbon pyrolysis and demonstrate the need for careful verification.

Bowser and Weinberg [95] suggest the ions produced in pyrolysis of hydrocarbons are due to the reaction:

$$C_2 + CH_3 \rightarrow C_3H_3^+ + e^- \tag{15}$$
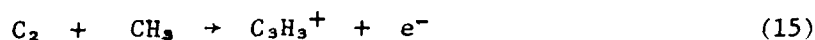
Because C_2 has been observed in both absorption and emission in pyrolysis experiments while CH has not [43,96-99], they conclude that the reaction:

$$CH^* + C_2H_2 \rightarrow C_3H_3^+ + e^- \tag{16}$$
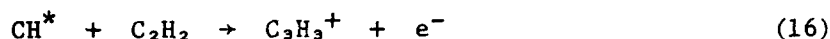
sometimes considered as a primary ion produced by chemi-ionization in flames [100], cannot be important in pyrolysis systems. If C_2 is in the ground state Reaction (15) is endothermic by 195 kJ mol^{-1} for a linear structure of $C_3H_3^+$ or 95 kJ mol^{-1} for a cyclic structure of $C_3H_3^+$. For C_2 ($A^3\Pi g$) Reaction (15) is exothermic by 27 to 167 kJ mol^{-1} depending upon the excitation energy of C_2 and the structure of $C_3H_3^+$. The basic problem of accounting for C_2 or C_2^* as well as CH and CH* in pyrolysis or flames is brought into focus by their apparent importance in ionization in pyrolysis or in rich flames (see subsequent discussion). Their source and relationship to each other are not at all clear [101], Knewstubb and Sugden [56] suggested the reverse of Reaction (15) to account for C_2^* in flames. Gaydon and Wolfhard [3,101] propose that C_2 is in fact produced by the decomposition of a polyacetylene, e.g.:

$$C_8H_2 \rightarrow C_6 \text{ (graphite nucleus)} + C_2 + H_2 \tag{17}$$
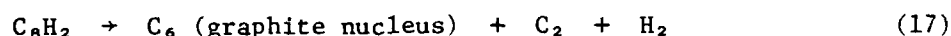
Using the data of Cowperthwaite and Bauer [102] this reaction would be endothermic by more than 1000 kJ mol^{-1}.

The nature of the ions produced in pyrolysis, their mechanism of formation, and their relationship to soot production in pyrolysis deserves further attention.

Thermal Ionization

The above discussion makes it clear that ions are associated with soot formation and that ionic mechanisms can be used to explain soot formation under many experimental conditions. Before proceeding further with an ionic mechanism, however, the possibility that ions are a byproduct and not a major intermediate in soot formation should be examined. The first possibility which must be considered is that the ions are produced thermally, i.e., that they are simply a result of equilibrium due to the high flame temperature. This proposal can be tested by calculating equilibrium ion concentrations using Saha's equation [5,103,104]

$$K_n = \frac{n_+ n_e}{n} = G \left(\frac{2\pi m_e kT}{h^2} \right)^{3/2} \exp\left(-\frac{I}{kT} \right) \qquad (A)$$

for the reaction:

$$A \rightleftharpoons A^+ + e^- \qquad (18)$$

where:

K_n = equilibrium constant

$G = \dfrac{g_+ g_e}{g}$ where the g's are statistical weights of ion, g_+, electron, g_e, and neutral species, g

T = absolute temperature

m_e = mass of the electron

k = Boltzmann's constant

h = Planck's constant

I = ionization potential for species A

For small ions it is readily demonstrated that the concentrations of ions observed in nonseeded flames (i.e., without alkali or alkaline earth atoms added) cannot be accounted for by thermal ionization [105,106]. However, when large particles are present and the ionization potential is replaced by the

26

work function of the particle, the number of charged particles and the number
of charges (positive) on the particle can be accounted for by thermal ioniza-
tion [5,43,58,92,106] (see also Ref. 107). The calculation for multicharged
particles is more complicated than described by Eq. (A); the reader is referred
to the literature [103,104,108]. The question here is to what extent might the
large molecular ions observed in the early part of the flame, Table 2, be
accounted for by simple ionization of large molecules whose ionization potential
must at some point approach the work function of large particles?

Since ionization potentials of very large molecular ions are not avail-
able, the first task is to determine how the ionization potential varies with
the size of the molecular ion and how it approaches the work function of a
large particle. To do this the variation of the work function of a particle
with size will be calculated and the work function of small particles approach-
ing the size of large molecular ions will be calculated and compared with the
known ionization potential of large molecular ions. The equation for the
energy to remove one electron from a particle is given by [104]

$$I = V + \frac{e^2}{2C} \qquad (B)$$

where V = work function of the substance making up the particle

    e = charge on the electron

    C = capacitance of the particle

where C = $2\pi\epsilon_0 d$ for a sphere of diameter d

 and C = $4\epsilon_0 d$ for a planar disc of diameter d

    ϵ_0 = dielectric constant of free space

Assuming the work function for soot to be the same as that for graphite, 4.6 eV,
(0.74 aJ or 0.74×10^{-18} J), the curves in Fig. 9 have been calculated. To deter-
mine the validity of these curves for large molecules and to determine whether the

spherical or planar disc curve should be used, calculated ionization potentials were compared with experimental values (see also Refs. 5, 104). The agreement was remarkably good for planar discs so that the upper curve, Fig. 9, can be used with confidence in calculating the ionization potential or work function of large molecules and small particles.

The first objective will be to compare measured concentrations of "large positive ions" (> 300 amu) with calculated concentrations using the above procedures. The experimental large positive ion concentration is given in Fig. 6 and the large molecular mass concentration is given in Fig. 5. It is necessary to know the molecular weight to transfer the mass concentration into the number density required for the calculation. The molecular weight is not given but since the ion molecular weights were > 300 amu the molecules from which they were derived must be > 300 amu. Further, since in the experiments from which these data were derived the smallest particle distinguished from large molecules had a diameter of 3 nm, the molecular weight of the large molecules must be < 10,000 amu (see Fig. 9). A linear variation of molecular weight from 300 to 10,000 amu was assumed over the distance of interest, from 1.5 to 5.0 cm, in estimating I and n to be used in calculating positive ion concentration by Eq. (A). The temperature was that given in Fig. 3. When this is done the experimental values are more than two orders of magnitude more than the calculated values, e.g., at 2 cm above the burner the experimental concentration is 8×10^{10} ions cm^{-3} and the calculated value is 3×10^{8} ions cm^{-3}. Thus the large molecular weight ions (amu > 300) observed in sooting flames cannot be accounted for by thermal ionization of

the large molecules present, a conclusion previously deduced by Prado and Howard [5].

Another compelling argument for rejecting thermal ionization of large molecules is that the ions observed, Table 2, do not resemble the molecules, Table 1; ions typically have an odd number of hydrogen atoms, implying proton or hydride transfer, while the molecules have even numbers of hydrogen atoms.

Now consider the possibility of a thermal source of the ionized particles. For this calculation the average particle diameter taken from Fig. 4 is used to obtain the ionization potential, I, from Fig. 9, to be used in Eq. (A). The neutral particle number density, soot, is taken from Fig. 6. The temperature is taken from Fig. 3 as above. The agreement, shown in Fig. 10, is amazing. It must be concluded that the small charged soot particles with diameters $\gtrsim 3$ nm observed in flames are explained simply as due to thermal emission of electrons from the particles. This must also explain the increase in total charged species, >300 amu, observed by Wersborg et al. [11] for increasing equivalence ratios in sooting acetylene-oxygen flames measured by the current delivered to a Faraday cage. It must also explain similar results obtained by Delfau et al. [13] with an electrostatic probe; as the equivalence ratio increased to the critical equivalence ratio for soot formation, ϕ_c, the maximum ion concentration decreased but as the equivalence was increased beyond ϕ_c the maximum ion concentration increased.

The problem posed by Fig. 4, also observed by Homann [43], that at any position downstream of the formation of soot the neutral soot particles are larger than the charged particles is contrary to what would be expected for

thermal ionization of the particles because larger particles have smaller

ionization potentials, Fig. 9. Homann explains the observation by a "kind

of chemi-ionization" in which exothermic growth reactions heat the small

particles preferentially. It is difficult to imagine the particle gaining

sufficient temperature above that of the environment by this mechanism

because of the large number of collisions with nonreactive molecules which

will remove the energy as fast as it is added. An explanation might be

sought in the observation that electron-particle recombination coefficients,

already large, are proportional to the particle diameter [109]. Thus smaller

particles may be in thermal equilibrium but larger particles may not because

the rapid charged particle electron recombination may exceed the rate of

thermal ionization. Obviously a more quantitative analysis is required. If

this explanation is correct, how does one account for the good agreement in

Fig. 10 or the observation by Homann [43] that the work function he derives

for soot particles by the application of Saha's equation to his data is

about 0.8 aJ, consistent with what would be expected for thermal ionization

of the particles present? There is, in fact, additional evidence for thermal

ionization of soot particles. When electrons are withdrawn from a nonsooting

flame, e.g., in flame ionization detectors [88, 110], a saturation current

is obtained where the rate of ion removal by the electric field is equal to

the rate of ion production. Delfau et al. [13] have observed that the slope

of the saturation current-voltage curve increases at the equivalence ratio

at which soot is formed and continues to increase as the equivalence ratio is

increased and more soot is produced. This indicates an equilibrium source

of electrons, e.g., thermal ionization of particles in which the electrons

are replaced as fast as they are removed. This phenomenon has also been

observed by Olson [111], and both Delfau et al. [13] and Olson [111] observed

a similar result when alkali metals, which are thermally ionized and in

30

equilibrium, are added to nonsooting flames. Others [112,113] who have reported saturation current measurements in sooting flames have not reported this same observation. However, Boothman et al. [112] observed that in sooting flames electric charge was generated throughout the total flame volume rather that in just the flame front and they interpreted this as due to thermionic emission from soot particles. An explanation of Fig. 4 consistent with thermionic emission of electrons from soot particles is needed, or a means of explaining the evidence for thermal emission which is consistent with Fig. 4 is needed. Could the data in Fig. 4 be in error?

To sum up this discussion: thermal ionization cannot account for the ionization of small or large molecules (amu $\leqslant$ 10,000) in sooting flames but does seem to account for the charged particles ($\geqslant$ 10,000 amu) which are observed when soot is formed.

Mechanism of Incipient Soot Formation

It has been demonstrated in the above discussion that none of the nucleating mechanisms involving neutral species proposed to account for soot formation in fuel rich flames are wholly consistent with the experimental observations. A mechanism will be presented here which borrows the acceptable elements of several previously proposed free radical mechanisms and merges them with an ionic mechanism to overcome the objections raised to the neutral species mechanisms. This involves a chemical nucleation step where ion molecule reactions are important in contrast to physical nucleation on ions [8]. The overall scheme is depicted in Fig. 11. All of the species proposed in the various steps have been observed in sooting flames. The main neutral building blocks, $C_x H_y$, include acetylene, the polyacetylenes, and such species as $C_2 H$, CH_2, and $C_4 H$. The reactions producing these reactants have already been discussed.

31

The primary ions are produced by chemi-ionization:

$$CH + O \rightarrow CHO^+ + e^- \qquad (19)$$

or
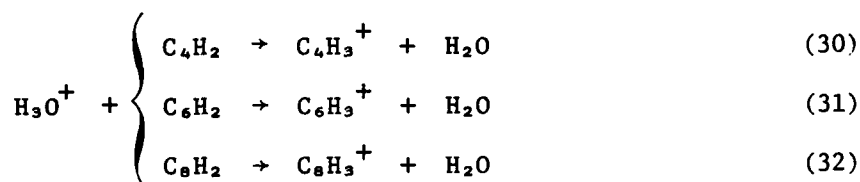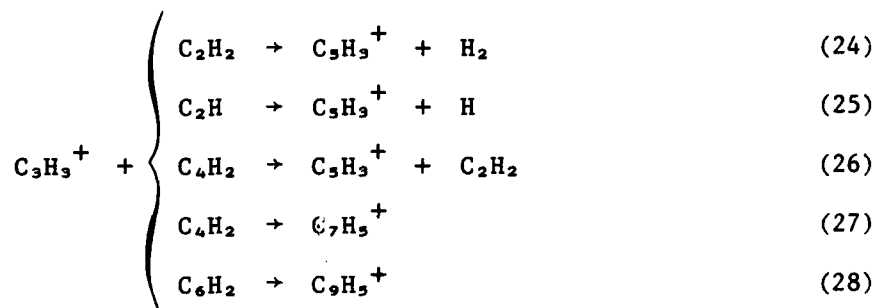$$CH^* + C_2H_2 \rightarrow C_3H_3^+ + e^- \qquad (16)$$
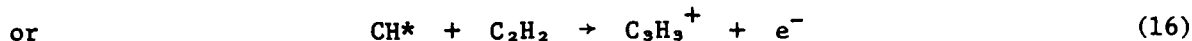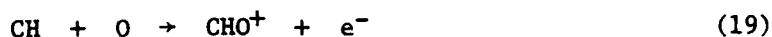
Reaction (19) is generally accepted as the source of ions in hydrocarbon flames [82,84,114]. Reaction (16) is often proposed as the source of the large concentration of $C_3H_3^+$ observed in fuel rich flames; however, the proof is still very fragile [82,100,114]. The mechanism of formation of $C_3H_3^+$ in fuel rich flames merits additional study.

Ion-molecule reactions follow very rapidly [82,83] so that CHO^+ is never observed in large concentrations:

$$CHO^+ + C_2H_2O \rightarrow C_2H_3O^+ + CO \qquad (20)$$

$$C_2H_3O^+ + C_2H_2 \rightarrow C_3H_3^+ + CH_2O \qquad (21)$$

$$CHO^+ + H_2O \rightleftarrows H_3O^+ + CO \qquad (22)$$

$$CHO^+ + C_2H_2 \rightarrow C_2H_3^+ + CO \qquad (23)$$
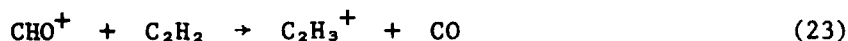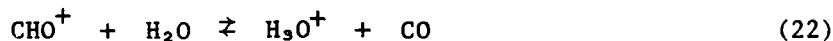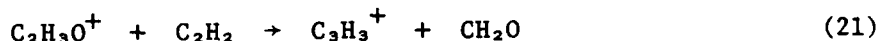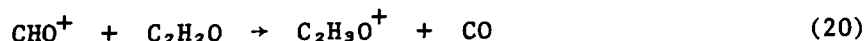
Reactions (20) and (21) are representative of a number of mechanisms going from CHO^+ to $C_3H_3^+$ [83]. Reaction (22) is in equilibrium [83] and is the principal source of the dominant H_3O^+ observed in near stoichiometric and lean flames. The dominant ion observed in rich flames is $C_3H_3^+$. At the critical equivalence ratio for soot formation the concentration of $C_3H_3^+$ falls very rapidly and is replaced by larger ions, Fig. 12. Reaction (23) is from O-atom reaction studies in flow tubes by Vinckier et al. [57] who observed this ion polymerize to produce larger ions and suggested that these polymeric ions are nucleating centers for soot formation in flames. Although $C_2H_3^+$ is not observed in large quantities in flames [82] this does not eliminate the possibility of Reaction (23)--$C_2H_3^+$ may simply react very rapidly.
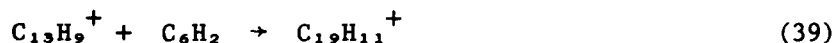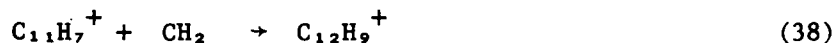
32

The next step in the scheme, Fig. 11, the formation of $C_zH_w^+$ ions from the primary ions and C_xH_y building blocks would be represented by fast ion–molecule reactions such as:

$$C_3H_3^+ + \begin{cases} C_2H_2 \rightarrow C_5H_3^+ + H_2 & (24) \\ C_2H \rightarrow C_5H_3^+ + H & (25) \\ C_4H_2 \rightarrow C_5H_3^+ + C_2H_2 & (26) \\ C_4H_2 \rightarrow C_7H_5^+ & (27) \\ C_6H_2 \rightarrow C_9H_5^+ & (28) \end{cases}$$

$$C_2H_3^+ + C_2H_2 \rightarrow C_4H_5^+ \qquad (29)$$

$$H_3O^+ + \begin{cases} C_4H_2 \rightarrow C_4H_3^+ + H_2O & (30) \\ C_6H_2 \rightarrow C_6H_3^+ + H_2O & (31) \\ C_8H_2 \rightarrow C_8H_3^+ + H_2O & (32) \end{cases}$$

All of the above reactions are exothermic.[2] Incidently, one of the problems in separating out possible reactions to account for the observed ions is the lack of thermodynamic values for the heats of formation of the ions involved.

The next step in the process, Fig. 11, is the growth to larger ions by further addition of the building blocks, C_xH_y, to the C_zH_w ions produced above. The following set of reactions is typical of this step:

---

[2] These calculations assumed the cyclic structure of $C_3H_3^+$ for which $\Delta H_f^{298} = 1075$ kJ mol^{-1} [116] and the recently obtained value of Michaud et al. [117] for $C_5H_3^+$ of $\Delta H_f^{298} = 1280$ kJ mol^{-1}. The literature value for $C_5H_3^+$, $\Delta H_f^{298} = 1490$ kJ mol^{-1} (derived from the appearance potentials in Ref. 116) would make some of these reactions endothermic.

$$C_5H_3^+ + C_2H_2 \rightarrow C_7H_5^+ \tag{33}$$

$$C_7H_5^+ + C_2H_2 \rightarrow C_9H_7^+ \tag{34}$$

$$C_9H_7^+ + C_2H_2 \rightarrow C_{11}H_7^+ + H_2 \tag{35}$$

$$C_{11}H_7^+ + C_2H_2 \rightarrow C_{13}H_9^+ \tag{36}$$

$$C_9H_7^+ + C_4H_2 \rightarrow C_{13}H_9^+ \tag{37}$$

$$C_{11}H_7^+ + CH_2 \rightarrow C_{12}H_9^+ \tag{38}$$

$$C_{13}H_9^+ + C_6H_2 \rightarrow C_{19}H_{11}^+ \tag{39}$$

The ions $C_{13}H_9^+$ and $C_{19}H_{11}^+$, amu = 165 and 239, respectively, are dominant ions [17] and probably have the stable structures:

$$C_{13}H_9^+ \qquad\qquad C_{19}H_{11}^+$$
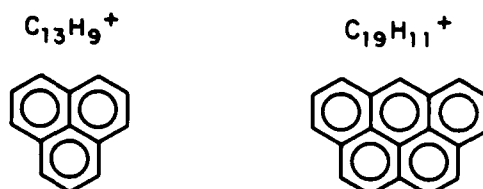
Rearrangement to a polynuclear or aromatic structure which is far more stable than a linear structure is assumed to occur very rapidly because of the propensity of gaseous ions to rearrange to their most stable structure [118-120].

This rapid rearrangement of ions overcomes one of the problems associated with the neutral species theories discussed earlier, namely the problem of forming a polycyclic structure from a linear structure. Another problem of the poly-acetylene or polyaromatic polymerization theories, the observation that the concentrations of these species remained high while the rate of soot formation decreased, is also accounted for. Since the source of ions is chemi-ionization, which only occurs in the flame front [82,84,114], the ion concentration will continually decrease by ion recombination so that the rate of soot formation will also decrease. It is easy to visualize reactions similar to Reactions (33) to (39) which would continue to produce even larger ions, with increasing carbon to hydrogen ratio. Oxidation of the growing ion would continue to remove hydrogen, further increasing the C/H ratio. As the ions and neutral

34

molecules (from neutralized ions which probably continue to grow) become larger, their properties continually approach those of particles instead of molecules, e.g., Fig. 9, and they become ionized because of their low work function as discussed above. The change from molecular to particle properties occurs at a molecular weight of about 10^4 which corresponds to an incipient particle diameter of about 3 nm.

Another argument for the ionic nucleation and growth mechanism, not yet mentioned, is that starting with chemi-ions which are far out of equilibrium is like starting on the top of an energy mountain. The excess energy in the chemi-ions is available to drive the process downhill to a lower energy level.

Another interpretation could be placed on the source of large ions observed in near sooting and sooting flames; they could be formed by equilibrium ion-molecule reactions between $C_3H_3^+$ and larger neutral species, as suggested by Michaud et al. [117]. In fact they showed that in a slightly sooting flame the heats of formation of several ions could be derived from the observed relative concentrations of ions and neutral species. This is consistent with the mechanism of formation of most of the ions in lean and stoichiometric flames [83]. Michaud et al. always observe much greater concentration of $C_3H_3^+$ than the concentration of other ions; this is not true in richer sooting flames, Fig. 12, where the $C_3H_3^+$ concentration becomes very small, presumably because of reactions forming larger ions. Further, the equilibrium argument requires a rapid mechanism forming the large neutral species and, as already discussed, these are not easy to write down. Then the large-ion forming reaction,

$$C_{12}H_8 + C_3H_3^+ \rightleftharpoons C_{13}H_9^+ + C_2H_2 \tag{40}$$

would be generally endothermic by about 170 or 390 kJ mol^{-1} depending upon

whether $C_{12}H_8$ is biphenylene or acenaphthylene.[3] For comparison $C_{13}H_9^+$ could

be produced by an ion growth process employing Reactions (24), (33), (34), (35),

and (36) which all add acetylene in an exothermic reaction.

Clearly more work should be done to quantify the above ionic mechanism

of soot nucleation; this should include more detailed experimental species

concentration measurements especially of ions through the flame front, better

estimation of the heats of formation of ions involved to be used in estimating

reaction rates, and the development of detailed computer models [115] which

can be compared with experiments to determine whether or not the above mecha-

nism will hold up under quantitative scrutiny.

---

[3] The heats of formation of the ions for which data are not available are

estimated from Fig. 12 in Ref. 115.

ACKNOWLEDGMENT

REFERENCES

[1]   Palmer, H.B. and Cullis, C.F., in Chemistry and Physics of Carbon
       (P.L. Walker, Jr., Ed.), Marcel Dekker, New York, 1965, Vol. 1, p. 265.

[2]   Lahaye, J. and Prado, G., in Chemistry and Physics of Carbon
       (P.L. Walker, Jr. and P.A. Thrower, Eds.), Marcel Dekker, New York,
       1978, Vol. 14, p. 167.

[3]   Gaydon, A.G. and Wolfhard, H.G., Flames, Their Structure, Radiation and
       Temperature, Chapman and Hall, London, Fourth Ed., 1979, Chap. VII.

[4]   Homann, K.H., in The Mechanisms of Pyrolysis, Oxidation and Burning of
       Organic Materials (L.A. Wall, Ed.), National Bureau of Standards Spec.
       Publ. 357, Washington, DC, 1972, p. 143.

[5]   Prado, G.P. and Howard, J.B., in Evaporation-Combustion of Fuels,
       (J.T. Zung, Ed.), American Chemical Society, Advances in Chemistry
       Series 166, Washington, DC, 1978, p. 153.

[6]   Bittner, J.D. and Howard, J.B., in Alternative Hydrocarbon Fuels:
       Combustion and Chemical Kinetics (C.T. Bowman and J. Birkeland, Eds.),
       Progress in Astronautics and Aeronautics, AIAA, New York, 1978,
       Vol. 62, p. 335.

[7]   Homann, K.H., Combust. Flame 11:265-287 (1967).

[8]   Lahaye, J. and Prado, G.P., in Petroleum Derived Carbons (M.L. Deviney
       and T.M. O'Grady, Eds.), American Chemical Society, Symposium Series 21,
       Washington, DC, 1976, p. 335.

[9]   Wagner, H.Gg.,   Seventeenth Symposium (International) on Combustion,
       The Combustion Institute, Pittsburgh, 1979, p. 3.

[10]   Wersborg, B.L., Fox, L.K., and Howard, J.B., Combust. Flame 24:1-10
       (1975).

[11]   Wersborg, B.L., Yeung, A.C., and Howard, J.B., Fifteenth Symposium
        (International) on Combustion, The Combustion Institute, Pittsburgh,
        1975, p. 1439.

[12]   Herlan, A., Combust. Flame 31:297-307 (1978).

[13]   Delfau, J.L., Michaud, P., and Barassin, A., Combust. Sci. Technol.
        20:165-177 (1979).

[14]   D'Alessio, A., Di Lorenzo, A., Beretta, F., and Venitozzi, C.,
        Fourteenth Symposium (International) on Combustion, The Combustion
        Institute, Pittsburgh, 1973, p. 941.

[15]   Prado, G.P., Lee, M.L., Hites, R.A., Hoult, D.P., and Howard, J.B.,
        Sixteenth Symposium (International) on Combustion, The Combustion
        Institute, Pittsburgh, 1977, p. 649.

[16]   Homann, K.H. and Wagner, H.Gg., Eleventh Symposium (International) on
        Combustion, The Combustion Institute, Pittsburgh, 1967, p. 371.

[17]   Olson, D.B. and Calcote, H.F., "Ions in Fuel Rich and Sooting Acetylene
        and Benzene Flames," to be published in proceedings of The Eighteenth
        Symposium (International) on Combustion.

[18]   Bittner, J.D. and Howard, J.B., "Pre-particle Chemistry in Soot Formation,"
        to be published in Particulate Carbon: Formation During Combustion,
        Proceedings of the General Motors Symposium, Warren, MI, 15-16 October
        1980.

[19]   Di Lorenzo, A. and Masi, S., Second European Symposium on Combustion,
        Orleans, France, 1-5 September 1975, Vol. I, p. 368.

[20]   Crittenden, B.D. and Long, R., Envir. Sci. Technol. 7:742-744 (1973).

[21]   Crittenden, B.D. and Long, R., Combust. Flame 20:359-368 (1973).

[22]   Tompkins, E.E. and Long, R., Twelfth Symposium (International) on
        Combustion, The Combustion Institute, Pittsburgh, 1969, p. 625.

[23]   Chakroborty, B.B. and Long, R., Combust. Flame 12:226-236; 237-242; 469-476 (1968).

[24]   Franceschi, A., Gerbaz, G.P., and Mangolini, S., Combust. Sci. Technol. 14:33-41 (1976).

[25]   Millikan, R.C. and Foss, W.I., Combust Flame 6:210-211 (1962).

[26]   Millikan, R.C., J. Phys. Chem. 66:794-799 (1962).

[27]   Graham, S.C., Homer, J.B., and Rosenfeld, J.L.J., Proc. Roy. Soc. London A344:259-285 (1975).

[28]   Bonne, U., Homann, K.H., and Wagner, H.Gg., Tenth Symposium (International) on Combustion, The Combustion Institute, Pittsburgh, 1965, p. 503.

[29]   Bonne, U. and Wagner, H.Gg., Ber. Bunsenges. Phys. Chem. 69:35-48 (1965).

[30]   Homann, K.H. and Wagner, H.Gg., Ber. Bunsenges. Phys. Chem. 69:20-35 (1965).

[31]   Jensen, D.E., Proc. Roy. Soc. London A338:375-396 (1974).

[32]   D'Alessio, A., Di Lorenzo, A., Borghese, A., Beretta, F., and Masi, S., Sixteenth Symposium (International) on Combustion, The Combustion Institute, Pittsburgh, 1977, p. 695.

[33]   Homann, K.H. and Wagner, H.Gg., Proc. Roy. Soc. London A307:141-152 (1968).

[34]   Homann, K.H., Mochizuki, M., and Wagner, H.Gg., Z. Phys. Chem. 37:299-313 (1963).

[35]   Bittner, J.D. and Howard, J.B., "Composition Profiles and Reaction Mechanisms in a Near-Sooting Premixed Benzene/Oxygen/Argon Flame," to be published in proceedings of The Eighteenth Symposium (International) on Combustion.

[36]   Glassman, I., "Phenomenological Models of Soot Processes in Combustion Systems," Presented at 1980 Technical Meeting, Eastern Section of the Combustion Institute, Princeton Univ. Princeton, NJ, 12-14 November 1980; see also Princeton Univ. Mechanical and Aerospace Engineering Report No. 1450, July 1979.

[37]   Ferguson, C.R. and Keck, J.C., Combust. Flame 34:85-98 (1979).

[38]   Calcote, H.F., Miller, W.J., and Olson, D.B., Unpublished work.

[39]   Homann, K.H., Morgeneyer, W., and Wagner, H.Gg., Combustion Institute European Symposium (F.J. Weinberg, Ed.), Academic Press, London, 1973, p. 394.

[40]   Wagner, H.Gg., Personal communication.

[41]   Wagner, H.Gg., Comment following Ref. 28.

[42]   Wersborg, B.L., Howard, J.B., and Williams, G.C., Fourteenth Symposium (International) on Combustion, The Combustion Institute, Pittsburgh, 1973, p. 929.

[43]   Homann, K.H., Ber. Bunsenges. Phys. Chem. 83:738-745 (1979).

[44]   Cullis, C.F., in Petroleum Derived Carbons (M.L. Deviney and T.M. O'Grady, Eds.), American Chemical Society, Symposium Series 21, Washington, DC, 1976, p. 348.

[45]   Thomas, A., Tenth Symposium (International) on Combustion, The Combustion Institute, Pittsburgh, 1965, p. 511.

[46]   Thomas, A., Combust. Flame 6:46-62 (1962).

[47]   Homann, K.H., Warnatz, J., and Wellmann, C., Sixteenth Symposium (International) on Combustion, The Combustion Institute, Pittsburgh, 1977, p. 853.

[48]   Tanzawa, T. and Gardiner, W.C., Jr., Seventeenth Symposium (International) on Combustion, The Combustion Institute, Pittsburgh, 1979, p. 563.

[49]   Jessen, P.F. and Gaydon, A.G., Twelfth Symposium (International) on Combustion, The Combustion Institute, Pittsburgh, 1969, p. 481.

[50]   Mann, D.M., J. Appl. Phys. 49:3485-3489 (1978).

[51]   Smith, E.C.W., Proc. Roy. Soc. London A174:110-125 (1940).

[52]   Cabannes, F., J. Phys. Radium 17:492-496 (1956).

[53]   Stehling, F.C., Frazee, J.D., and Anderson, R.C., Eighth Symposium (International) on Combustion, Williams and Wilkins, Baltimore, 1962, p. 774.

[54]   Franceschi, A., Zanelli, S., and Cornetti, G.M., Combust. Sci. Technol. 14:57-62 (1976).

[55]   Stein, S.E., J. Phys. Chem. 82:566-571 (1978).

[56]   Knewstubb, P.F. and Sugden, T.M., Seventh Symposium (International) on Combustion, Butterworths, London, 1959, p. 247.

[57]   Vinckier, C., Gardner, M.P., and Bayes, K.D., Sixteenth Symposium (International) on Combustion, The Combustion Institute, Pittsburgh, 1977, p. 881.

[58]   Howard, J.B., Twelfth Symposium (International) on Combustion, The Combustion Institute, Pittsburgh, 1969, p. 877.

[59]   Abrahamson, J., Nature 266:323-327 (1977).

[60]   Howard, J.B., Wersborg, B.L., and Williams, G.C., Faraday Society Symposia 7:109-119 (1973).

[61]   Ball, R.T. and Howard, J.B., Thirteenth Symposium (International) on Combustion, The Combustion Institute, Pittsburgh, 1971, p. 353.

[62]   Mayo, P.J. and Weinberg, F.J., Proc. Roy. Soc. London A319:351-371 (1970).

[63]   Weinberg, F.J., Faraday Society Symposia 7:120-132 (1973).

[64] Place, E.R. and Weinberg, F.J., Eleventh Symposium (International) on Combustion, The Combustion Institute, Pittsburgh, 1967, p. 245.

[65] Place, E.R. and Weinberg, F.J., Proc. Roy. Soc. London A289:192-205 (1965).

[66] Heinsohn, R.J. and Becker, P.M., in Combustion Technology: Some Modern Developments (H.B. Palmer and J.M. Beer, Eds.), Academic Press, New York, 1974, p. 239.

[67] Lester, T.W. and Wittig, S.L.K., Sixteenth Symposium (International) on Combustion, The Combustion Institute, Pittsburgh, 1977, p. 671.

[68] Wittig, S.L.K. and Lester, T.W., in Evaporation-Combustion of Fuels (J.T. Zung, Ed.), American Chemical Society, Advances in Chemistry Series 166, Washington, DC, 1978, p. 167.

[69] Miller, W.J., Eleventh Symposium (International) on Combustion, The Combustion Institute, Pittsburgh, 1967, p. 252.

[70] Salooja, K.C., Combustion Institute European Symposium 1973 (F.J. Weinberg, Ed.), Academic Press, London, 1973, p. 400.

[71] Bowser, R.J. and Weinberg, F.J., Nature 249:339-341 (1974).

[72] Bartholome, E. and Sachsse, H., Z. Elektrochem. 53:326-331 (1949).

[73] Haynes, B.S., Jander, H., and Wagner, H.Gg., Seventeenth Symposium (International) on Combustion, The Combustion Institute, Pittsburgh, 1979, p. 1365.

[74] Addecott, K.S.B. and Nutt, C.W., "Mechanism of Smoke Reduction by Metal Compounds," presented at American Chemical Society Meeting, New York City, September 7-12, 1969.

[75] Feugier, A., Combustion Institute European Symposium (F.J. Weinberg, Ed.), Academic Press, London, 1973, p. 406.

[76] Feugier, A., Second European Symposium on Combustion, Orleans, France, 1-5 September 1979, Vol. I, p. 362.

[77] Feugier, A., in Evaporation-Combustion of Fuels (J.T. Zung, Ed.),
      American Chemical Society, Advances in Chemistry Series 166,
      Washington, DC, 1978, p. 178.

[78] Bulewicz, E.M., Evans, D.G., and Padley, P.J., Fifteenth Symposium
      (International) on Combustion, The Combustion Institute, Pittsburgh,
      1975, p. 1461.

[79] Goodings, J.M., Ng, C-W., and Bohme, D.K., Int. J. Mass Spectr. Ion
      Phys. 29:57-75 (1979).

[80] Friauf, G.F., Jordan, M.E., and Cole, H.M., U.S. Patent 3,413,093,
      November 26, 1968.

[81] Cotton, D.H., Friswell, N.J., and Jenkins, D.R., Combust. Flame
      17:87-98 (1971).

[82] Calcote, H.F. and Miller, W.J., in Reactions Under Plasma Conditions
      (M. Venugopalan, Ed.), Wiley, New York, 1971, Vol. II, p. 327.

[83] Calcote, H.F., in Ion-Molecule Reactions (J.L. Franklin, Ed.),
      Plenum Press, New York, 1972, Vol. 2, p. 673.

[84] Page, F.M., in Physical Chemistry of Fast Reactions, Vol. I, Gas Phase
      Reactions of Small Molecules (B.P. Levitt, Ed.), Plenum Press, London,
      1973, p. 161.

[85] Albers, E.A. and Homann, K.H., Z. Phys. Chem. 58:220-222 (1968).

[86] King, I.R., J. Chem. Phys. 31:855 (1959).

[87] Bulewicz, E.M. and Padley, P.J., Ninth Symposium (International) on
      Combustion, Academic Press, New York, 1963, p. 647.

[88] Sternberg, J.C., Galloway, W.S., and Jones, D.T.L., in Gas Chromatography
      (N. Brenner, J.E. Cullen, and M.D. Weiss, Eds.) Academic Press, London,
      1962, p. 231.

[89] Krejci, J.C. and Johnson, P.H., U.S. Patent 3,240,565, March 15, 1966.

[90] Bredo, M.A., Guillaume, P.J., and Van Tiggelen, P.J., <u>Fifteenth Symposium (International) on Combustion</u>, The Combustion Institute, Pittsburgh, 1975, p. 1003.

[91] Bulewicz, E.M. and Padley, P.J., <u>Ninth Symposium (International) on Combustion</u>, Academic Press, New York, 1963, p. 638.

[92] Arrigoni, V., Cornetti, G.M., Gerbaz, G.P., Giavazzi, G., and Pozzi, U., Society of Automotive Engineers, Automotive Engineering Congress, Detroit, MI, 25 February - 1 March 1974, Paper 740192.

[93] Peeters, J., Lambert, J.F., Hertoghe, P., and Van Tiggelen, A., <u>Thirteenth Symposium (International) on Combustion</u>, The Combustion Institute, Pittsburgh, 1971, p. 321.

[94] Abrahamson, J. and Kennedy, E.R., in <u>Twelfth Biennial Conference on Carbon</u>, Extended Abstracts, American Carbon Society and the School of Engineering, University of Pittsburgh, Pennsylvania State University, 1975, p. 167.

[95] Bowser, R.J. and Weinberg, F.J., <u>Combust. Flame</u> 27:21-32 (1976).

[96] Tsang, W., Bauer, S.H., and Waelbroeck, F., <u>J. Phys. Chem.</u> 66:282-287 (1962).

[97] Cathro, W.S. and Mackie, J.C., <u>J. Chem. Soc. Faraday II</u> 69:237-245 (1973).

[98] Fairbairn, A.R. and Gaydon, A.G., <u>Proc. Roy. Soc. London</u> A239:464-475 (1957).

[99] Fairbairn, A.R., <u>Eighth Symposium (International) on Combustion</u>, Williams and Wilkins, Baltimore, 1962, p. 304.

[100] Hayhurst, A.N. and Kittelson, D.B., <u>Combust. Flame</u> 31:37-51 (1978).

[101] Gaydon, A.G., <u>The Spectroscopy of Flames</u>, Chapman and Hall, London, 2nd ed., 1974, p. 269.

[102] Cowperthwaite, M. and Bauer, S.H., J. Chem. Phys. 36:1743-1753 (1962).

[103] Sodha, M.S. and Gaha, S., Adv. Plasma Phys. 4:219-309 (1971).

[104] Smith, F.T., J. Chem. Phys. 34: 793-801 (1961).

[105] Calcote, H.F., Combust. Flame 1:385-403 (1957).

[106] Sodha, M.S., Sagoo, M.S., Chandra, A., and Ghatak, A.K., J. Appl. Phys. 46:3806-3808 (1975).

[107] Newman, R.N., Page, F.M., and Woolley, D.E., in Evaporation-Combustion of Fuels (J.T. Zung, Ed.), American Chemical Society, Advances in Chemistry Series 166, Washington, DC, 1978, p. 141.

[108] Smith, F.T., J. Chem. Phys. 28:746-747 (1958).

[109] Bates, D.R., Adv. Atom. Molec. Phys. 15:235-262 (1979).

[110] Bolton, H.C. and McWilliam, I.G., Proc. Roy. Soc. London A321:361-380 (1971).

[111] Olson, D.B., Publication in preparation.

[112] Boothman, D., Lawton, J., Melinek, S.J., and Weinberg, F., Twelfth Symposium (International) on Combustion, The Combustion Institute, Pittsburgh, 1969, p. 969.

[113] Taran, E.N., Nesterko, N.A., and Tsikora, I.L., Combustion Institute European Symposium (F.J. Weinberg, Ed.), Academic Press, London, 1973, p. 279.

[114] Miller, W.J., Fourteenth Symposium (International) on Combustion, The Combustion Institute, Pittsburgh, 1973, p. 307.

[115] Olson, D.B. and Calcote, H.F., "Ionic Mechanisms of Soot Nucleation in Premixed Flames," to be published in Particulate Carbon: Formation During Combustion, Proceedings of the General Motors Symposium, Warren, MI, 15-16 October 1980.
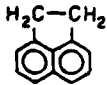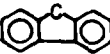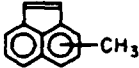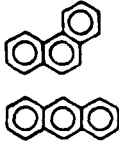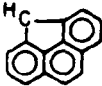
[116] Rosenstock, H.M., Draxl, K., Steiner, B.W., and Herron, J.T., *J. Phys. Chem. Ref. Data* 6 (1977), Supplement No. 1.

[117] Michaud, P., Delfau, J.L., and Barassin, A., "The Positive Ion Chemistry in the Post-Combustion Zone of Sooting Premixed Acetylene Low Pressure Flat Flames," to be published in proceedings of the Eighteenth Symposium (International) on Combustion.

[118] Ausloos, P. and Lias, S.G., in *Ion-Molecule Reactions* (J.L. Franklin, Ed.), Plenum Press, New York, 1972, Vol. 2, p. 707.

[119] McLoughlin, R.G., Morrison, J.D., and Traeger, J.C., *Organic Mass Spectr.* 14:104-108 (1979).

[120] Bowen, R.D. and Williams, D.H., *J. Am. Chem. Soc.* 100:7454-7459 (1978).

TABLE 1

Molecules Observed in Sooting Flames

Polycyclic aromatic hydrocarbons in the combustion products

of turbulent diffusion flames of kerosene and benzene.[a]

From Prado, Lee, Hites, Hoult, and Howard [15].

Molecular Weight	Name	Formula	Structure
116	Indene	C_9H_8	
128	Naphthalene	$C_{10}H_8$	
142	Methylnaphthalene	$C_{11}H_{10}$	
152	Biphenylene	$C_{12}H_8$	
152	Acenaphthylene	$C_{12}H_8$	
154	Biphenyl	$C_{12}H_{10}$	
154	Acenaphthene	$C_{12}H_{10}$	
166	Fluorene	$C_{13}H_{10}$	
166	Methylacenaphthylene	$C_{13}H_{10}$	
168	Methylbiphenyl	$C_{13}H_{12}$	
176	Cyclopent(f,g)acenaphthylene	$C_{14}H_8$	
178	Phenanthrene + Anthracene	$C_{14}H_{10}$	
190	4H-cyclopenta(def)phenanthrene	$C_{15}H_{10}$	

[a]Essentially the same molecules are observed in rich nonsooting premixed

benzene-oxygen flames at 2.67 kPa [18].

48

TABLE 1 (continued)

Molecular Weight	Name	Formula	Structure
192	Methylphenanthrene	$C_{15}H_{12}$	
202	Fluoranthene	$C_{16}H_{10}$	
202	Benzacenaphthylene	$C_{16}H_{10}$	
202	Pyrene	$C_{16}H_{10}$	
204	2-phenylnaphthalene	$C_{16}H_{12}$	
216	Benzofluorene	$C_{17}H_{12}$	
216	Methylfluoranthene + Methylpyrene	$C_{17}H_{12}$	
226	Benzo(ghi)fluoranthene	$C_{18}H_{10}$	
226	Cyclopenta(cd)pyrene	$C_{18}H_{10}$	
240	Methylcyclopenta(cd)pyrene	$C_{19}H_{12}$	
252	Benzofluoranthene	$C_{20}H_{12}$	

TABLE 1 (continued)
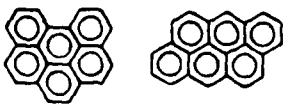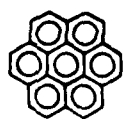
Molecular Weight	Name	Formula	Structure
252	Benzo(e)pyrene	$C_{20}H_{12}$	
	+		
	Benzo(a)pyrene		
252	Perylene	$C_{20}H_{12}$	
276	Indeno(1,2,3-cd)pyrene	$C_{22}H_{12}$	
276	Benzo(ghi)perylene + Anthanthrene	$C_{22}H_{12}$	
300	Coronene	$C_{24}H_{12}$	

TABLE 2

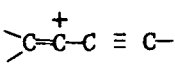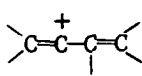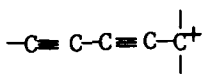Ions Observed in Sooting Acetylene-Oxygen Flames [13,17]
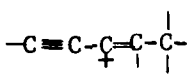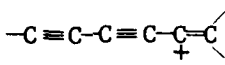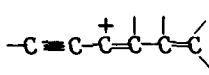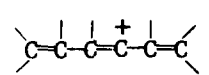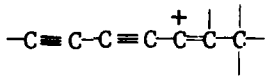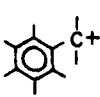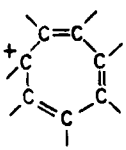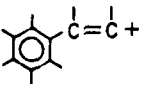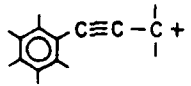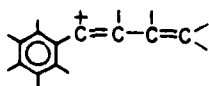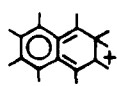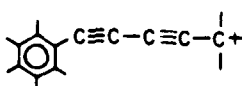
Molecular Weight	Formula	Suggested Structure
39	$C_3H_3^+$	(cyclopropenyl cation structure)
51	$C_4H_3^+$	$>C=\overset{+}{C}-C \equiv C-$
53	$C_4H_5^+$	$>C=\overset{+}{C}-C=C<$
63	$C_5H_3^+$	$-C \equiv C-C \equiv C-\overset{+}{C}<$
65	$C_5H_5^+$	$-C \equiv C-\underset{+}{C}=C-C-$
75	$C_6H_3^+$	$-C \equiv C-C \equiv C-\underset{+}{C}-C<$
77	$C_6H_5^+$	$-C \equiv C-\overset{+}{C}=C-C=C<$
79	$C_6H_7^+$	$>C-C-C=\overset{+}{C}-C=C<$ or (cyclohexadienyl cation)
89	$C_7H_5^+$	$-C \equiv C-C \equiv C-\overset{+}{C}-C-C-$
91	$C_7H_7^+$	(benzyl cation) or (tropylium cation)
103	$C_8H_7^+$	(phenyl-C=C+)
115	$C_9H_7^+$	(phenyl-C≡C-C+)
129	$C_{10}H_9^+$	(phenyl-C=C-C-C=C) or (naphthalene cation)
139	$C_{11}H_7^+$	(phenyl-C≡C-C≡C-C+)
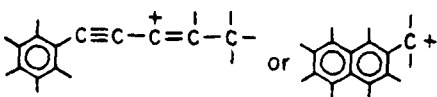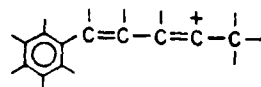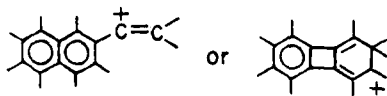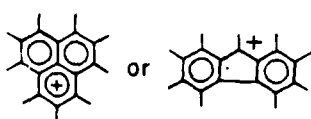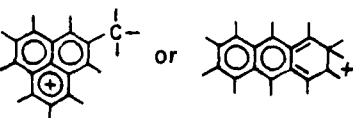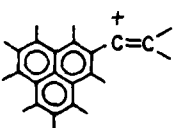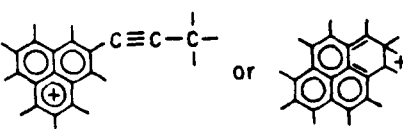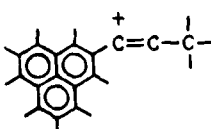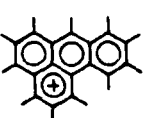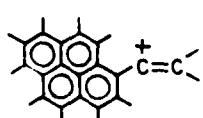
TABLE 2 (continued)

Molecular Weight	Formula	Suggested Structure
141	$C_{11}H_9^+$	C≡C−C⁺=C−C−C− or C⁺
143	$C_{11}H_{11}^+$	C=C−C=C⁺−C−
153	$C_{12}H_9^+$	C⁺=C< or ⁺
165	$C_{13}H_9^+$	⊕ or ⁺
179	$C_{14}H_{11}^+$	C− or ⁺
191	$C_{15}H_{11}^+$	C⁺=C<
203	$C_{16}H_{11}^+$	C≡C−C− or ⁺
205	$C_{16}H_{13}^+$	C⁺=C−C−
215	$C_{17}H_{11}^+$	⊕
227	$C_{18}H_{11}^+$	C⁺=C<

TABLE 2 (continued)
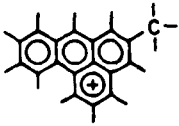
Molecular Weight	Formula	Suggested Structure
229	$C_{18}H_{13}^{+}$	
239	$C_{19}H_{11}^{+}$	

Table 3

Comparison of Thermodynamic and Experimental Equivalence Ratios

and Temperatures for Soot Formation

Premixed Bunsen burner flames at 1 atm.

Soot is assumed to be graphite.

The experimental temperature is the adiabatic flame temperature

corresponding to the measured ϕ_c.

	Thermodynamic		Experimental		Departure from Equilibrium	
	ϕ_c	T, K	ϕ_c	T, K	ϕ_{Th}/ϕ_{exp}	T_{exp}/T_{Th}
Acetylene	2.5	2140	2.05	2380	1.3	1.1
Benzene	2.5	1350	1.55	2200	1.6	1.6
n-Hexane	2.8	1100	1.63	1850	1.7	1.7

Figure Captions

Fig. 1. Growth from primary molecular species to soot aggregation, assuming ions as the nucleating agent.

Fig. 2. Typical sooting flame on a flat flame burner.

Fig. 3. Flame temperature and C_2, CH, and OH emission. Emission intensities from Bonne, Homann, and Wagner [28]. Temperature measurement by Bonne and Wagner [29] by Na-line reversal. Tompkins and Long [22] report T about 500 K lower at $\phi = 3.75$.

Fig. 4. Increase in soot and charged particle diameters. Bonne, Homann, and Wagner (BHW) [28]. Prado and Howard (PH) [5] at $\phi = 3.0$. The "soot" curve is an average with the original data defining the cross-hatched area of uncertainty.

Fig. 5. Mass concentration of soot and large molecules. "Total polymeric material" and "PCAH" from Tompkins and Long [22], $\phi = 3.75$, u = 31 cm s^{-1}; "soot" curve is average of Wersborg, Yeung, and Howard (WYH) [11], $\phi = 3.0$ (volume concentration converted to mass assuming $\rho = 1.5$ g cm^{-3}) and Bonne, Homann, and Wagner (BHW) [28] (mass fraction converted to mass concentration). "Large molecules" curve is average of Wersborg et al. [11], $\phi = 3.0$ (volume concentration converted to mass concentration assuming $\rho = 1.5$ g cm^{-3}) and Bonne et al. [28] (mass fraction converted to mass concentration) (see also Ref. 39).

Fig. 6. Concentration profiles. O_2, CO, C_2H_2, H_2O, $C_{14}H_8$, and "precursors" from Homann and Wagner [16,33]; C_4H_2, C_6H_2, C_8H_2 from Bonne, Homann, and Wagner [28]; large positive ions and charged soot particles from Prado and Howard [5], $\phi = 3.0$, u = 38 cm s^{-1}; ions, 300-1000 amu from Olson and Calcote [17];determination of curve shape by mass spectrometry, concentration estimated by comparison of results with Prado et al. [5], Delfau et al. [13], and

Wersborg et al. [11] (see discussion following Ref. 17); soot number density

below 3.5 cm from Wersborg, Yeung, and Howard [11], ϕ = 3.0, u = 50 cm s^{-1}. Bonne

et al. [28] soot $\stackrel{\text{number densities}}{\wedge}$continue to rise to 6 x 10^{11} cm^{-3} at 2.8 cm. Above 3.5 cm

the data of above two groups, which were very close, have been averaged.

Fig. 7. Concentration profiles for ϕ = 2.4. Data from Homann and Wagner [30].

u = 50 cm s^{-1}, p = 2.7 kPa.

Fig. 8. Size distribution of charged and neutral particles.

Charged Particles	Neutral Particles
ϕ = 2.25	ϕ = 3.0
u = 31 cm s^{-1}	u = 50 cm s^{-1}

Distance above burner indicated above each curve. Charged particle data from

Wersborg, Yeung, and Howard [11]; neutral particle data from Wersborg, Howard,

and Williams [42]; data normalized so area under each curve is 100%. Charged

species measured by determining electric current to a Faraday cage in the

detection chamber of a molecular beam flame sampling instrument. Neutral parti-

cles determined by electron $\stackrel{\text{microscopic}}{\wedge}$ analysis of beam deposits collected in

same sampling instrument used for charged particles.

Fig. 9. Ionization potential or work function for large molecules and small

particles. Assumes: Particle density = 1.5 g cm^{-3}; for planar disc assumed

$d = \left(\dfrac{20.4 \times 10^{-20} \times N}{\pi} \right)^{1/2}$ where N = number of polycyclic hexagonal rings. The

20.4 is 4 x area of ring (in 10^{-20} m^2 units) which is taken as 5.1; it is

5.24 for graphite or 5.02 for benzene. 1 eV = 0.160 aJ.

Fig. 10. Comparison of calculated (equilibrium) and experimental charged

particle number density.

Fig. 11.   Ionic mechanism of incipient soot formation.

Fig. 12.   Effect of equivalence ratio on peak ion currents for 2.0 kPa acetylene-oxygen flames.   The shaded area indicates the minimum equivalence ratio for soot formation.   From Ref. 115.
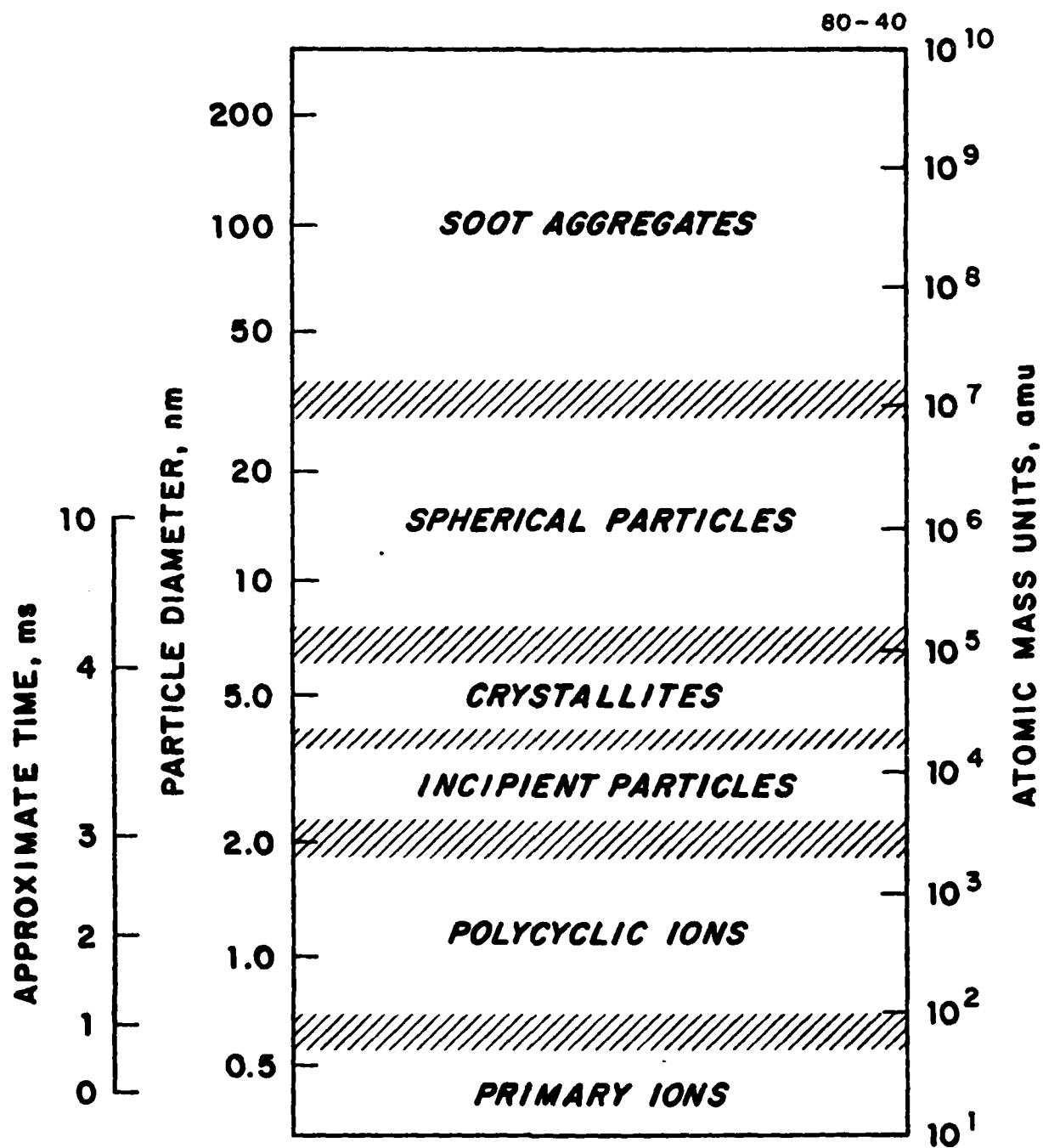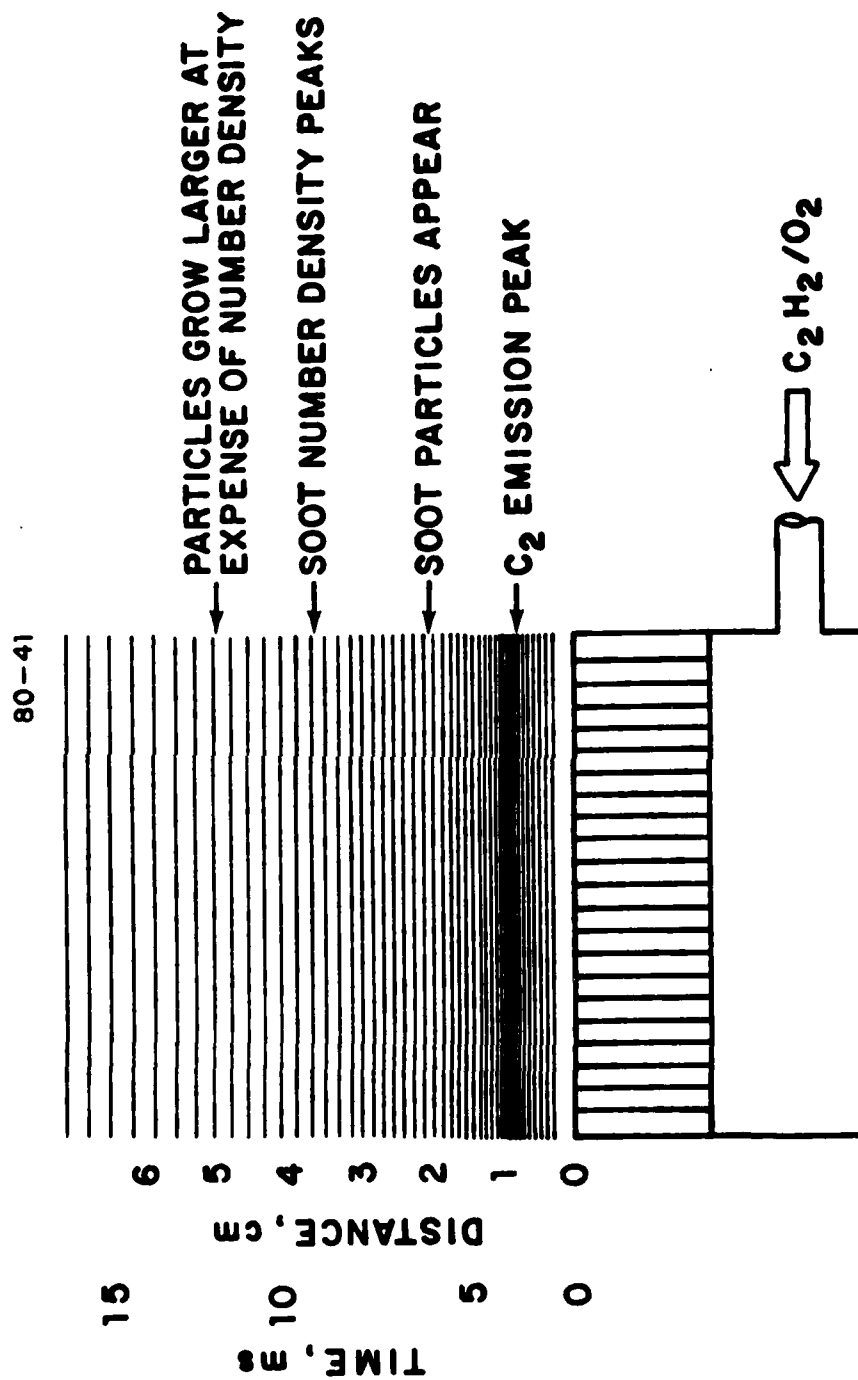
80-40

SOOT AGGREGATES

SPHERICAL PARTICLES

CRYSTALLITES

INCIPIENT PARTICLES

POLYCYCLIC IONS

PRIMARY IONS

APPROXIMATE TIME, ms

10
4
3
2
1
0

PARTICLE DIAMETER, nm

200
100
50
20
10
5.0
2.0
1.0
0.5

ATOMIC MASS UNITS, amu

10^{10}
10^{9}
10^{8}
10^{7}
10^{6}
10^{5}
10^{4}
10^{3}
10^{2}
10^{1}

Figure 1

58

Figure 2

80-42

Figure 3

60

Figure 4

61

Figure 5

Figure 6

Figure 7

Figure 8

80-46

65

Figure 9

Figure 10

67
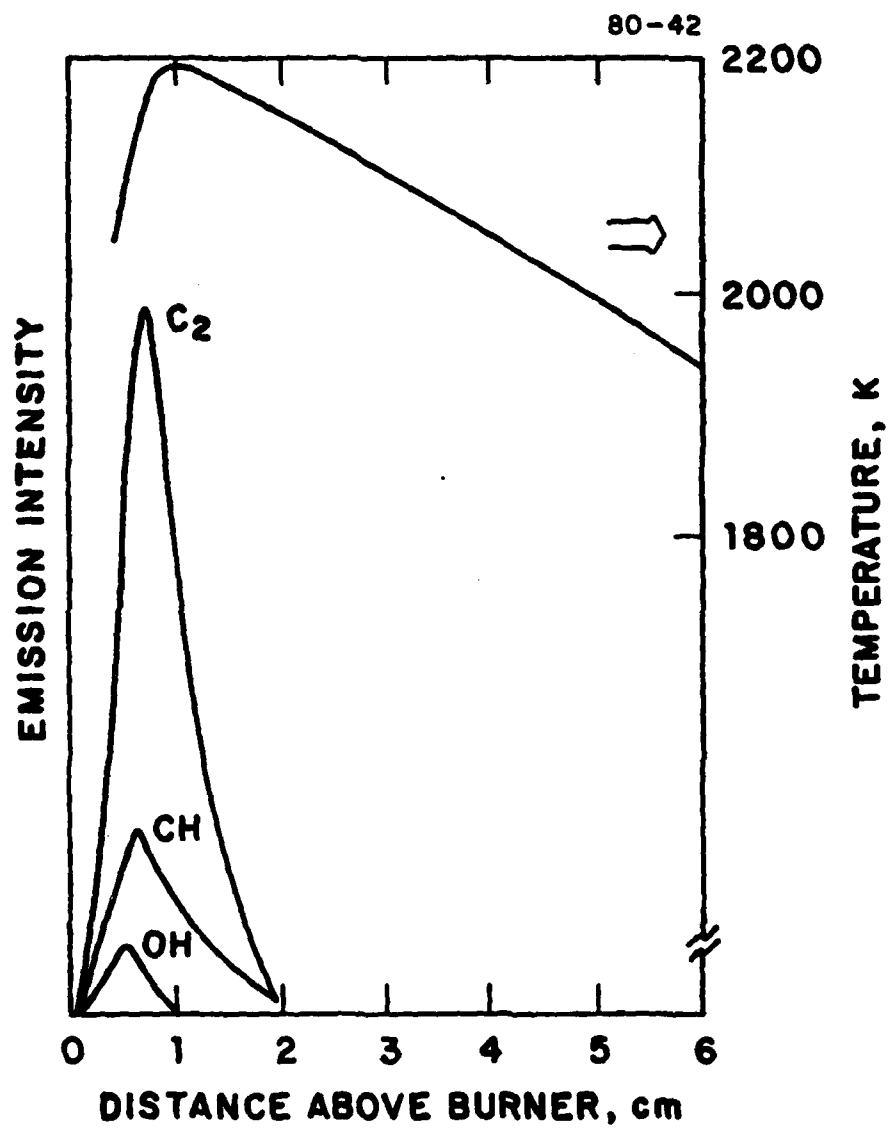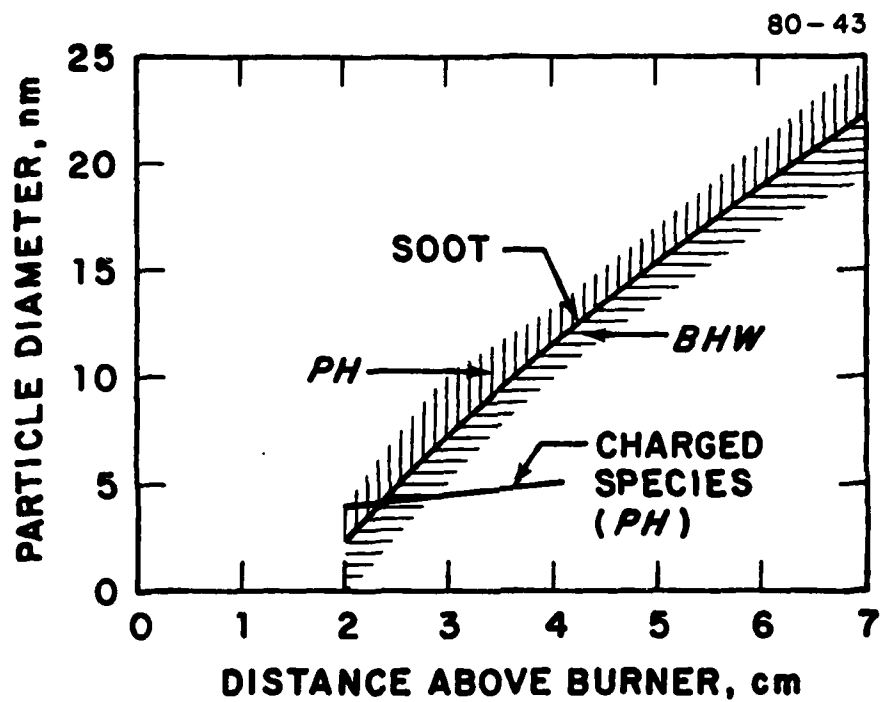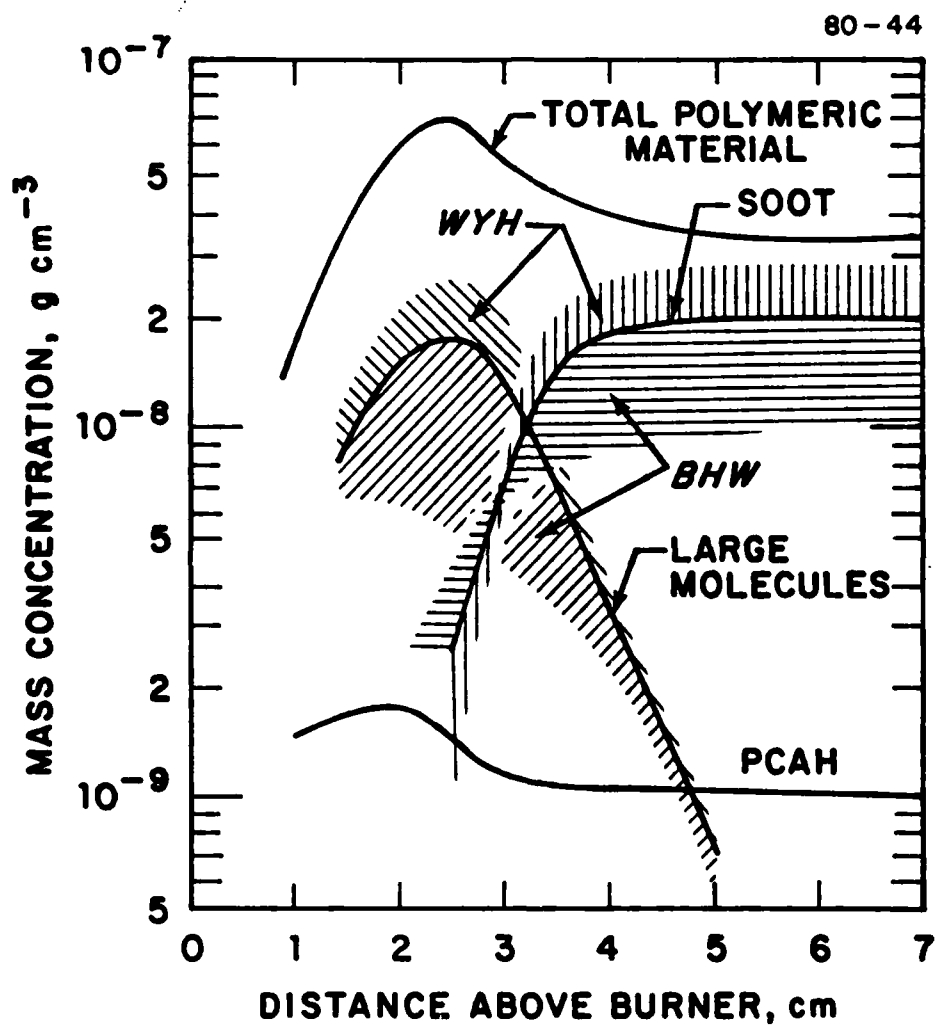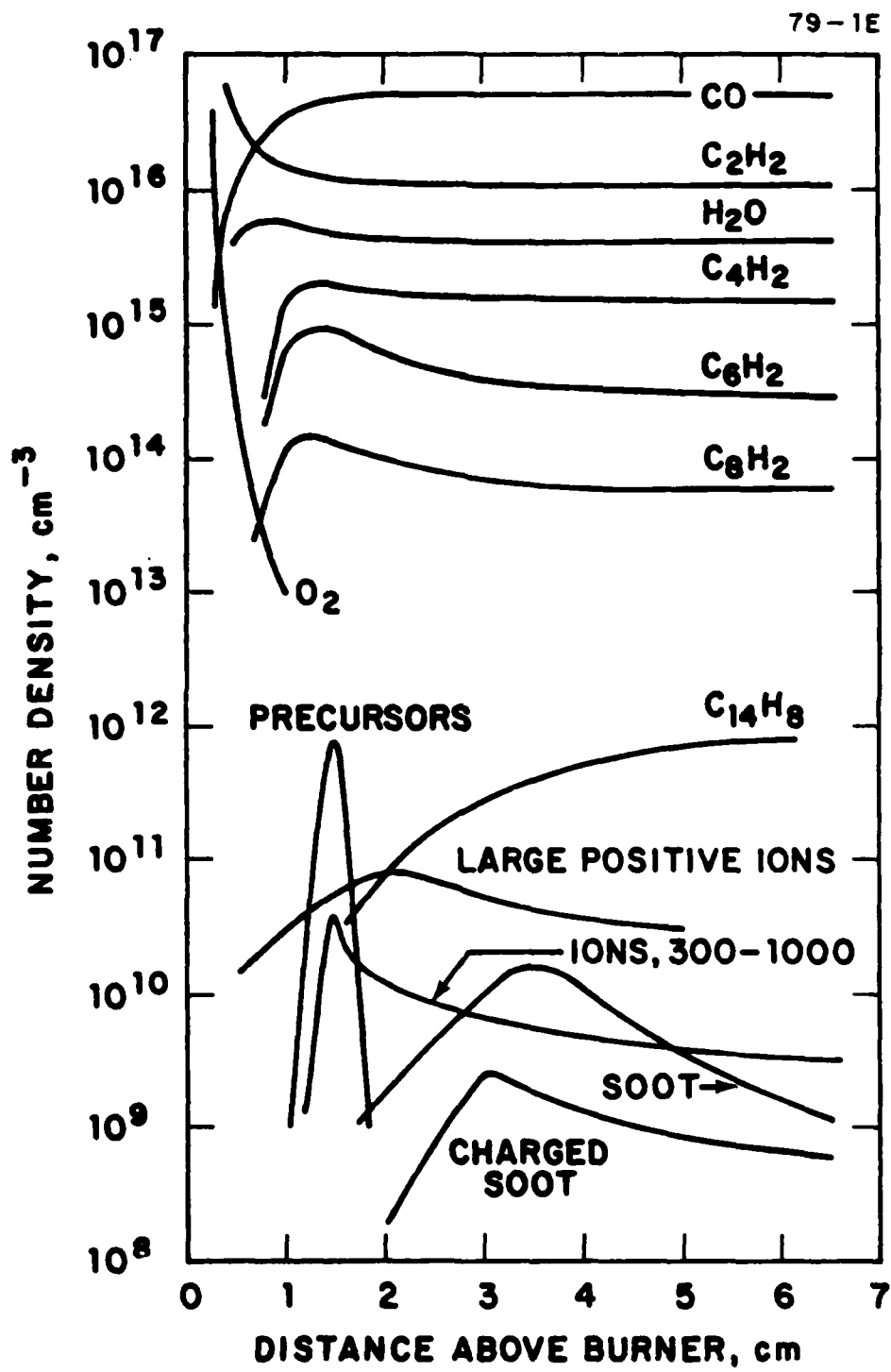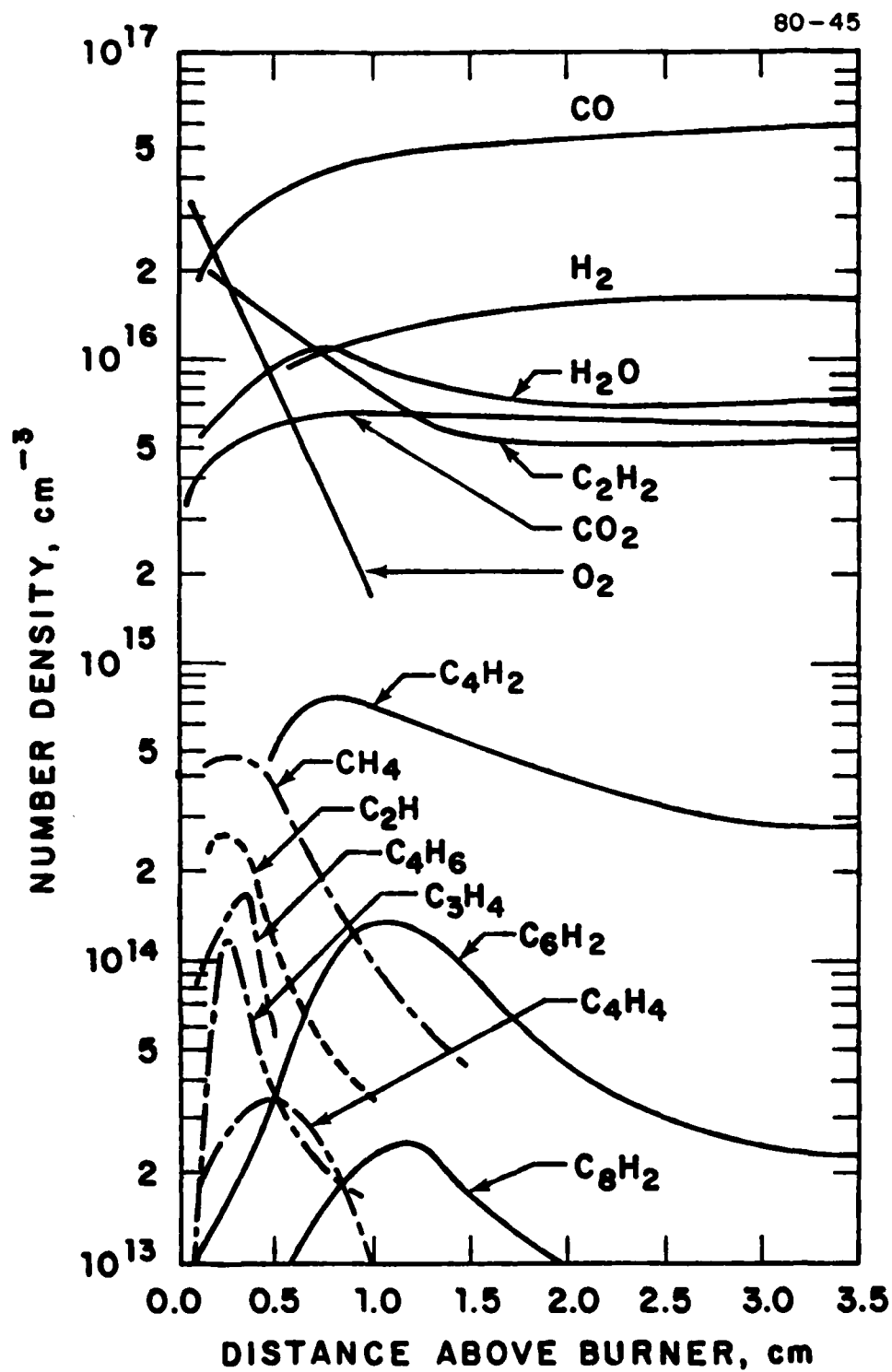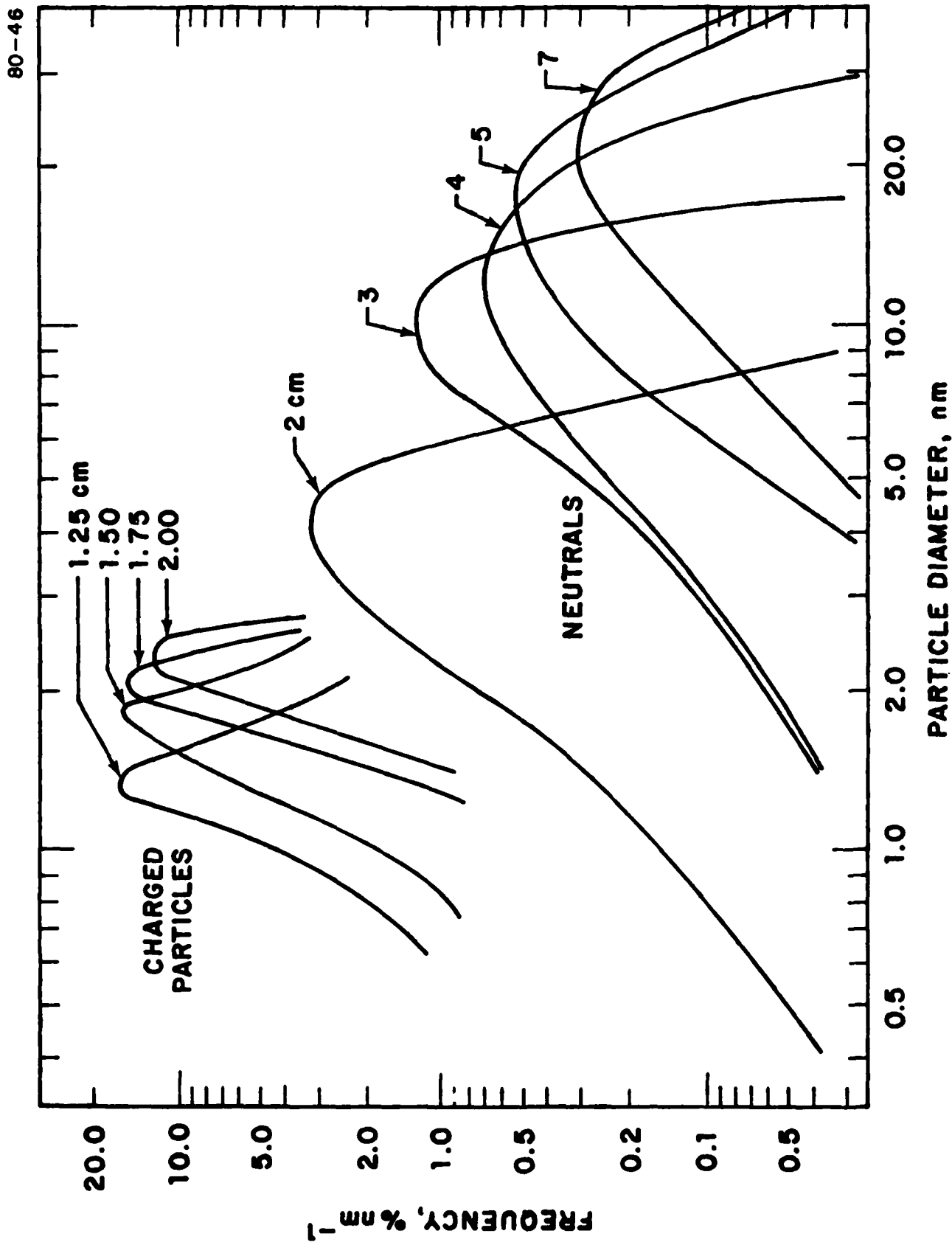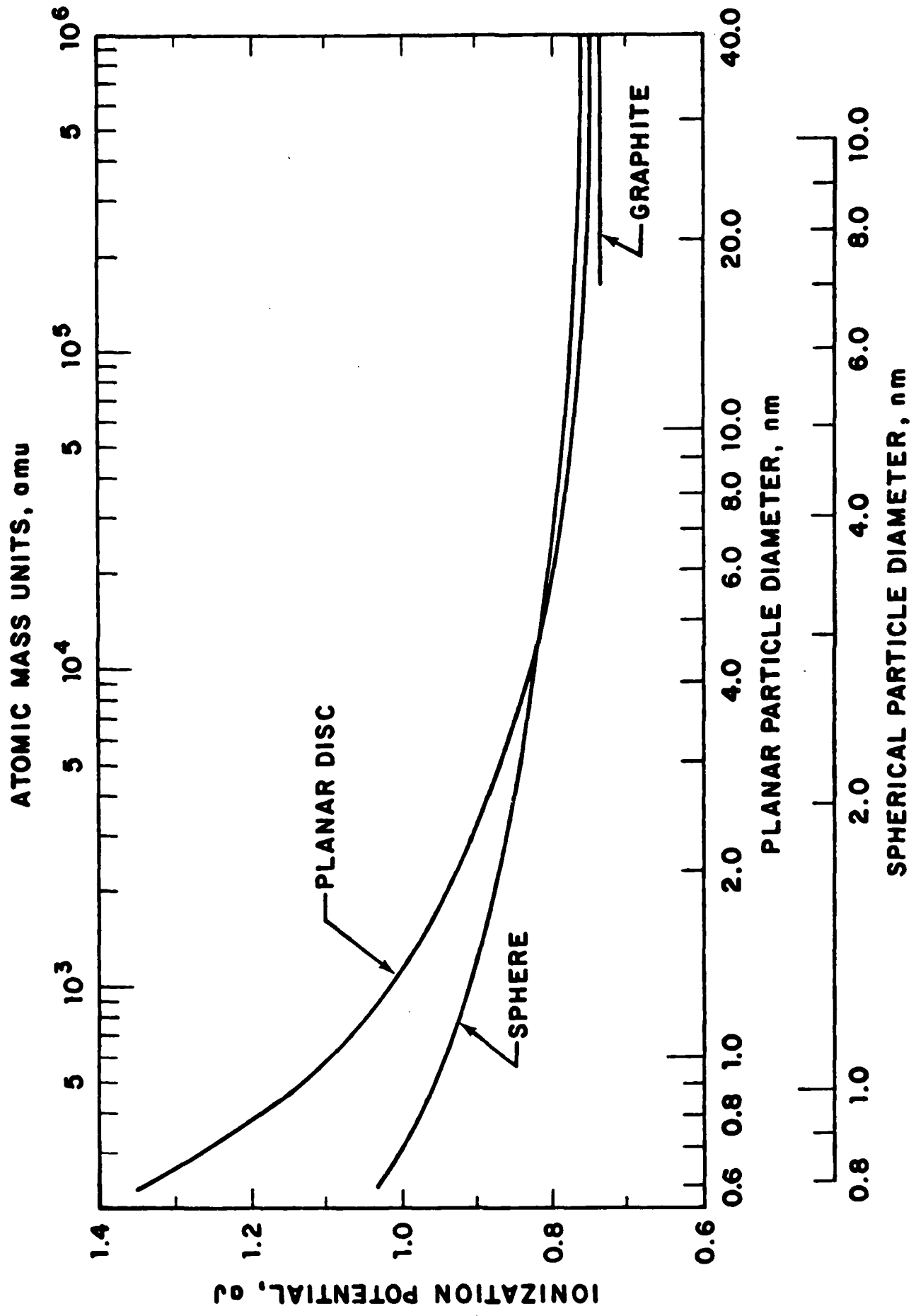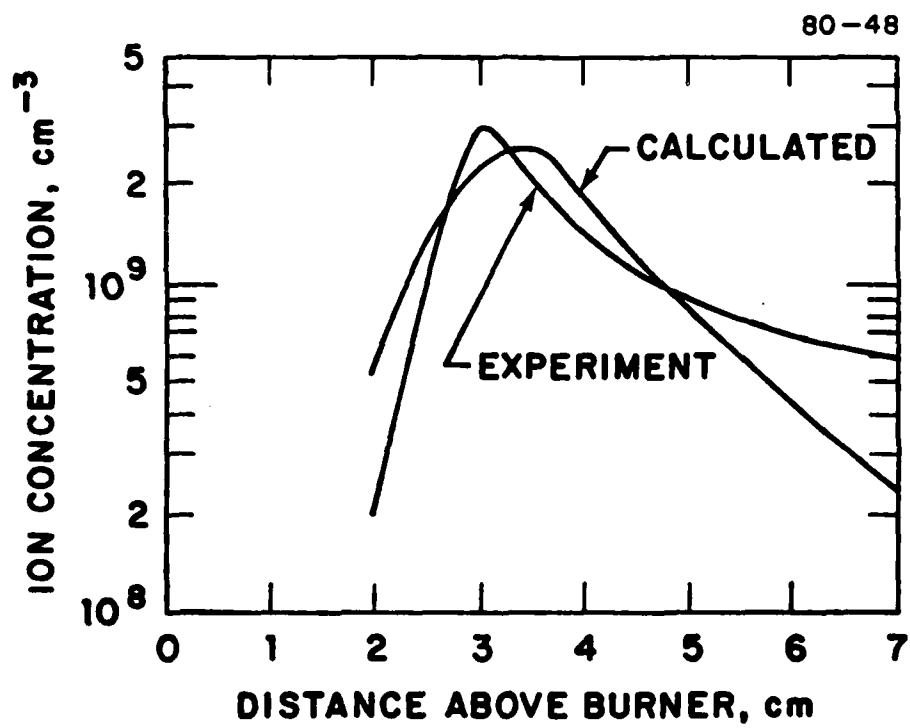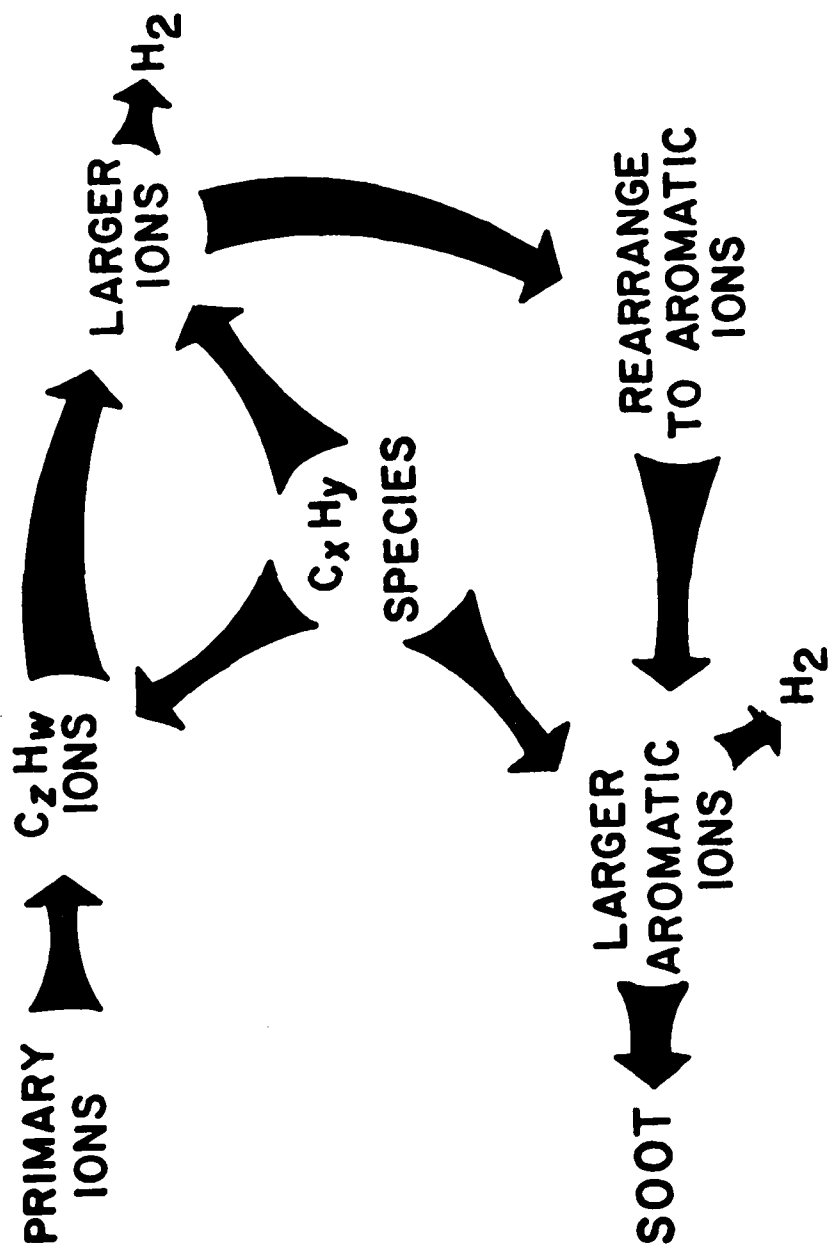
Figure 11

Figure 12

69
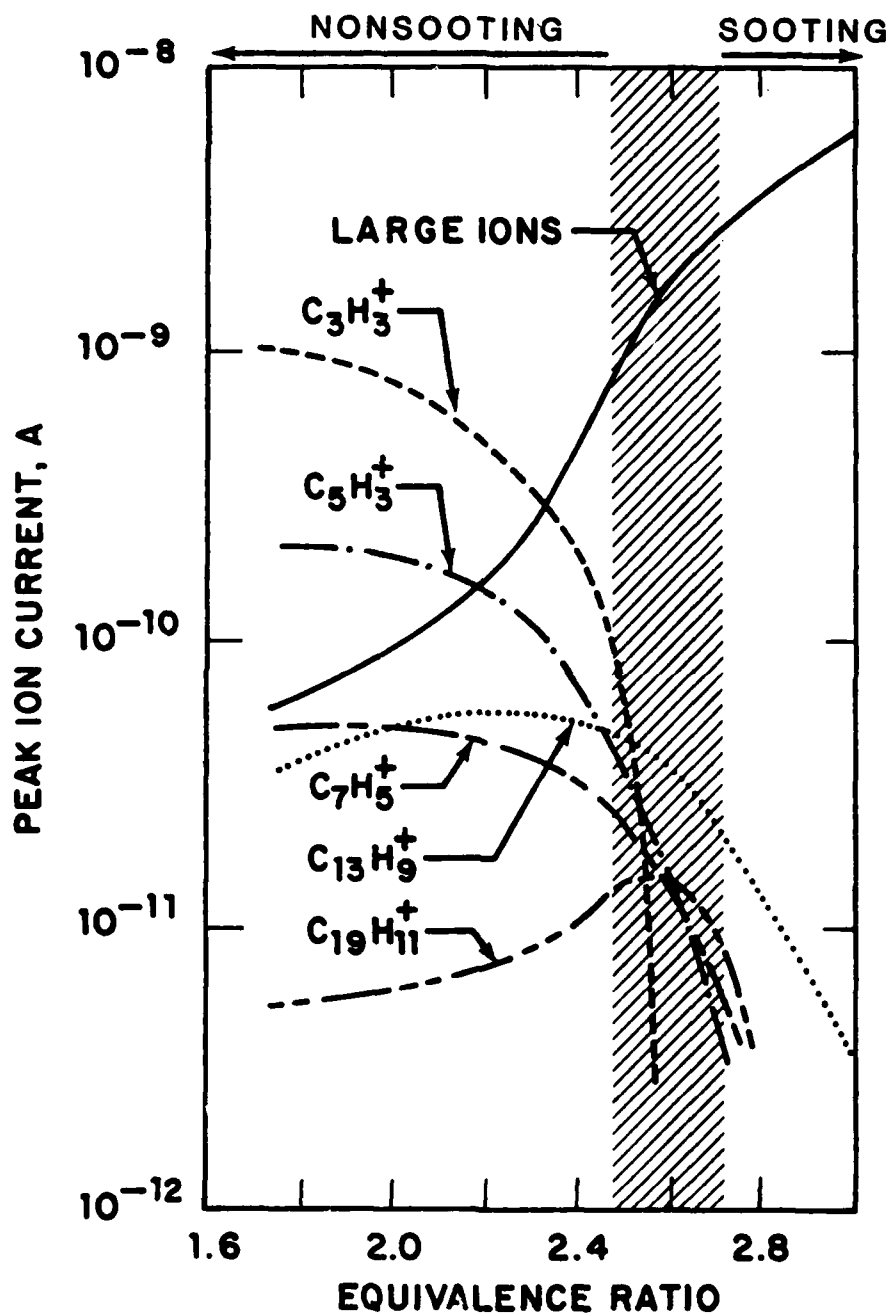
APPENDIX B

IONS IN FUEL-RICH AND SOOTING ACETYLENE AND BENZENE FLAMES

D.B. Olson and H.F. Calcote

AeroChem Research Laboratories, Inc.
P.O. Box 12
Princeton, New Jersey 08540

ABSTRACT

Mass spectrometric measurements of flame ion concentration profiles have been made in low pressure rich and sooting acetylene/oxygen and benzene/oxygen flames. As both flames are made richer and approach sooting the predominant ion $C_3H_3^+$ is replaced by large positive aromatic ions with mass greater than 300. The profile of these ions corresponds with a previously identified class of "soot precursor" species. Similarities and differences between the ion spectra in the two flames are discussed along with possible reasons for dual maxima in individual ion concentration vs distance profiles observed in sooting flames.

The data are consistent with an ionic mechanism of soot nucleation.

I. INTRODUCTION

The formation of soot in combustion of hydrocarbon fuels has received much attention, yet the basic chemical processes controlling the transition from gas-phase species to parti les remain unclear. In a recent review of the mechanism of soot formation in flames[1] the evidence was assembled for an ionic nucleation mechanism based upon chemi-ions. The chemi-ions CHO^+ and $C_3H_3^+$ were the key to the initial growth of molecular species to large polycyclic aromatic ions which ultimately became incipient soot particles. Detailed steps in the process were suggested. It is thus important to understand the ion chemistry of fuel-rich flames in order to verify this process and to explain the key chemical steps to soot formation. We here report mass spectrometric measurements of ion concentration profiles in fuel-rich and sooting low pressure premixed acetylene- and benzene-oxygen flames. Acetylene was chosen for study because it is the most extensively studied sooting flame so our results can be compared to previous data to obtain a detailed picture of the process. Benzene with the same C/H ratio was chosen as representative of aromatic substances whose tendency to soot is markedly greater than aliphatic substances and because aromatic substances will be important as "new fuels". It should be noted that acetylene is unique in having a very low tendency to soot in premixed flames, so from that point represents a poor choice. More typical hydrocarbons will be studied in future work.

Many similarities and some distinct differences are found between the two flames; the basic trend being the predominance of $C_3H_3^+$ in non-sooting flames with large aromatic ions growing in concentration very rapidly as the critical equivalence ratio, ϕ_c, for sooting is approached.

In the benzene flame front oxygen-containing aromatic ions are also observed but downstream the ions in acetylene and benzene flames are the same. Ions with $300 <$ mass $\gtrsim 1000$ amu become dominant very early in both flames at ϕ_c.

II. EXPERIMENTAL

The low pressure flame apparatus and ion sampling quadrupole mass spectrometer, shown in Fig. 1, have been described previously.[2] Briefly, the flames were stabilized on a 12 cm diam flat flame burner and were surrounded by a fuel-rich annular shield flame 16 cm in diam to prevent air or combustion product entrainment. Gases were controlled using critical flow orifices while benzene was metered by a syringe pump. The liquid benzene was sprayed into a flash evaporator and the vapor fed to the burner-mixing chamber through heated lines. The mass spectrometer sampling cone was constructed from 316 stainless steel with a 90° outer angle and a 0.25 mm orifice. Ion profiles through the flame were obtained by moving the burner with respect to the mass spectrometer sampling cone.

The majority of the results were obtained from acetylene/oxygen and benzene/oxygen flames at 2.0 kPa (15 Torr) although some work was performed at 2.7 kPa (20 Torr). The unburned gas velocity at the burner was 50 cm s^{-1} in all the work reported here. Detailed individual ion species profiles were measured for masses up to 300 at equivalence ratios above and below the critical equivalence ratio, ϕ_c, for soot formation as determined by the appearance of the yellow-orange continuum soot emission. In addition, the spectrometer was operated as a high-pass mass filter and profiles were recorded of ions with mass larger than 300 up to the cutoff of the filter, estimated to be about mass 1000. Ion current data from high-pass operation of the filter are not directly comparable to individual mass profiles

3

because the throughput of the instrument is much greater when acting as a
high-pass mass filter. Ion currents are reported instead of ion concentra-
tions because of the difficulties in quantitatively and reproducibly
calibrating the instrument.

III. RESULTS

Representative ion spectra from rich non-sooting acetylene and benzene
flames are shown in Fig. 2 taken at a distance of 1 cm from the burner
surface in the blue-green reaction zone which extends from about 0.5 to
1.5 cm. These data are from a $\phi = 2.0$ acetylene flame ($\phi_c = 2.7$) and a
$\phi = 1.8$ benzene flame ($\phi_c = 1.85$). The essential features for the acetylene
spectrum are the high concentration of $C_3H_3^+$ and the following series of
peaks spaced evey 13 or 14 mass units. Only odd number ion masses are
observed while for neutral species sampled from sooting flames the number
of hydrogens is even.[1] Other large peaks, for example mass = 63, 91, and
165, correspond to $C_5H_3^+$, $C_7H_7^+$, and $C_{13}H_9^+$. In these rich flames H_3O^+,
the dominant ion in near stoichiometric flames, is observed only at low
concentrations not visible on the scale of Fig. 2.

Figure 2 shows ions characteristic of the early benzene oxidation zone.
The spectrum is atypical in that beyond the flame zone the observed mass
spectrum rapidly becomes very similar to that observed in the acetylene
flame. Unique peaks are observed at mass 95, 109, 131, etc., with only a
small amount of mass 39, although further downstream at 2 cm from the
burner the concentration of $C_3H_3^+$ dominates the spectrum. These unique
benzene ions are identified as oxygen-containing aromatic species $C_6H_7O^+$,
$C_7H_9O^+$, $C_9H_7O^+$, etc. Notable is the lack of species smaller than C_6
indicating little ring opening has occurred at this time.

Figures 3 and 4 show additional data for these same two flames in the
form of concentration profiles vs distance from the burner surface for
selected important species and the $300 < $ mass $\lesssim 1000$ group identified as
ions > 300. Note in Fig. 3 the early appearance of mass 165, 239, and
> 300 ions in addition to mass 39. The equivalence ratio of this flame
was considerably below the critical equivalence ratio at the sooting point
($\phi = 2.0$ vs $\phi_c = 2.7$). Similar data are shown in Fig. 4 for a benzene
flame just below the critical equivalence ratio for soot formation
($\phi = 1.80$ vs $\phi_c = 1.85$). Several profiles show dual maxima; the first
in the flame front and the second just beyond the point where soot emission
is first observed visually. This dual peak behavior is characteristic of
both fuels near and beyond sooting with the same ions occurring in both
peaks. Delfau, Michaud, and Barassin[3] have observed similar dual peaked
behavior with small ions dominating the first peak and large ions dominating
the second peak.

The dramatic increase in large ion concentration at the expense of
smaller ions is the most significant change that occurs in the mass spectra
as the flames are made increasingly richer and finally produce soot.
Figure 5 shows the profiles for the > 300 group of ions from six acetylene
flames. A hundredfold greater peak concentration is obtained in a $\phi = 3.0$
flame compared to the $\phi = 1.75$ flame, accompanied by a corresponding
decrease in total concentration of small ions (determined separately using
bandpass operation of the mass spectrometer, 13-300 amu). The total ion
concentration remains nearly constant (within a factor of two--the
precision of the measurements) over the wide range of equivalence ratios
investigated. Figure 5 also demonstrates the decay of the first ion peak
and the growth of the second ion peak as soot is produced. It should be

5

remarked that soot does not form--by visual observation of the well known yellow appearance--abruptly in acetylene flames but rather slowly over a range of equivalence ratios of 2.5 to 2.7. In benzene the appearance of soot as the equivalence ratio is increased is very sudden and very reproducible.

The variation in peak ion concentrations as a function of equivalence ratio for the two fuels is shown in Figs. 6 and 7. The absolute currents, and thus concentrations, for ions > 300 and the other ions are not directly comparable. We find it significant that at the soot point, indicated in the figures, the large ion concentration, i.e., > 300 amu, reaches the same level in both flames even though the equivalence ratios at which this occurs are very different for the two fuels.

IV. DISCUSSION

The ion profiles of acetylene and benzene flames exhibit many similarities and some distinct differences. The basic trend is for $C_3H_3^+$ (mass 39) to dominate in rich non-sooting flames with larger species becoming increasingly more important as the soot point is approached by increasing the equivalence ratio. In a strongly sooting flame (yellow-orange in color) these ions are replaced by ions with mass > 300. The most important species in addition to $C_3H_3^+$ are masses 63, 65 ($C_5H_3^+$, $C_5H_5^+$), 89, 91 ($C_7H_5^+$, $C_7H_7^+$), 165 ($C_{13}H_9^+$), and 239 ($C_{19}H_{11}^+$). Table I shows the species observed at two positions in each flame, corresponding nominally to first and second peak compositions. In addition, a suggested structure for each ion is given; the mass spectrometer only identifies the mass but in most cases there is little choice in what the structure might be. First looking at the non-oxygen-containing ions, the small ions other than $C_3H_3^+$ have C/H

ratios corresponding to molecules with conjugated double or triple bonds.
For C_6 and larger species aromatic structures become more and more dominant.
Aromatic structures are chosen because of their greater stability over
other structures and the propensity of ions to rapidly rearrange to the more
stable structures. Beyond C_{10} fused ring structures are observed.

The ions observed in the second peak, i.e., at about 2 cm in the
benzene flame are very similar to those observed in acetylene. The spectrum
at 1 cm is strikingly different; each of the unique ions in the benzene
flame contains an oxygen atom. Other flame studies[4,5] have identified
C_6H_6O as a neutral intermediate in rich benzene flames present in signifi-
cant concentration. It is difficult to speculate on the mechanism of
formation of ions in benzene flames because so little is known about benzene
combustion including the identity of the reaction which fractures the ring
structure. Nevertheless some of the unique ions can be accounted for as
follows:

$$C_6H_6O + CHO^+ \rightarrow C_6H_7O^+ + CO$$
$$95 \text{ amu}$$

$$C_6H_6O + C_3H_3^+ \rightarrow C_9H_7O^+ + H_2$$
$$131$$

$$C_9H_7O^+ + C_2H_2 \rightarrow C_{11}H_9O^+$$
$$157$$

$$C_9H_7O^+ + C_4H_2 \rightarrow C_{13}H_9O^+$$
$$181$$
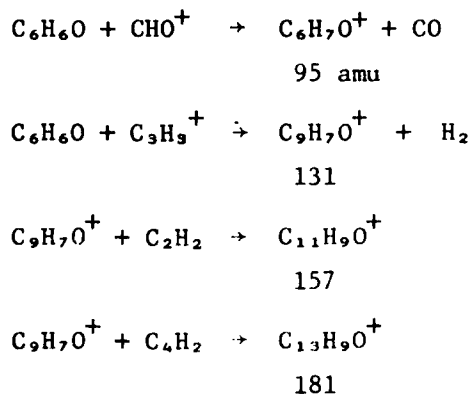
A mechanism which explains the essential features of the ion spectra
observed in the C_2H_2 flame has been formulated. The primary ions are
assumed to be formed by the usual flame chemi-ionization reactions

$$CH + O = CHO^+ + e^-$$

$$CH^* + C_2H_2 = C_3H_3^+ + e^-$$
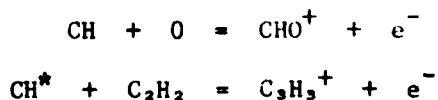
followed by rapid charge transfer from CHO^+ to H_2O to give H_3O^+ or by

several reaction paths from CHO^+ to give additional $C_3H_3^+$.[6] If $C_3H_3^+$ is

allowed to grow by reaction with only the three major neutral species,

C_2H_2, C_2H_4, and C_2H, the following sequence of reactions would occur:

$$C_3H_3^+ + \begin{cases} C_2H_2 & \rightarrow & C_5H_5^+ & \quad 65 \text{ amu} \\ C_4H_2 & \rightarrow & C_7H_5^+ & \quad 89 \\ C_2H & \rightarrow & C_5H_3^+ + H & \quad 63 \end{cases}$$
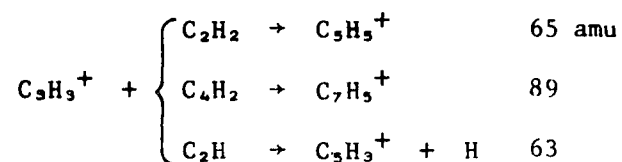
followed by continuing reaction of C_2H, C_2H_2, and C_4H_2 with the above

product ions and with each subsequently produced ion. Only exothermic

reactions in the forward direction are considered. If this type of addition

to the ions is continued with all rates assumed equal then the ion distri-

butions would be dependent upon the concentrations of C_2H_2, C_4H_2, and C_2H

(assumed to be 100:10:1)[7] and the number of reaction channels. Several

observed features are predicted by this mechanism: large concentrations of

the 89-91 and 63-65 pairs; higher concentrations of 103, 115, 129, and 153

than 101, 113, 127, and 151; and mass 165 being the main ion larger than

$\approx$ 110. Obviously this is only a preliminary argument. More detailed and

quantitative calculations are needed to establish whether this type of

mechanism can ultimately lead to soot formation.

The reason for the double peaks is not clear. They do not appear to

be an experimental artifice. The second peak arises further downstream

than the leaner mixture first peak and includes the same ion species as the

first peak. It is not just a shift in location. The total number of

charged species is not significantly larger when the second peak appears;

it may increase slightly, the data are not that definitive because of an

unknown variation in mass spectrometer throughput with mass. Flames with

dual maxima are always sooting or near sooting and therefore contain particles

which can be thermally ionized if they are larger than mass 10^4 or so[1] for these specific flames. These, however, are not the species being observed, and charge transfer from a small charged particle, P^+, to a molecular or radical species, M

$$P^+ + M = M^+ + P$$

is unlikely since the ionization potential of the molecule is higher than that of the particle. Also the ions contain an odd number of hydrogens and the neutral species observed[8] contain an even number of hydrogens. Alternatively the process

$$PH^+ + M = MH^+ + P$$

is thermodynamically unfavored but cannot be completely eliminated at this time. The observed ions are the same in the first and second peaks; not what would be expected from radically different production processes. One possible explanation would be a reduced loss rate of ions leading to a secondary increase in concentration. Since $C_3H_3^+$ and the neutral building blocks are still present at high concentrations at the second peak, the ion growth processes are still producing larger ions. If the rate of ion recombination was suddenly reduced by electron attachment to particles, a second rise in species concentration would occur. There is some evidence that only positively charged particles are present,[9,10] but the data may not be applicable to the flame front, and even downstream we think it is very possible that a significant concentration of negative particles, less than the concentration of positive particles, could have been overlooked. In a recent paper Homann[11] reported the presence of both negatively charged ions and particles in similar flames.

The sudden appearance and disappearance of "ions > 300" in the flame front, e.g., Fig. 3, followed by ions of lower mass, which must be

9

intermediates in forming "ions > 300," appears to be incongruous. The

formation of these large ions so early in the flame front implies extremely

rapid ion-molecule reactions--a basic tenet of our argument. The rapid

decay of this group of large ions, presumably due to ion-electron recombination

or oxidation--leaving a smaller ion--and the persistence of smaller ions,

can be interpreted as a decrease in the availability of building blocks

necessary for sustaining the > 300 ions downstream. The smaller ions can

continue to be formed from $C_3H_3^+$. More quantitative data on absolute ion

concentrations will be required to test this interpretation. We are in

the process of obtaining such data.

The data obtained in this study are consistent with a mechanism for

soot formation in which chemi-ions are the precursors of soot in spite of

the unexplained observations mentioned above. We find large ions formed

early in non-sooting rich flames and see their concentrations fall very

rapidly. In near sooting flames the concentration of these species remains

high and there is an abrupt change from small ions to large ions. It is

difficult to explain these ions as resulting from the soot particles or the

transfer of protons from chemi-ions such as $C_3H_3^+$ to large molecules being

formed in a neutral reaction sequence to soot. The thermodynamics are

unfavorable. The large ions can be explained by very rapid exothermic

ion-molecule reactions and it is easy to extrapolate these growing by the

same processes to incipient soot particles. The energetics are favorable.

An additional argument for chemi-ions as precursors for soot formation

is obtained by comparing our results, Fig. 8, for the > 300 ion profile in

a 2.7 kPa (20 Torr) ϕ = 3.5 C_2H_2/O_2 flame with data measured in the same

flame by other workers. Homann and Wagner[12] identified a class of species,

other than polyaromatic hydrocarbons which had a unique profile, and called

10

them soot "precursors". The > 300 ion profile from our work corresponds closely with Homann and Wagner's precursor peak. The decay shape is somewhat different, possibly since our ion profile includes a broader mass class than the "precursors". Thus, a progression from small ions to large ions to incipient charged soot particles would be apparent.

V. CONCLUSIONS

A significant difference in the ion spectrum is observed between non-sooting and sooting flames, with the increasing dominance of ions with mass larger than 300 amu as the flame is made fuel richer. Dual maxima are observed in individual species concentration vs distance profiles from sooting flames. The ion profiles of acetylene and benzene exhibit many similarities and some distinct differences. High concentrations of oxygen-containing aromatic ions are observed in the benzene flame front; they are not observed downstream of the flame front where the ions in benzene and acetylene flames are similar.

The data and arguments presented here are consistent with an ionic mechanism of soot formation in which the initial ions are chemi-ions and the building blocks are C_2H_2, C_4H_2, and C_2H, which add to the growing ion by ion-molecule reactions.

ACKNOWLEDGMENT

11

REFERENCES

1. Calcote, H.F., Combust. Flame, submitted (1980).

2. Jensen, D.E. and Miller, W.J., J. Chem. Phys. 53, 3287 (1970).

3. Delfau, J.L., Michaud, P., and Barassin, A., Combust. Sci. and Technol. 20, 165 (1979).

4. Homann, K.H., Mochizuki, M., and Wagner, H.Gg., Z. Physik. Chem. N.F. 37, 299 (1963).

5. Bittner, J.D. and Howard, J.B., personal communication, 1979.

6. Calcote, H.F., in Ion-Molecule Reactions (J.L. Franklin, Ed.), Plenum Press, New York, 1972, Vol. 2, p. 673.

7. Bonne, U., Homann, K.H., and Wagner, H.Gg., Tenth Symposium (International) on Combustion, The Combustion Institute, Pittsburgh, 1965, p. 503.

8. Homann, K.H. and Wagner, H.Gg., Eleventh Symposium (International) on Combustion, The Combustion Institute, Pittsburgh, 1967, p. 371.

9. Place, E.R. and Weinberg, F.J., Twelfth Symposium (International) on Combustion, The Combustion Institute, Pittsburgh, 1969, p. 245.

10. Wersborg, B.L., Yeung, A.C., and Howard, J.B., Fifteenth Symposium (International) on Combustion, The Combustion Institute, Pittsburgh, 1975, p. 1439.

11. Homann, K.H., Ber. Bunsenges. Phys. Chem. 83, 738 (1979).

12. Homann, K.H. and Wagner, H.Gg., Proc. Roy. Soc. London A307, 141 (1968).

13. Prado, G.D. and Howard, J.B., in Evaporation-Combustion of Fuels, B.T. Zung, Ed., American Chemical Society, Advances in Chemistry Series 166, Washington, DC, 1978, p. 153.

Table 1
Ions identified in acetylene and benzene flames
Relative concentrations indicated by number of *. Ions unique
to benzene indicated by *.

Mass	Species	Structure	C$_2$H$_2$/O$_2$, φ = 2.0		C$_6$H$_6$/O$_2$, φ = 1.8	
			1 cm	2 cm	1 cm	2 cm
19	H$_3$O$^+$					*
39	C$_3$H$_3^+$	(cyclopropenyl triangle)$^+$	***	***	*	***
51	C$_4$H$_3^+$	C=C$^+$–C≡C–				**
53	C$_4$H$_5^+$	C=C$^+$–C=C	*	*	*	*
63	C$_5$H$_3^+$	–C≡C–C$^+$–C≡C–		**		***
65	C$_5$H$_5^+$	–C≡C–C$^+$–C=C	*	*		
67	C$_4$H$_3$O$^+$	C=C$^+$–C=C=O			*̲	
75	C$_6$H$_3^+$	–C≡C–C≡C–C$^+$=C		*		**
77	C$_6$H$_5^+$	–C≡C–C=C$^+$–C=C	*	*		*
79	C$_6$H$_7^+$	C=C$^+$–C–C–C=C		*		
81	C$_5$H$_5$O$^+$	C=C–C=C$^+$–C=O			*̲*̲	
89	C$_7$H$_5^+$	–C≡C–C≡C–C$^+$=C–C	*	**		**
91	C$_7$H$_7^+$	(benzyl ring)CH$^+$	**	**	**	**
95	C$_6$H$_7$O$^+$	(ring with O)$^+$			*̲*̲	
103	C$_8$H$_7^+$	(ring)–C$^+$=C	*	*		**
105	C$_7$H$_5$O$^+$	–C≡C–C=C$^+$–C=C–(ring=O)			*̲*̲	

13
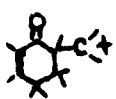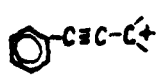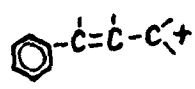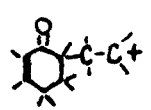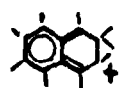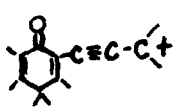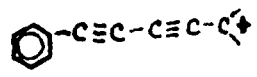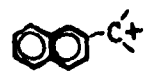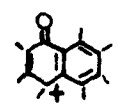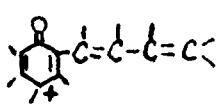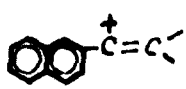
TABLE I (Continued)

Mass	Species	Structure	$C_2H_2/O_2, \phi = 2.0$		$C_6H_6/O_2, \phi = 1.8$	
			1 cm	2 cm	1 cm	2 cm
109	$C_7H_9O^+$				**	
115	$C_9H_7^+$			*		
117	$C_9H_9^+$		*			*
119	$C_8H_{11}O^+$				**	
129	$C_{10}H_9^+$		*	*		*
131	$C_9H_7^+$				***	
139	$C_{11}H_7^+$			*		
141	$C_{11}H_9^+$		*	*		*
143	$C_{10}H_7O^+$				**	
145	$C_{10}H_9O^+$				**	
153	$C_{12}H_9^+$		**	**		

4
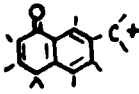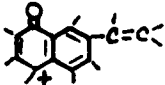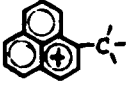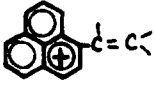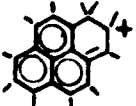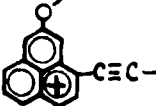
TABLE I (Continued)

Mass	Species	Structure	C_2H_2/O_2, $\phi = 2.0$		C_4H_6/O_2, $\phi = 1.8$	
			1 cm	2 cm	1 cm	2 cm
157	$C_{11}H_9O^+$				**	*
165	$C_{13}H_9^+$		***	***	***	***
169	$C_{12}H_9O^+$				**	
179	$C_{14}H_{11}^+$		*	*	*	
181	$C_{13}H_9O^+$				**	*
191	$C_{15}H_{11}^+$		**	*	**	*
203	$C_{16}H_{11}^+$		*	*	*	*
205	$C_{15}H_9O^+$				**	
215	$C_{17}H_{11}^+$		*	*	**	*

15

TABLE I (Continued)
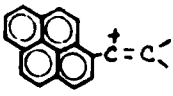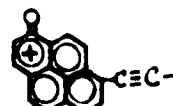
Mass	Species	Structure	C_2H_2/O_2, $\phi = 2.0$		C_6H_6/O_2, $\phi = 1.8$	
			1 cm	2 cm	1 cm	2 cm
217	$C_{16}H_9O^+$				*	
227	$C_{18}H_{11}^+$		*	*	*	*
231	$C_{17}H_{11}O^+$				*	
239	$C_{19}H_{11}^+$		**	*		
241	$C_{18}H_9O^+$				*	**

16

FIGURE CAPTIONS

Fig. 1   FLAME ION SAMPLING MASS SPECTROMETER

Fig. 2   ION SPECTRA FOR ACETYLENE AND BENZENE FLAMES

Data taken 1 cm above burner correspond to "first peak" compositions

at 2.0 kPa. (a) acetylene/O_2, ϕ = 2.0; (b) benzene/O_2, ϕ = 1.8.

Fig. 3   ION PROFILES FOR ACETYLENE/OXYGEN NON-SOOTING FLAME

2.0 kPa, ϕ = 2.0, calculated adiabatic flame temperature,

T_a = 2300 K.

Fig. 4   ION PROFILES FOR BENZENE/OXYGEN NEARLY SOOTING I LAMES

2.0 kPa, ϕ = 1.8, calculated adiabatic flame temperature,

T_a = 1900 K.

Fig. 5   EFFECT OF EQUIVALENCE RATIO ON > 300 amu ION PROFILES FOR

ACETYLENE/OXYGEN FLAMES

Ions 300 < amu $\gtrsim$ 1000, 2.0 kPa. Transition to sooting occurs

between ϕ = 2.5-2.75.

Fig. 6   EFFECT OF EQUIVALENCE RATIO ON PEAK ION CURRENTS FOR

ACETYLENE/OXYGEN FLAMES

2.0 kPa.

Fig. 7   EFFECT OF EQUIVALENCE RATIO ON PEAK ION CURRENTS FOR

BENZENE/OXYGEN FLAMES

2.0 kPa.

Fig. 8   CONCENTRATION PROFILES FOR AN ACETYLENE/OXYGEN FLAME

2.7 kPa, ϕ = 3.5 (after Ref. 1); ions > 300, this work--use ion

current scale, all others use number density scale. "Charged Soot"

particles from Prado and Howard[13]; "Soot" from Wersborg, Yeung, and

Howard[10] and Bonne, Homann, and Wagner[7]; "Precursors" and "$C_{14}H_8$",

typical of polycyclic aromatic hydrocarbon, from Homann and Wagner[8].

17

TO
RECORDER

ION MULTIPLIER

QUADRUPOLE
MASS FILTER

ENERGY CONTROL
AND FOCUSING
LENSES

TO
DIFFUSION PUMP

QUADRUPOLE
LENSES

TO
DIFFUSION PUMP

EXTRACTION LENS

SAMPLING CONE

FLAT FLAME

OUTER FLAME
GAS MIXTURE

INNER FLAME
GAS MIXTURE

FIGURE 1

18

FIGURE 2

19

FIGURE 3

FIGURE 4

21

FIGURE 5

FIGURE 6

23
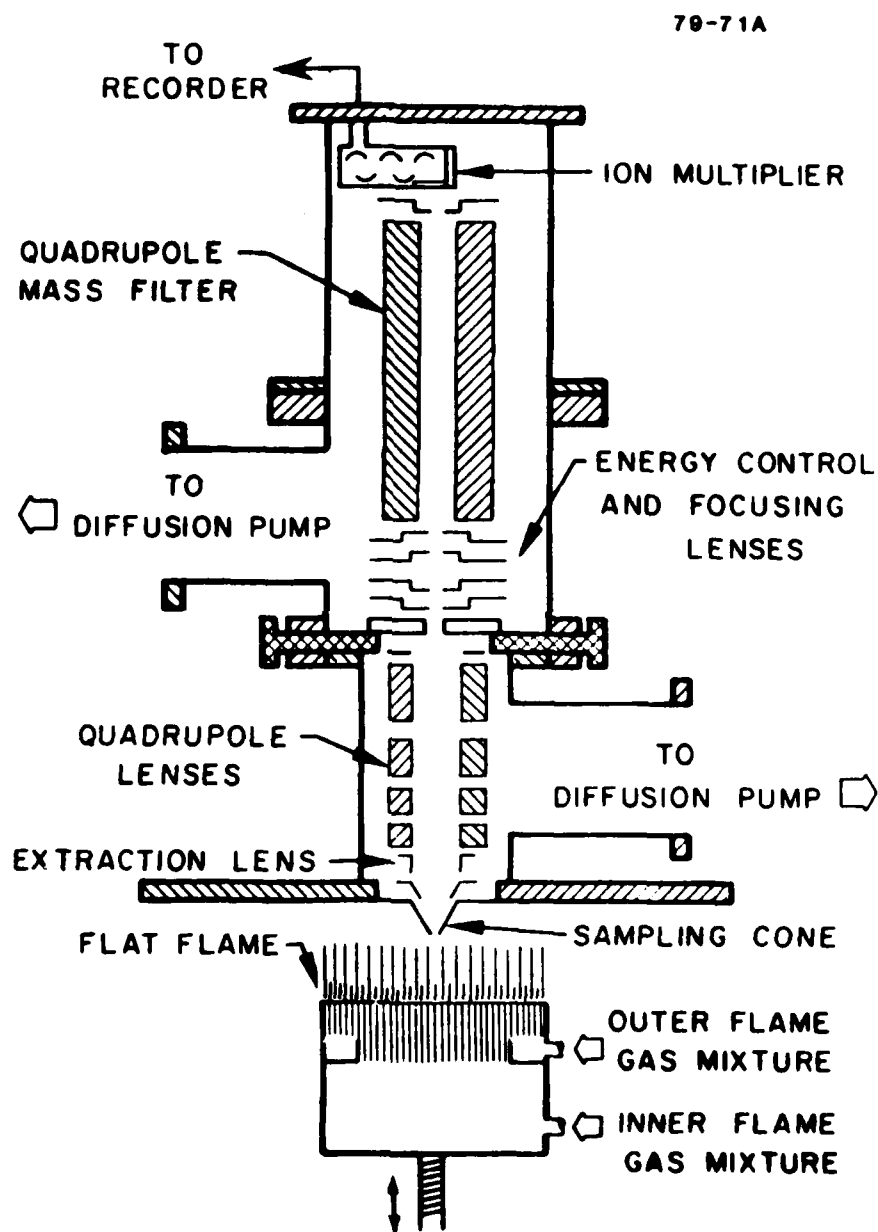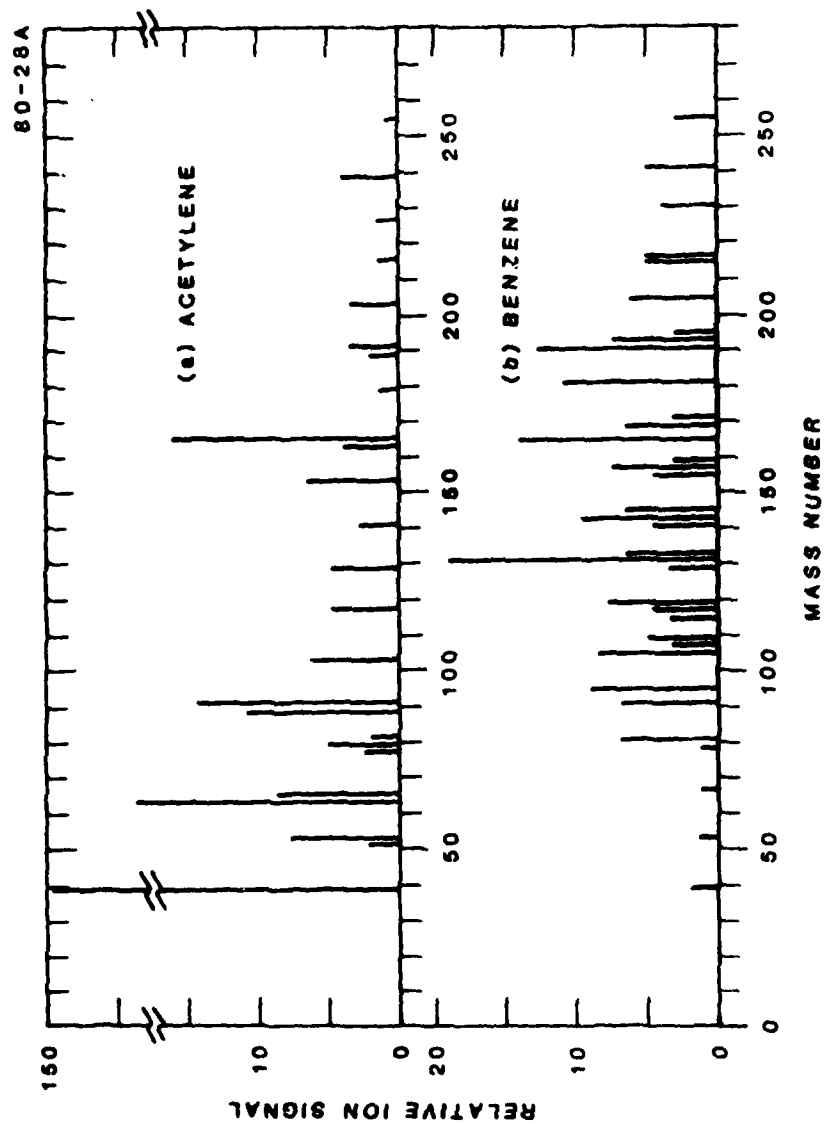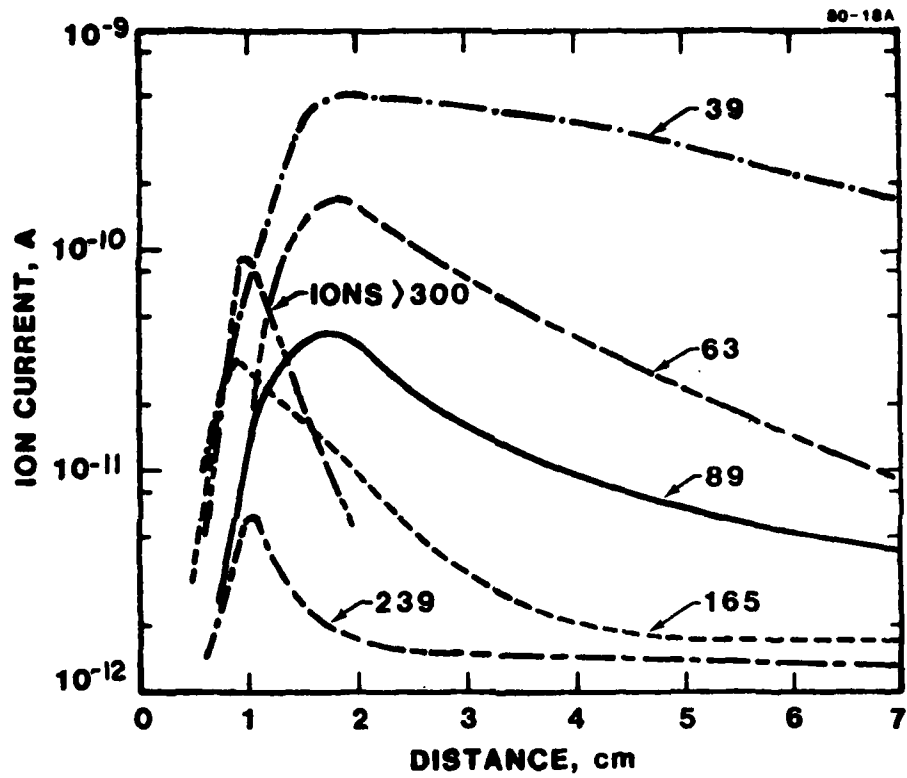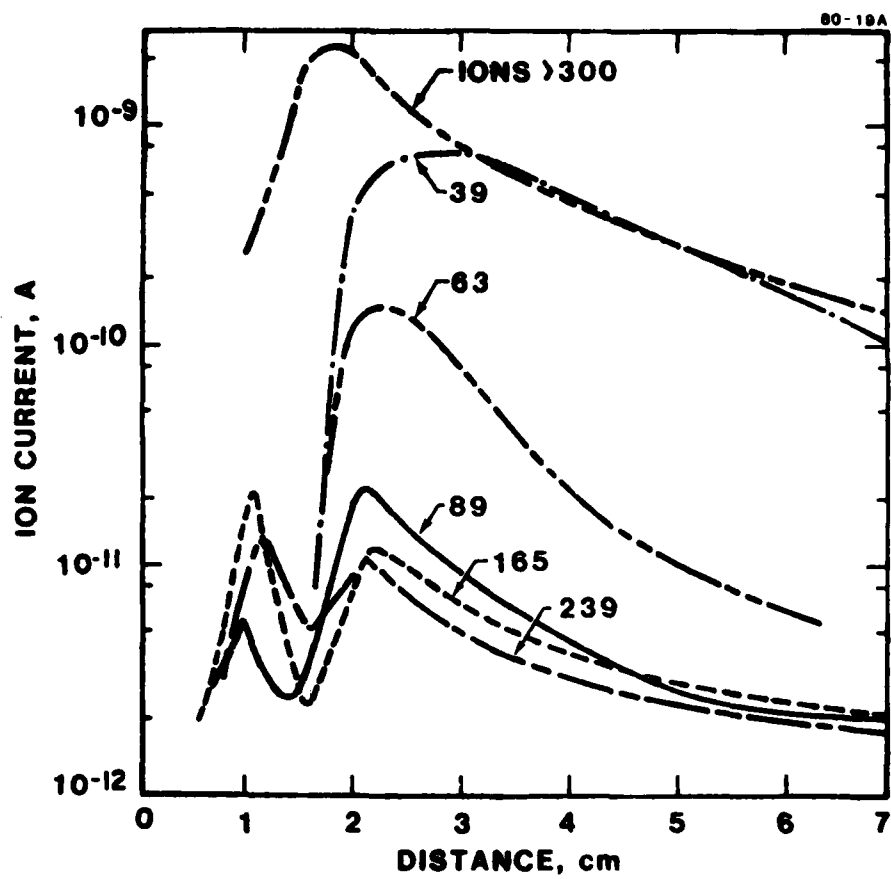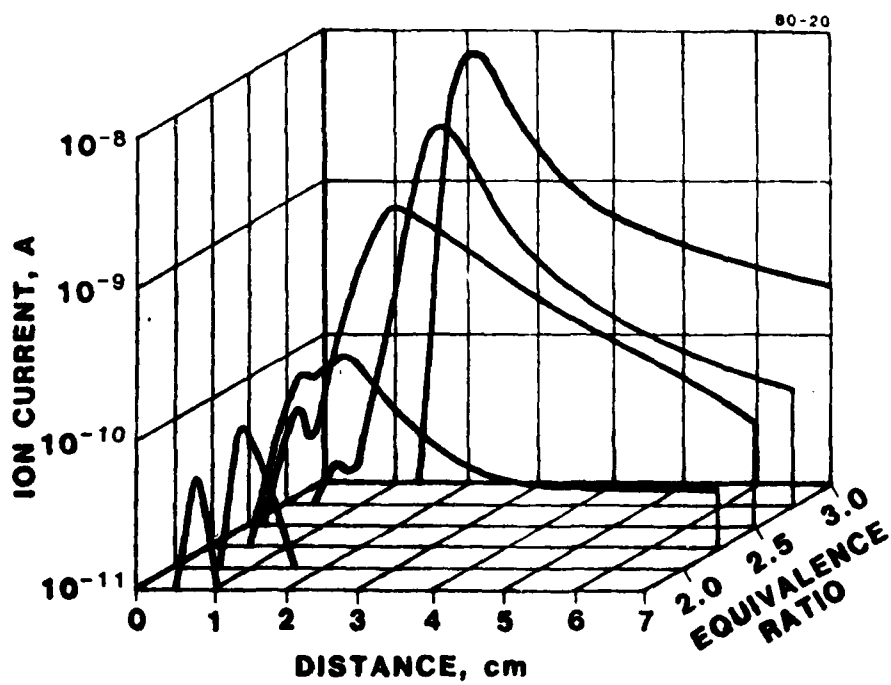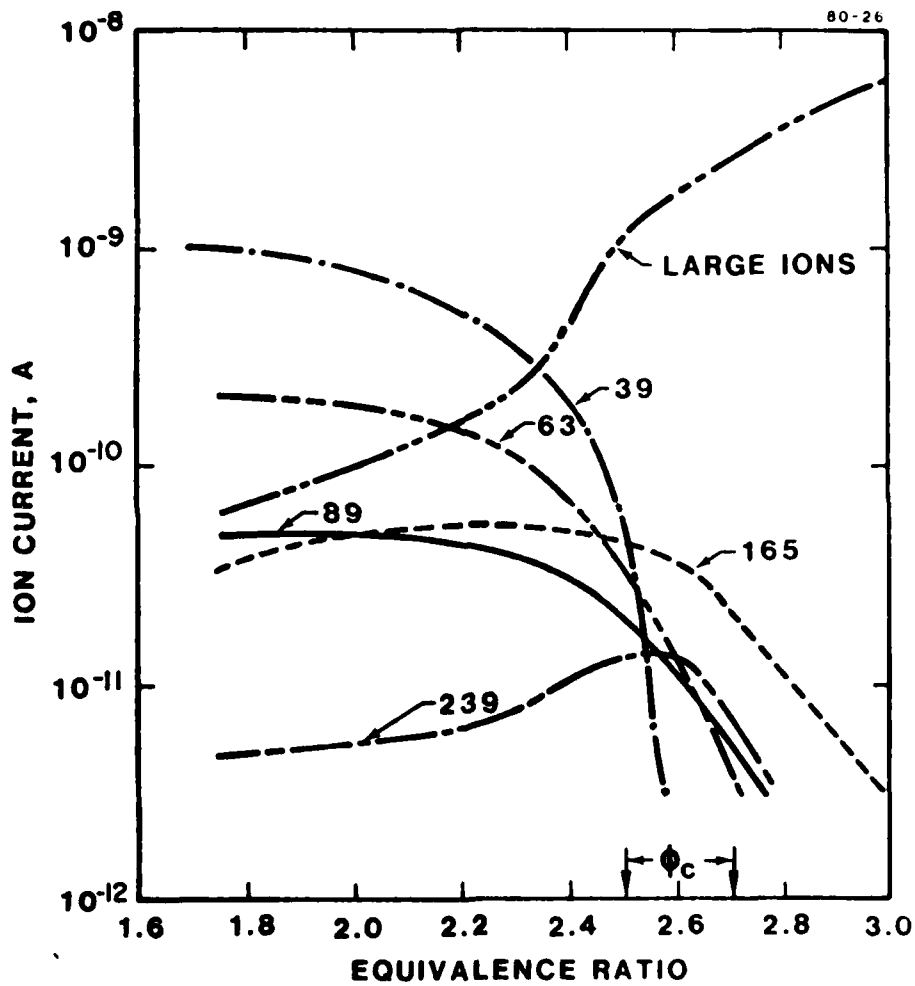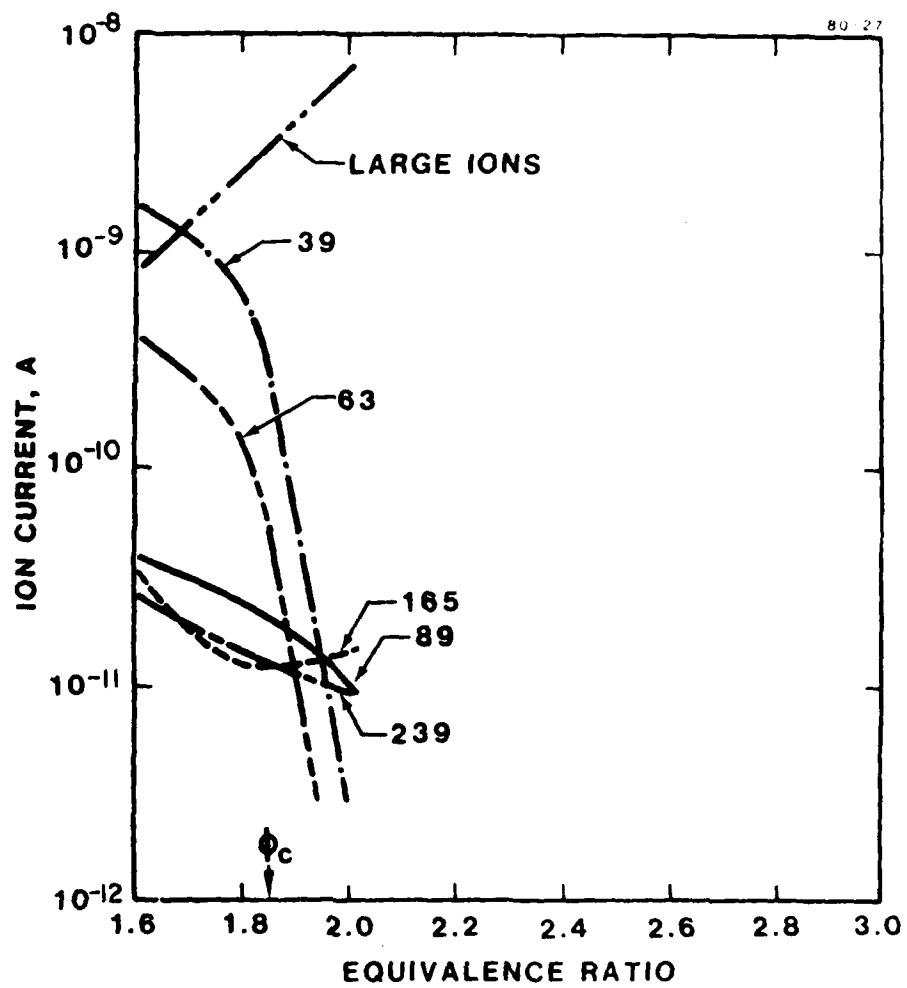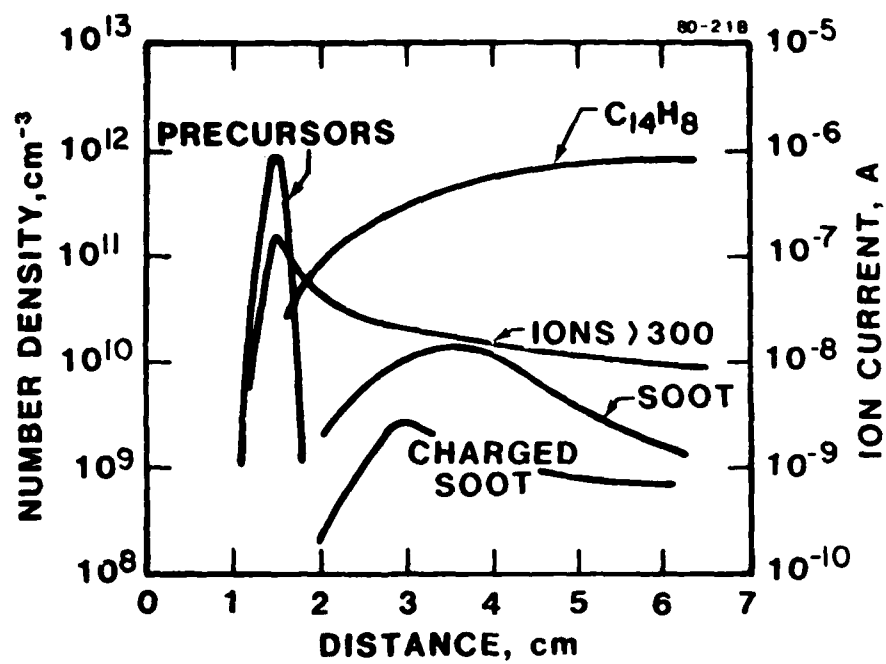
FIGURE 7

FIGURE 8

APPENDIX C

IONIC MECHANISMS OF SOOT NUCLEATION IN PREMIXED FLAMES

D.B. Olson and H.F. Calcote

AeroChem Research Laboratories, Inc.
P.O. Box 12, Princeton, NJ 08540

ABSTRACT

Although numerous chemical mechanisms have been postulated for the formation of soot in hydrocarbon combustion, none have received quantitative support. Understanding of this process is complicated by the large number of species involved and by the phase change associated with nucleation.

An experimental program is underway at AeroChem to determine the role of ionic processes in soot formation in premixed hydrocarbon flames. The hypothesis being tested is that ions produced via chemi-ionization serve as nuclei for initial formation of soot particles. Rapid ion-molecular kinetics, rapid structural rearrangements, and thermochemistry favorable toward growth to larger species are characteristics of the ion chemistry, in agreement with observations about the soot formation process.

Mass spectrometric measurements of flame ion concentration profiles have been made in low pressure rich and sooting acetylene/oxygen and benzene/oxygen flames. As both flames are made increasingly fuel rich and approach sooting the predominant ion $C_3H_3^+$ is replaced by large positive aromatic ions with mass greater than 300. It is argued that these ions are the soot precursors.

Similarities and differences between the ion spectra of rich and sooting acetylene and benzene flames are discussed along with possible reasons for dual maxima in ion concentration profiles observed in sooting flames. A detailed chemical mechanism considering both neutral and ionic flame chemistry is being

---

developed for which it is necessary to estimate the thermochemical parameters for large ionic species. Preliminary results of computer simulations of the chemical kinetics using this scheme are presented. The results are consistent with an ionic mechanism of soot formation.

INTRODUCTION

The mechanism of soot formation has been recognized for many years as an extremely complex problem and the nucleation step--the transition from molecular species where chemical reactions dominate to incipient soot particles where physical processes dominate--has been recognized as the least understood step in the process. Many diverse theories have been put forward to explain the nucleation step and all of them seem to have been refuted.[1,2] One of the troublesome problems is that there may be many mechanisms operating simultaneously or that different mechanisms may dominate under different conditions. We are exploring the hypothesis[2,3] that the basic nucleation mechanism in most systems involves growth through rapid ion-molecule reactions producing larger and larger ions. The initial ion is assumed to be the chemi-ion $C_3H_3^+$ which is observed in large concentrations in rich flames. Thus the energetics which drive the process are originally derived from the nonequilibrium chemi-ionization process. In the ionic hypothesis, the large ions are subsequently neutralized by ion-electron and ion-ion recombination to become incipient particles. As the neutral particles grow via coagulation and/or surface growth to a critical size they are thermally ionized. Thus there are two stages of ionization, a situation which has led to some of the confusion in interpreting previous experiments where it has not been clear whether the chemi-ions or thermally ionized particles are being observed. In two recent publications[2,3] we have compared the chemi-ionization soot nucleation mechanism

to the various neutral species mechanisms and shown the ionic mechanism to be more consistent with observations. In this paper we present further evidence for the proposed ionic mechanism and examine some of its problems. These problems include the lack of a satisfactory pathway for the production of $C_3H_3^+$ in rich flames, the value of the absolute concentration of chemi-ions in sooting flames, and the inadequately explained observation that, at equivalence ratios near sooting, individual large ions show double-peaked profiles as a function of distance through the flame.

Two basic non-ionic mechanisms are currently postulated. One involves the growth of large polyacetylenes (or other unsaturated molecules) and subsequent ring formation to produce species with aromatic structures. These then grow by addition of unsaturated groups to form larger and larger polycyclic aromatic hydrocarbons, eventually to become soot particles. The other mechanism, consistent with the observation that aromatics soot more readily than do aliphatics, assumes the continual growth of larger and larger aromatic structures by condensation of intact polycyclic aromatic hydrocarbons. There are severe problems with either of these mechanisms. Carbon blacks and soot are not large linear polyacetylene molecules but are multi-ring structures, so the polyacetylenes must in some way produce a ring structure. Any reaction scheme one can envision for this process would be expected to be slow because of the complicated rearrangement geometry involved. Furthermore, the concentration of polyacetylenes remains large even downstream in the flame beyond the point where soot nucleation has ceased. If no other ingredient were required, the number of particles would be expected to continue to increase as long as significant concentrations of polyacetylenes were present. Polycyclic hydrocarbon nucleating (condensation) mechanisms are similarly inconsistent because the concentration of these molecules continues to increase in the flame front beyond the point where soot nucleation ceases. Furthermore, thermodynamic

3

considerations appear to limit the growth of larger and larger polycyclic aromatic hydrocarbons in an intermediate size range.

Much of the evidence for an ionic nucleation mechanism is circumstantial, and much of what has been interpreted as verification of ionic nucleation is related to large charged particles. As we noted above these particles can arise from thermal ionization and have nothing to do with the nucleation process. The essential remaining evidence supporting an ionic nucleation mechanism can be summarized[2,3] as:

1. A strong positive correlation is observed in premixed flames between the growth of large ions and the appearance of soot.

2. Carbon tetrachloride (and other electrophilic molecules) increase the concentration of large ions in diffusion flames and the subsequent onset of soot formation.

3. Fuels which produce ions also produce soot, while fuels which do not produce ions do not produce soot.

4. Reactions of O atoms with excess acetylene demonstrate very rapid ionic polymerization to form $C_{2n}H_{2n+1}^{+}$ and $C_{2n}H_{2n-1}^{+}$ ions.

5. Large concentrations of ions are also produced in pyrolysis experiments.

6. The location of the molecular ion peak concentration in the flame front corresponds to the maximum concentration of a group of poorly characterized molecules previously identified as soot precursors.

7. The concentration of chemi-ions has been estimated[2] to be large enough and at an appropriate location in the flame to account for the rate and concentration of particles formed.

Additional thermodynamic and chemical kinetics arguments will be presented in this paper.

FORMATION OF CHEMI-IONS

The ion concentrations observed in hydrocarbon flames are far in excess of what can be accounted for by thermal ionization. There is overwhelming evidence that in lean and close-to-stoichiometric compositions this is due to the chemi-ionization reactions first proposed[4] by Calcote

$$CH + O \rightarrow CHO^+ + e^- \qquad (1)$$

The rate coefficient[5] for this reaction in the temperature range 2000 to 2400 K is about 2.3×10^{-13} cm^3 s^{-1}. The observed concentrations of CHO^+ are, however, almost three orders of magnitude smaller than the maximum total ion concentration because of very rapid ion-molecule reactions, especially

$$CHO^+ + H_2O \rightarrow H_3O^+ + CO \qquad (2)$$
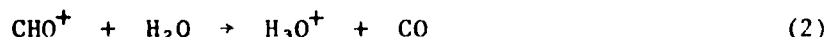
The ions are removed mostly by dissociative recombination:

$$H_3O^+ + e^- \rightarrow H_2O + H \qquad (3)$$

The rate constant[6,7] for this reaction is 2×10^{-7} cm^3 s^{-1} at 2000 K with a temperature dependence of $T^{-1/2}$.

Many other superequilibrium concentrations of ions are observed[8,9] due to very rapid ion-molecule reactions with the neutral species present which are in local equilibrium with each other. The various ion concentrations all decay at nearly the same rate, probably by reaction with O, OH, O_2, or H_2O to form H_3O^+ with a bimolecular rate coefficient[10] of 4×10^{-11} cm^3 s^{-1}. Some of these species are displayed[11] in Fig. 1. In lean flames the dominant ion is $C_2H_3O^+$ which is formed by

$$CHO^+ + CH_2CO \rightarrow C_2H_3O^+ + CO \qquad (4)$$

5

However, in even slightly rich flames (where the equivalence ratios, ϕ, are small compared to those at which soot is formed), the dominant ion is $C_3H_3^+$. Note that the maximum equivalence ratio shown in Fig. 1 is 1.3 and soot formation begins at $\phi \approx 2.6$ (see Fig. 2 for example). At concentrations approaching those where soot is formed $C_3H_3^+$ is still the dominant ion and H_3O^+ and $C_2H_3O^+$ are no longer important. They have been replaced by non-oxygen-containing ions like $C_5H_3^+$ and larger ions containing only carbon and hydrogen. In an ethylene/oxygen flame at 0.5 kPa Miller[10] measured the $C_3H_3^+$ concentration at $\phi = 1.0$, 1.3, and 1.5 to be about 1×10^{10} ions cm^{-3}; he observed a slightly higher value at $\phi = 1.3$ but within experimental error, his observations are all equal.

In lean and stoichiometric flames the appearance of $C_3H_3^+$ is generally explained[8,9] by a series of reactions deriving from CHO^+

$$CHO^+ + CH_2O \rightarrow CO + CH_3O^+ \xrightarrow{C_2H_2} C_3H_3^+ + H_2O \qquad (5)$$

$$CHO^+ + CH_4O \rightarrow CO + CH_5O^+ \xrightarrow{C_2H_2} C_3H_3^+ + H_2O + H_2 \qquad (6)$$

$$CHO^+ + C_2H_2O \rightarrow CO + C_2H_3O^+ \xrightarrow{C_2H_2} C_3H_3^+ + CO + H_2 \qquad (7)$$
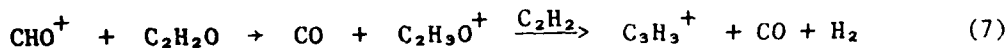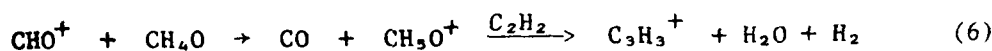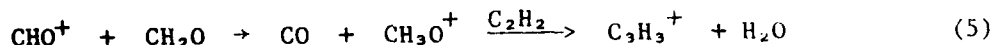
Reaction (7) probably goes through two steps:

$$C_2H_3O^+ + O \rightarrow H_2O + C_2HO^+ \xrightarrow{C_2H_2} C_3H_3^+ + CO \qquad (8)$$
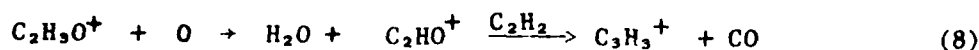
However, all of the above reactions require oxygen-containing species and it seems unlikely that in very rich flames the concentration of oxygenated species is sufficient to account for the large observed concentrations of $C_3H_3^+$. One possible reaction route which does not require oxygenated species is

$$CHO^+ + CH_2 \rightarrow CO + CH_3^+ \xrightarrow{C_2H_2} C_3H_3^+ + H_2 \qquad (9)$$
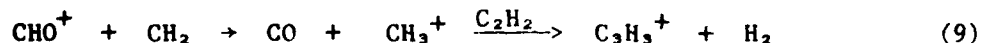
Besides the CH/O reaction (1), other pathways to account for the large concentration of $C_3H_3^+$ observed in flames have been proposed. The most commonly quoted is[12,13]

$$CH^* + C_2H_2 \rightarrow C_3H_3^+ + e^- \qquad (10)$$

6
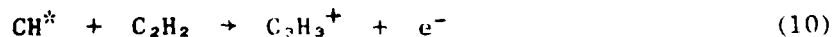
Efforts by several groups to find supporting evidence for the occurrence of this reaction by correlating the concentrations of CH in the $A^2\Lambda$ or $B^2\Sigma$ state with the rate of ion formation have been unsuccessful. Miller[10] thoroughly considered the mechanism of $C_3H_3^+$ formation in C_2H_4/O_2 and C_2H_2/O_2 flames and concluded that it is complex. He measured the dependence of the $C_3H_3^+$ on concentrations of C_2H_4 or C_2H_2 added to H_2/O_2 flames and found a a $[C_2H_4]^{3.5}$ and a $[C_2H_2]^2$ dependence. Yet in both cases the CH^* dependence on the hydrocarbon concentration was 2. If Reaction (10) were the dominant mechanism the order should be 3 in both cases (C_2H_2 and C_2H_4). It was suggested[10,14] that proton transfer from some unidentified species to C_3H_2 might account for the formation of $C_3H_3^+$ but insufficient data were available to examine this hypothesis.

Evidence for other proposed independent sources[15] of $C_3H_3^+$, e.g.

$$C_2^* + CH_3 \rightarrow C_3H_3^+ + e^- \tag{11}$$
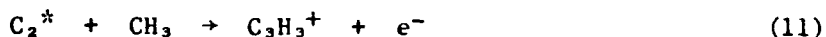
is nonexistent.

On the basis of thermodynamics there are other conceivable chemi-ionization reactions which can explain some of the large ions observed in the flame front of fuels approaching sooting, e.g.,

$$C_{16}H_{10} + C_6H \rightarrow C_{22}H_{11}^+ + e^- \qquad \Delta H \approx -30 \text{ kcal mol}^{-1} \tag{12}$$

While reactions of this type cannot be eliminated with available information it seems unlikely that in such a large molecule all of the energy of reaction should be concentrated in one electronic state.

For the purposes of developing an ionic mechanism of soot formation in flames we accept the presence of large concentrations of $C_3H_3^+$ as the initial ion but recognize that its source has yet to be explained.

7

ABSOLUTE ION CONCENTRATIONS

To quantitatively evaluate our proposed mechanism of soot nucleation it would indeed be desirable to know not only the absolute ion concentrations but also the rates of formation of the chemi-ions which we propose initiate the growth of soot nuclei. It is difficult to obtain absolute ion concentrations with a mass spectrometer, especially over a mass range for which a good calibration is impossible, as in the case of large positive ions in sooting flames. Absolute measurements with electrostatic probes are also difficult in the presence of a large range of ion masses.

Previously we have relied on the results of Howard and coworkers[16,17] for establishing that the ion concentrations were sufficiently large to be important in soot nucleation. Recent measurements, however, by Delfau et al.[18] and Homann[19] disagree with the earlier results. It thus seems reasonable in view of the importance of these results to review those measurements. We chose four sets of data obtained in rich and sooting low pressure acetylene/oxygen flames as close to the same experimental conditions as possible; they are summarized in Table I.

Howard and associates used both an electrostatic probe[16] and a molecular beam sampling system[17] with a Faraday cage detector. Delfau et al.[18] used an electrostatic probe while Homann[19] used a molecular beam sampling system with an ion collector immediately behind the flame sampling orifice with electrostatic grids to control the sampling process. First, the data have been obtained over such a range of conditions that it is surprising that they agree as well as they do; the highest ion concentration was measured by Howard et al. and the lowest by Homann, both with molecular beam sampling. The difference is about a factor of 40.

The Prado and Howard electrostatic probe data were taken under the conditions we have previously chosen[2] for comparisons because of the availability of data from various investigators at those conditions. It thus is instructive to compare the conditions of this work and other data sets in the table to see if the variations are reasonable, i.e., expected. The Delfau et al. ion concentration result would be expected to be lower because of the diluent N_2 and the lower equivalence ratio, while the higher pressure and flow velocity would increase the value. Wersborg et al.'s molecular beam data would be expected to be higher because of the higher flow velocity but lower because of the lower equivalence ratio. Homann's data would be expected to be lower because of the lower flow velocity and lower equivalence ratio. Finally, it is interesting that from Wersborg et al. the effect of equivalence ratio is considerably greater than in the data of Homann or Delfau et al.!

It is significant that the authors describe the quantity they are measuring as quite different. For example, Prado and Howard describe their data as "total positive ions" but assume in the calculation that the measured value represents 4 nm diam charged particles. They present another set of data in the same paper for charged particles which peaks at about 3 cm with a maximum value of about 4×10^9 cm^{-3}, rather close to the concentration of what Homann calls "positively charged soot particles," 2.4×10^9 cm^{-3} peaking at 2.0 cm.

The very large difference between Homann's concentration value, Table I, and the others is difficult to explain. Indeed, the greatest difference in ion concentrations is between the two sets of molecular beam sampling data (Refs. 17 and 19). Homann's use of the equation for isentropic flow through the sampling nozzle as the basis for absolute calculation of ion flux and neutral gas flux may not, as he recognizes, be valid since ions are probably lost on every collision with the wall. Wersborg et al. similarly assumed isentropic nozzle flow

and made absolute concentration measurements in the flame from measured molecular beam flux. Comparing Homann's data directly with that of Wersborg et al. is somewhat uncertain because it is not clear that the same mass range was being measured. Furthermore, the different measurement conditions (equivalence ratio and flow velocity) would emphasize any other differences because of the idiosyncrasies of individual burner systems; for example, increasing the flow velocity caused the flame to move closer to the burner rather than further away. Thus, Homann found that increasing the unburned gas flow velocity by about 10 cm s^{-1} decreased the observed peak concentration of charged soot particles by a factor of 2 to 3. Wersborg et al. on the other hand observed a decrease of a factor of about 100 for a similar change in flow velocity. Apparently these workers are not measuring the same quantities and in any case, given the high sensitivity of their systems to various parameters, it is amazing that the values in Table I are as close as they are. Incidentally a value of about 10^{10} ion cm^{-3} is all that seems to be required for ionic soot nucleation.

Probably none of the measurements in Table I are relevant to the question of ionic nucleation. The proper question is whether there are sufficient small chemi-ions such as $C_3H_3^+$ to quantitatively account for the proposed mechanism. To answer this question one must look at data such as presented in Fig. 2. The instrument used in these experiments was not calibrated but the relative concentrations are approximately correct. A rough estimate of the calibration factor using an assumed ion-electron recombination rate constant (that for H_3O^+) and the observed ion disappearance rate leads to peak ion concentrations of about 10^{10} cm^{-3}.

However, there is another apparent difference between our work[9] and the work of Delfau et al.,[18] Wersborg et al.,[17] and Homann[19] which demands resolution. This is the change in total ion concentration with equivalence ratio

10

near the critical equivalence ratio for soot formation. If the data reported
in Fig. 2 are taken by operating the mass spectrometer in a mode to observe
ions in two ranges, 13 to 300 amu and greater than 300 amu, the ion concentra-
tion in the range 13 to 300 falls sharply at the soot point (see Fig. 3) while
the concentration above 300 amu increases such that the total ion concentration
is essentially constant from ϕ = 1.7 to 3.0 with only a small increase between
the soot point and ϕ = 3.0. In contrast Delfau et al. observed more than a
factor of 10 decrease in maximum ion concentration from ϕ = 1.7 to the soot
point and then an increase of more than a factor of 10 from the soot
point to ϕ = 3.0. Homann observed an increase from his soot point to
ϕ = 2.9 of a factor of about 25 and Wersborg et al. observed an increase of
about 25 from their soot point to ϕ = 3.0. We suspect that in all of the mea-
surements, including our own, the sensitivity of the measuring technique to
different ion masses has not been accurately accounted for.

Clearly there is need for some very careful measurements of ion concentra-
tions, especially individual species or groups of species, in rich and sooting
hydrocarbon flames. In the meantime the data in the literature are supportive,
although shaky, of an ionic mechanism of soot nucleation.

ION PROFILES

The low pressure flame apparatus and ion sampling quadrupole mass spectrom-
eter, shown in Fig. 4, have been described previously.[3,20] Briefly, the flames
were stabilized on a 12 cm diam flat flame burner and were surrounded by a
fuel-rich annular shield flame 16 cm in diam to prevent air or combustion prod-
uct entrainment. The mass spectrometer sampling cone was constructed from 316
stainless steel with a 90° outer angle and a 0.25 mm orifice. The ion beam is
focused in the first stage (P $\approx$ 30 mPa) using quadrupole lenses to minimize mass
discrimination onto a 1 mm diam aperture into the second pumping stage. The
custom-made quadrupole mass filter uses 2.5 cm diam rods and is characterized as

11

a relatively low resolution, high transmission instrument, operating at 0.5 MHz and covering the mass range 13 to 300 amu. A Bendix Model 306 magnetic electron multiplier is used off-axis as detector; its output is amplified by a Keithley 602 electrometer and displayed on an X-Y recorder. Ion profiles through the flame were obtained by moving the burner with respect to the mass spectrometer sampling cone. Gases were controlled using critical flow orifices while benzene was metered by a precision syringe pump. The liquid benzene was sprayed into a low pressure flash evaporator and the vapor fed to the burner-mixing chamber through heated lines.

Initial experiments were performed at 2.7 kPa with an unburned gas velocity of 50 cm s^{-1} at the burner. Rather serious interactions of the flame with the burner were reduced by lowering the total pressure. Unless otherwise noted the work reported here corresponds to a pressure of 2.0 kPa and unburned gas velocity of 50 cm s^{-1}.

An example of the sensitivity of the system at 2.7 kPa to flow velocity is shown in Fig. 5. The total small (< 300 amu) ion profile is observed to increase in magnitude and move closer to the burner surface with increasing gas velocity. This increase in maximum current is in contrast to results reported by Homann and by Wersborg et al. who found the maxima to decrease with increasing flow velocity at 4.0 kPa and 2.7 kPa, respectively. These results emphasize the care one must exercise in comparing data from different sources or taken under different conditions. We selected experimental conditions under which the results were less sensitive to flow velocity.

Detailed individual ion species profiles were measured for masses up to 300 amu at equivalence ratios above and below the critical equivalence ratio, ϕ_c, for soot formation as determined by the appearance of the yellow-orange continuum soot emission. In addition, the spectrometer was operated as a

12

high-pass mass filter and profiles were recorded of ions with mass larger than 300 up to cutoff of the filter, estimated to be about mass 1000. Ion current data from high-pass operation of the filter are not directly comparable to individual mass profiles because the throughput of the instrument is greater when acting as a high-pass mass filter. Relative ion currents are reported instead of ion concentrations because of the difficulties in quantitatively and reproducibly calibrating the instrument, although quantitative evaluation of soot nucleation mechanisms will require knowledge about absolute levels of ion concentrations in future experiments, and these are planned.

Data were taken by scanning the mass range at fixed distances from the burner to establish which ions were present at high concentrations; individual concentration profiles of selected species were then recorded by setting the spectrometer to that mass and moving the burner. Figure 6 shows spectra taken in nonsooting and sooting acetylene/oxygen flames at 1 cm distance in the blue-green oxidation zone. The essential features of the spectra are the dominance of mass 39, $C_3H_3^+$, followed by a series of peaks spaced every 13 or 14 amu. Only odd numbered ion masses are observed in contrast to neutral species sampled from similar flames[21] whose masses (number of hydrogens) are even. For most species the identity may be assigned with good confidence although the assigned structures[3] are somewhat speculative. At lower masses more than one isomer is observed, e.g., 63/65 amu, 89/91 amu. This latter pair is interesting because mass 89 must be an open-chained isomer but 91 can be either open-chained, a seven-membered ring, or a toluene-derived species. The most prevalent heavier species observed are masses 165 and 239 corresponding respectively to relatively stable three and five ringed compounds. In these rich flames H_3O^+ is observed only at low concentrations. At $\phi = 2.75$ the concentrations of the masses shown in the figure have all dramatically fallen and have been replaced by ions of larger mass.

Figure 7 shows mass spectra taken at two different positions in a nearly

sooting benzene flame. In the oxidation zone at 1 cm from the burner unique

oxygenated ionic species are observed at masses 95, 109, 131, etc., whereas

mass 39, $C_3H_3^+$, is essentially absent. At 2 cm the $C_3H_3^+$ concentration has grown

several orders of magnitude and the ions unique to benzene have disappeared.

These ions are identified as containing oxygen, and appear to be derived from

the neutral C_6H_6O species previously observed in similar flames.[21] Notable at

1 cm is the lack of species smaller than C_6 indicating little ring opening has

occurred in this region. The ion spectra in benzene flames beyond the flame

front are quite similar to those of acetylene flames with little or no informa-

tion about the parent fuel persisting. One speculates that it may be a general

rule that rich flames differ in the relative concentrations of ionic species

(as opposed to identities of ions present) downstream of the oxidation zone.

That is not to say that if ions nucleate soot that all flames would soot at the

same equivalence ratio since the chemistry of the oxidation zone may dominate

the process or the relative concentration of some ions may be more important

than others.

Figures 8 and 9 show profiles of selected ions in nonsooting, $\phi = 2.0$, and

sooting, $\phi = 2.7$, acetylene flames ($\phi_c \sim 2.6$). In Fig. 8 each ion profile is

observed to rise rapidly at the beginning of the flame front, at 0.6 cm. The

concentrations peak and slowly decay due mainly to ion-electron recombination

beyond $\sim$ 2 cm where oxidation is no longer occurring.

Also shown in these figures is the signal obtained using high-pass opera-

tion of the mass spectrometer, attributed to ions larger than 300 amu up to

about 1000 amu (labeled ions > 300). In the nonsooting flame, Fig. 8, this pro-

file peaks rapidly and disappears by 2 cm downstream. In the sooting flame,

Fig. 9, somewhat different ion profiles are observed. The initial flame front

maxima are followed by second larger, broad peaks, at about 2-4 cm. Although
$C_3H_3^+$ is still the dominant small ion, the heavier species (> 300 amu) are
much higher in relative concentrations. Note that the $C_{13}H_9^+$ first
peak is larger than the $C_3H_3^+$ first peak. The ions > 300 are ten times higher
in concentration than at $\phi = 2.0$. To further illustrate the behavior of these
larger ions, Fig. 10 shows their profiles in several flames. The dramatic
increase in large ion concentration at the expense of smaller ions is the most
significant change that occurs in the mass spectra as the flames are made
increasingly richer and finally produce soot. A hundredfold greater peak concen-
tration for the large ions is obtained in a $\phi = 3.0$ flame compared to the $\phi = 1.75$
flame, accompanied by a corresponding decrease in total concentration of small
ions (determined separately using bandpass operation of the mass spectrometer,
13-300 amu). The total ion concentration remains nearly constant (within a
factor of two—the precision of the measurements) over the wide range of equiva-
lence ratios investigated, see Fig. 3. Figure 10 also demonstrates the decay of
the first ion peak and the growth of the second ion peak as soot is produced.

SECOND ION PEAKS

Comparing the ion profiles from a nonsooting acetylene flame, Fig. 8, with
a sooting flame, Fig. 9, the appearance of the second broad maxima is puzzling.
Benzene flames have the same behavior, as shown in Fig. 11. The ions observed
in the second peak are the same as those observed in the first (flame front) peak,
although relative levels of different species change. Double peaks are observed
in profiles of a single species. Delfau et al.[18] have observed dual maxima in
electrostatic probe measurements in low pressure flames, but only present data
where the identity of the ions in the two peaks may be different. Neutral
beam sampling from benzene flames does not show dual peaked behavior.[21] On the
other hand, Homann[19] performed ion beam sampling from C_2H_2/O_2 flames in a

simple mass discriminator and found a strong increase in ionization at the beginning of the sooting zone (a second peak).

The source of this second peak is not clear. It cannot be due to the primary chemi-ionization reaction of CH + O since the O-atom and CH concentration are very small beyond the flame front. Other proposed chemi-ionization steps such as $CH^* + C_2H_2$ would also have peaked in the primary reaction zone. Thermal ionization of soot particles probably occurs when the particles become large enough to be characterized by ionization potentials near that of graphite. Calcote[2] used experimentally observed particle size distributions, temperature profiles, and estimated ionization potential vs. particle size variations to calculate charged particle concentrations in sooting low pressure acetylene flames. The agreement with observed values was excellent. This means that the molecular-sized ions which we are observing are not necessary to explain charged soot particles. However, it does not explain the source of the second peak for small ions.

A difficult question arises of whether these results could be due to experimental problems in sampling. Several different burners were used in conjunction with several different sampling cones and over a range of pressures. Specific details could be changed some, but not the general character of the results. The dual peaked behavior persisted under all conditions and we think the results are valid. Other laboratories[22] have found dual peaked behavior which they believe to be false. The question is not settled at this point and further experimental work will be necessary to resolve the issue.

The second peak arises further downstream than the leaner mixture first peak and includes the same ion species as the first peak. It is not just a shift in location. The total number of charged species is not significantly larger when the second peak appears; it may increase slightly. The data are not that definitive because of an unknown variation in mass spectrometer throughput with mass. Flames with dual maxima are always sooting or near sooting. Charge

16

transfer from a small thermally ionized charged particle, P^+, to a molecular or radical species, M

$$P^+ + M = M^+ + P$$

is unlikely since the ionization potential of the molecule is higher than that of the particle. Also, the ions contain an odd number of hydrogens and the neutral species observed contain an even number of hydrogens. Alternatively the process

$$PH^+ + M = MH^+ + P$$

will proceed in the direction such that the proton will end up on the species which has the highest proton affinity (PA). For hydrocarbon molecules the PA generally increases with size. Also the PA of molecules in a homologous series is inversely related to the ionization potentials of the members[23] so this would also indicate that large molecules (or particles) would have high PAs and therefore scavenge charge from molecular-sized ions rather than create them.

Condensation reactions of the type

$$M_1 + M_2 = M_3$$
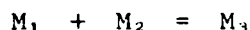
produce M_3 molecules with large excess internal energies. The M_3 species may dissociate if the collision rate is insufficient for it to be stabilized. We here point out that such condensation processes involving large molecules (particles ?) release sufficient energy in some cases for ionization to occur. The reaction

$$C_{16}H_{10} + C_6H = C_{22}H_{11}^+ + e^- \qquad \Delta H \stackrel{\sim}{\sim} -30 \text{ kcal mol}^{-1} \qquad (12)$$

is a (merely illustrative) example.

The sudden appearance and disappearance of "ions > 300" in the flame front, e.g., Fig. 8, followed by ions of lower mass, which must be intermediates in forming "ions > 300," appears to be incongruous. The formation of these large ions so early in the flame front implies extremely rapid ion-molecule reactions--

17

a basic tenet of our argument. The initially produced small ions rapidly pro-
duce larger ions before they can be detected. This also occurs in lean flames
where the chemi-ion CHO^+ is not the first or most dominant ions observed.[7] The
rapid decay of these large ions, presumably due to ion-electron recombination
or oxidation—leaving a smaller ion—and the persistence of smaller ions, can
be interpreted as a decrease in the availability of building blocks necessary
for sustaining the > 300 ions downstream. The smaller ions can continue to be
formed from $C_3H_3^+$. More quantitative data will be required to test this
interpretation.

THERMODYNAMIC ARGUMENTS

Tanzawa and Gardiner[24],[25] studied the pyrolysis of acetylene and were able
to develop a kinetic mechanism capable of explaining their data and all previous
shock tube data from 600 to 3400 K. As a minor part of this work they examined
which species were likely to play an important role in soot formation. They
concluded thermodynamically that large C_nH_2 and C_nH species would never reach
high enough concentrations to form soot at the observed rate. A kinetic system
of faster reactions and involving species of greater stability at high tempera-
ture was required.

Stein[26] investigated the high temperature equilibrium of selected polycyclic
aromatic hydrocarbons (PCAH) with acetylene and hydrogen using the group additivity
techniques developed by Benson and coworkers[27] to obtain thermochemical param-
eters. He found that above 1700 K, for a series of PCAH the equilibrium concen-
trations pass through a minimum dependent upon the temperature and concentration
of C_2H_2 and H_2. Essentially a benzene condensation mechanism forming large
cyclic molecules was studied and some characteristics of a nucleation process
found. The molecules for which lowest concentrations were predicted could act

as critical species and be involved in the rate limiting reaction. The identity of these critical species is dependent upon specific conditions, but they were found to be approximately in the 20 to 50 carbon range.

Thermodynamic arguments are very useful, but it is likely that the dynamics of intact benzene ring condensation are too slow for this simple picture to be very realistic. The crucial question is how to obtain molecular species, almost certainly PCAHs, larger than some critical size on a very short time scale. We think this is the essence of the nucleation problem of soot formation and that these molecules may grow as ions and be neutralized after they have passed the critical size. Beyond that point they would continue to grow into particles.

It is informative to look at the thermodynamics of the ionic species observed in rich and sooting flames. These data are also required for kinetic modeling of the process. We find, however, that experimental data are not available for many of these low H/C ratio species. Most ionic hydrocarbon thermodynamic information has been obtained by electron impact at room temperature so that flame ion species are relatively uncharacterized. For example, a recent comprehensive source of thermodynamic data[28] on gaseous ions lists 22 odd and 61 even mass species between C_{14} and C_{30} which have been studied. Flame ions are all odd mass species. Since tabulated thermodynamic data are not available for many ionic species observed in our rich flames, we have used the group additivity technique to calculate these data for some of the species experimentally observed and proposed to be important in soot formation. Properties of the relevant neutral molecules were calculated as functions of temperature and the ionization potential (IP) used to calculate the ΔH_f of the ionic species. To estimate the IP of molecules for which experimental values are not available we examined the available data[28] for trends and used a smooth curve through the experimental results to estimate ($\pm$ 50 kJ mol^{-1}) needed values. There are probably much better methods to estimate these data. Even so, the major uncertainty

19

in estimating heats of formation is not the technique but the choice of iso-
mers at a particular mass. Even though ions are known to rearrange very rapidly
to more stable structures[23,29,30] (an advantage of the ionic mechanism over neu-
tral mechanisms), we do not know where kinetic constraints will be present so
that the observed ion is a less stable isomer.

Figure 12 shows estimated heats of formation (298 K) for hydrocarbon ions
between C_1 and C_{23} along with selected neutral species. The data are plotted
vs. carbon number where linearly increasing trends in the ΔH_f of $C_x H_n$ vs. X
indicate that group additivity is followed. Data for $C_n H_2$, $C_n H$, and PCAH neu-
trals are also shown. The curve for the largest ions, $C_n H_{12}{}^+$, is seen to be
approximately parallel to that for PCAH neutrals and separated by 550–650 kJ
mol^{-1} (6 to 7 eV), a reasonable ionization potential for such molecules. One
sees that thermodynamically you cannot create larger and larger molecules (or
ions) with the same number of hydrogens (such as increasingly larger polyacety-
lenes); the lines are simply too steep. On the other hand, for the proposed
ionic mechanism the major species would move across this figure at about the
same level of heat of formation, ± about 100 kJ mol^{-1}. Clearly more careful
thermodynamic considerations are warranted using better data (estimated or
measured) and free energy rather than heat of formation and including other
reactants and products.

KINETIC ARGUMENTS

A chemical kinetic mechanism for soot formation is necessarily very compli-
cated since many species are involved and the physical change from gaseous to
condensed matter requires many steps. Nucleation phenomena in general are
only poorly understood. Our basic hypothesis is that, in parallel to a
neutral-radical chain reaction mechanism of $C_2 H_2$ pyrolysis and combustion,

there exists an ion-molecule mechanism which very rapidly produces large
aromatic ions and by ion recombination large aromatic molecules (incipient
soot particles) which then grow further by neutral and/or ion-molecule sur-
face growth and coagulation. The objective is to develop a mechanism of
"getting over the hump" to these large molecules; this is the nucleation
process.

A series of ion molecule reactions is shown in Table II which comprises a
subset of an overall mechanism considering only gaseous species. The primary
ions are assumed to be produced by the usual flame chemi-ionization reactions
although (cf. Section 2) these are not well established under fuel rich condi-
tions. Whatever the actual chemi-ionization reaction, we assume $C_3H_3^+$ to be
produced and propose the ion-molecule sequence for growth to large PCAH ions.
Most of the growth flux is probably due to reaction of ionic species with C_2H_2
and C_4H_2, although C_2H, C_4H, and C_6H_2 may be present in large enough concentra-
tions to contribute under some conditions.

In order to test such a mechanism we have performed preliminary computer
simulations of an acetylene/oxygen system. The objective was not realistic
modeling of a flame but simply to see if this kinetic scheme would show rapid
growth of large ions, up to about C_{30}. Particles have not been considered up
to now.

Briefly, the computations were done using a computer program simulating an
adiabatic one-dimensional flow tube. Thermodynamic parameters for neutral
species were obtained from the JANAF tables[31] or other published data,[32] whereas
ionic species data were estimated as discussed above (using experimental data
where available). The calculation was initiated at 1100 K with a $C_2H_2/O_2/N_2$
mixture at 2.7 kPa containing small amounts of CO, H_2, and H atoms. About 65
reactions of 35 species were considered. This mixture was calculated to ignite

21

after 20 ms (1 cm distance at 50 cm s^{-1})* reaching a maximum temperature of 2200 K. The equivalence ratio of the initial mixture was 3.5.

The neutral portion of the reaction mechanism consists basically of an acetylene pyrolysis scheme[24] combined with an acetylene oxidation scheme.[33] Thirty ion molecule reactions were added to test whether species up to $C_{37}H_{11}^+$ could be produced. Only the CH^*/C_2H_2 chemi-ionization reaction was used. All ion-molecule reactions were arbitrarily given the same rate constant, $k = 2 \times 10^{-11}$ cm^3 s^{-1}.

A discussion of the results of these calculations should be prefaced by a clear statement that (1) we do not intend that this is a computationally accurate description of a flame, (2) the combustion mechanism is not complete and was not checked against any data, and (3) the ionic mechanism is only a part of what would be required to describe ion chemistry under these conditions. What we did want to test was whether, given a mechanism such as in Table II with reasonable rate constants, large ions would grow to high enough concentrations and rapidly enough to support our hypothesis. If so, calculations similar to these may help to analyze the complex processes going on in a sooting flame.

Results of a typical simulation run are shown in Fig. 13 for selected neutral and ionic species concentrations and the temperature. The total ion concentration peaks at about 1.8 cm at a value of 4×10^9 cm^{-3} with most species rapidly disappearing after the flame zone and $C_3H_3^+$ persisting and only slowly decaying. The neutral species profiles are reasonable for a nonsooting flame with large concentrations of polyacetylenes calculated. Except for the $C_7H_7^+$

---

* Diffusion of radical species from the flame zone toward the burner into the unburned gases is, of course, important in ignition processes. Realistic simulations of flame structure must consider mass and thermal diffusion. Our simplified calculation does, however, serve to investigate chemical processes on a semiquantitative basis.

22

profile, the ionic profiles are very similar to those observed experimentally in rich nonsooting acetylene flames with heavy species rapidly peaking and $C_3H_3^+$ persisting. Although we have only limited data on absolute concentrations of these species, the calculated values are close to experimental results. All of the ions are produced via the CH^*/C_2H_2 reaction (with CH^* from $C_2H + O = CH^* + CO$) with other possible sources ignored. The ion concentrations may therefore be artificially low. These results clearly point out a mistake that is often made deducing mechanistic information from relative positions of peak concentrations or even relative concentrations. This mechanism produces $C_3H_3^+$ as the only primary ion, yet the concentration of this ion is not always the highest even early in the reaction and in particular its profile does not peak prior to other species. In a complex reacting system the ranking of species profile peaks may bear little or no relationship to the sequence in which they are produced.

The $C_7H_7^+$ concentration shown in Fig. 13 is much larger than observed in experiments mainly due to a low heat of formation attributed to this ion (assumed to be benzyl, $\Delta H_f = 910$ kJ mol^{-1}). This unusually stable ion therefore forms a sink in the ion-molecule sequence and its concentration reaches a large value. Since high concentrations of this ion are not observed we conclude that the actual ion is not benzyl but some less stable isomer. The calculated results were found to be very sensitive to assumed thermodynamic properties of the more stable species leading us to the prediction that if there is a large ion of very high stability its concentration could quickly become large. If its stability is very large compared to the next species in the growth sequence this would act as a terminating point in the growth sequence. Again the importance of the thermodynamics of large ions to the arguments of the proposed ionic mechanism is emphasized. Further work will be necessary to test these ideas.

23

CONCLUSIONS

The data obtained in this study are consistent with a mechanism for soot formation in which chemi-ions are the precursors of soot in spite of several unexplained observations mentioned above. We find large ions formed early in nonsooting flames and see their concentrations fall very rapidly beyond the flame zone. In sooting and nearly sooting flames the concentration of this group of ions builds several orders of magnitude higher and remains high throughout the flame. The abrupt shift from $C_3H_3^+$ as the major charged species to large ions predominating is the main feature that changes in going from nonsooting to sooting flames. In sooting flames an unexplained second source of molecular ions increases the total ion concentration beyond the flame zone and gives dual peaked concentration profiles.

Thermodynamic properties of low H/C ratio hydrocarbon ions have been estimated to allow preliminary testing of the thermodynamics and kinetics of the proposed ionic mechanism of soot formation. Kinetic modeling shows that sufficient concentrations of multi-ring aromatic ions can be produced rapidly. Further work will consider particle formation and growth.

We conclude that the ionic mechanism of soot formation warrants further study.

ACKNOWLEDGMENTS

REFERENCES

1. Palmer, H.B. and Cullis, C.F., in Chemistry and Physics of Carbon, Vol. 1 P.L. Walker, Ed. (Marcel Dekker, New York, 1966) p. 265.

2. Calcote, H.F., March, 1980; Accepted for publication in Combust. Flame.

3. Olson, D.B. and Calcote, H.F., Eighteenth Symposium (International) on Combustion (The Combustion Institute, Pittsburgh, in press).

4. Calcote, H.F., Eighth Symposium (International) on Combustion (Williams and Wilkins Co., Baltimore, 1962) p. 184.

5. Peeters, J. and Vinckier, C., Fifteenth Symposium (International) on Combustion (The Combustion Institute, Pittsburgh, 1975) p. 969.

6. McGowan, J.W., Mul, P.M., D'Angelo, V.S., Mitchell, J.B.A., Defrance, P., and Froelich, H.R., Phys. Rev. Lett. 42, 373 (1979).

7. Calcote, H.F. and Miller, W.J., in Reactions Under Plasma Conditions, Vol. II, M. Venugopalan, Ed. (John Wiley & Sons, New York, 1971) p. 327.

8. Goodings, J.M., Bohme, D.K., and Sugden, T.M., Sixteenth Symposium (International) on Combustion (The Combustion Institute, Pittsburgh, 1977) p. 891.

9. Calcote, H.F., in Ion-Molecule Reactions, Vol. 2, J.L. Franklin, Ed. (Plenum Press, New York, 1972) p. 673.

10. Miller, W.J., Eleventh Symposium (International) on Combustion (The Combustion Institute, Pittsburgh, 1967) p. 311.

11. Calcote, H.F., Kurzius, S.C., and Miller, W.J., Tenth Symposium (International) on Combustion (The Combustion Institute, Pittsburgh, 1965) p. 605.

12. Glass, G.P., Kistiakowsky, G.B., Michael, J.V., and Niki, H., J. Chem. Phys. 42, 608 (1965).

13. Knewstubb, P.F. and Sugden, T.M., Seventh Symposium (International) on Combustion (Butterworths, London, 1959) p. 247.

14. Miller, W.J., Oxid. Combust. Rev. 3, 97 (1968).

15. Bowser, R.J. and Weinberg, F.J., Combust. Flame 27, 21 (1976).

16. Prado, G.D. and Howard, J.B., in Evaporation-Combustion of Fuels, J.T. Zung, Ed. (American Chemical Society, Washington, DC, 1978) p. 153.

17. Wersborg, B.L., Yeung, A.C., and Howard, J.B., Fifteenth Symposium (International) on Combustion (The Combustion Institute, Pittsburgh, 1975) p. 1439.

18. Delfau, J.L., Michaud, P., and Barassin, A., Combust. Sci. Technol. 20, 165 (1979).

19. Homann, K.H., Ber. Bunsenges. Phys. Chem. 83, 738 (1979).

20. Jensen, D.E. and Miller, W.J., J. Chem. Phys. 53, 3287 (1970).

21. Bittner, J.D. and Howard, J.B., Eighteenth Symposium (International) on Combustion (The Combustion Institute, Pittsburgh, in press).

22. Michaud, P., personal communication, 1980.

23. Lias, S.G. and Ausloos, P., Ion-Molecule Reactions. Their Role in Radiation Chemistry (The American Chemical Society, Washington, DC, 1975) p. 94.

24. Tanzawa, T. and Gardiner, W.C., Jr., Seventeenth Symposium (International) on Combustion (The Combustion Institute, Pittsburgh, 1979) p. 563.

25. Tanzawa, T. and Gardiner, W.C., Jr., J. Phys. Chem. 84, 236 (1980).

26. Stein, S.E., J. Phys. Chem. 82, 566 (1978).

27. Stein, S.E., Golden, D.M., and Benson, S.W., J. Phys. Chem. 81, 314 (1977).

28. Rosenstock, H.M., Draxl, K., Steimer, B.W., and Herron, J.T., J. Phys. Chem. Ref. Data 6, 1977, Suppl. No. 1.

29. McLoughlin, R.G., Morrison, J.D., and Troeger, J.C., Organic Mass Spectr. 14, 104 (1979).

30. Bowen, R.D. and Williams, D.H., J. Amer. Chem. Soc. $\underline{100}$, 7454 (1978).

31. Stull, D.R. and Prophet, H., JANAF Thermochemical Tables, Second Ed., NSRDS-NBS-37 (National Bureau of Standards, Washington, DC, 1971).

32. Duff, R.S. and Bauer, S.H., J. Chem. Phys. $\underline{36}$, 1754 (1962).

33. Jachimowski, C.J., Combust. Flame $\underline{29}$, 55 (1977).

TABLE I

Comparison of Total Ion Concentrations in Acetylene Flames.

	Electrostatic Probe		Molecular Beam Sampling	
	Prado et al.[16]	Delfau et al.[18]	Wersborg et al.[17]	Homann[19]
Oxidizer	O_2	$N_2/O_2 = 0.6$	O_2	O_2
Pressure, Torr	20	45	20	20
Flow velocity, cm s^{-1}	50	27	38	44
Equivalence ratio	3.5	3.0	3.0	2.9
Equivalence ratio at soot point	2.4	2.2	?	2.5
Height in flame for peak ion concentration, cm	2.0	1.5	2.0	1.3
Description of what is measured	≈ 4 nm particles	large ions > 700 amu	ions > 300 amu	large ions about 40–200 amu
Ion concentration, ions cm^{-3}	4×10^{10}	1.3×10^{10}	8×10^{10}	3×10^{8}

8

TABLE II

Proposed Ion-Molecule Mechanism

$$CH + O = CHO^+ + e^-$$

$$CH^* + C_2H_2 = C_3H_3^+ + e^-$$

$$C_2 + CH_3 = C_3H_3^+ + e^-$$

$$C_3H_3^+ + e^- = \text{neutral products}$$

$$C_3H_3^+ + \left\{ \begin{array}{l} C_2H_2 = C_5H_5^+ \\ C_4H_2 = C_5H_3^+ + C_2H_2 \\ C_4H_2 = C_7H_5^+ \end{array} \right.$$

$$C_5H_3^+ + \left\{ \begin{array}{l} C_2H_2 = C_7H_5^+ \\ C_4H_2 = C_7H_3^+ + C_2H_2 \\ C_4H_2 = C_9H_5^+ \end{array} \right.$$

$$C_5H_5^+ + \left\{ \begin{array}{l} C_2H_2 = C_7H_5^+ \\ C_4H_2 = C_7H_5^+ + C_2H_2 \\ C_4H_2 = C_9H_5^+ \end{array} \right.$$

$$C_7H_5^+ + \left\{ \begin{array}{l} C_2H_2 = C_9H_7^+ \\ C_4H_2 = C_9H_5^+ + C_2H_2 \\ C_4H_2 = C_{11}H_7^+ \end{array} \right.$$

$$C_7H_7^+ + \left\{ \begin{array}{l} C_2H_2 = C_9H_9^+ \\ C_4H_2 = C_9H_7^+ + C_2H_2 \\ C_4H_2 = C_{11}H_9^+ \end{array} \right.$$

$$C_9H_7^+ + \left\{ \begin{array}{l} C_2H_2 = C_{11}H_9^+ \\ C_4H_2 = C_{11}H_7^+ + C_2H_2 \\ C_4H_2 = C_{13}H_9^+ \end{array} \right.$$

etc.

FIGURE CAPTIONS

FIGURE 1 EFFECT OF FLAME COMPOSITION ON PEAK ION CURRENTS FOR 0.5 kPa
ACETYLENE/OXYGEN FLAMES. (From Ref. 11)

FIGURE 2 EFFECT OF EQUIVALENCE RATIO ON PEAK ION CURRENTS FOR 2.0 kPa
ACETYLENE/OXYGEN FLAMES. The shaded area indicates the minimum
equivalence ratio for soot formation.

FIGURE 3 EFFECT OF EQUIVALENCE RATIO ON TOTAL ION CURRENTS DIVIDED INTO
TWO BROAD MASS CLASSES FOR 2.0 kPa ACETYLENE/OXYGEN FLAMES.
The shaded area indicates the minimum equivalence ratio for
soot formation.

FIGURE 4 FLAME ION SAMPLING MASS SPECTROMETER.

FIGURE 5 EFFECT OF UNBURNED GAS VELOCITY, cm s^{-1}, ON TOTAL SMALL ION
PROFILE FOR 2.7 kPa ACETYLENE/ OXYGEN FLAMES.

FIGURE 6 ION MASS SPECTRA TAKEN 1.0 cm FROM THE BURNER SURFACE FOR A
NONSOOTING AND A SOOTING 2.0 kPa ACETYLENE/OXYGEN FLAME. ϕ_c = 2.6.

FIGURE 7 ION MASS SPECTRA TAKEN AT 1.0 cm AND 2.0 cm FROM THE BURNER SURFACE
FOR A NEARLY SOOTING 2.0 kPa BENZENE/OXYGEN FLAME. ϕ_c = 1.85.

FIGURE 8 ION PROFILES FOR A 2.0 kPa NONSOOTING, ϕ = 2.0, ACETYLENE/
OXYGEN FLAME. Calculated adiabatic flame temperature is 2300 K.

FIGURE 9 ION PROFILES FOR A 2.0 kPa SOOTING, ϕ = 2.7, ACETYLENE/OXYGEN
FLAME. Calculated adiabatic flame temperature is 2170 K.

FIGURE 10 EFFECT OF EQUIVALENCE RATIO ON LARGE ION PROFILES IN SIX 2.0
kPa ACETYLENE/OXYGEN FLAMES. Transition to sooting occurs
between ϕ = 2.5 to 2.75.

FIGURE 11 ION PROFILES FOR A 2.0 kPa NEARLY SOOTING, ϕ = 1.8, BENZENE/
OXYGEN FLAME. Calculated adiabatic flame temperature is 1900 K.

FIGURE 12 HEAT OF FORMATION TRENDS FOR $C_xH_y^+$ FAMILIES WHERE THE NUMBER
OF HYDROGENS, y, IS INDICATED FOR EACH LINE. Also shown are
C_nH, C_nH_2, and PCAH neutral species trends. Uniquely stable
ions differ somewhat from these lines.

FIGURE 13 CALCULATED CONCENTRATION PROFILES FOR A 2.7 kPa ACETYLENE/
OXYGEN/NITROGEN FLAME. The simulation is initialized at 1100 K
and considers 65 reactions of 35 species. All ion-molecule
reactions are given a k = 2 × 10^{-11} cm^3 s^{-1}. No condensed phase
is considered.

30

FIGURE 1

31
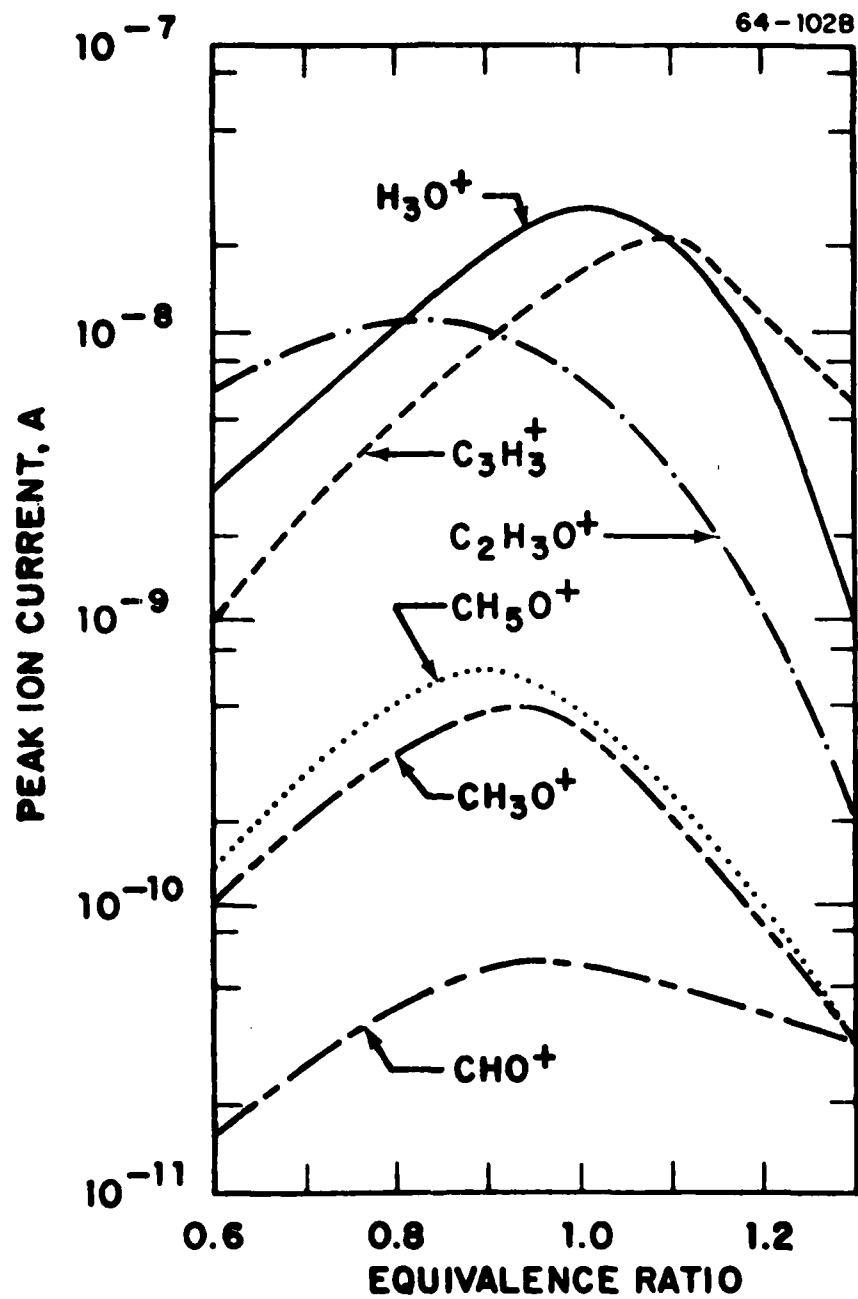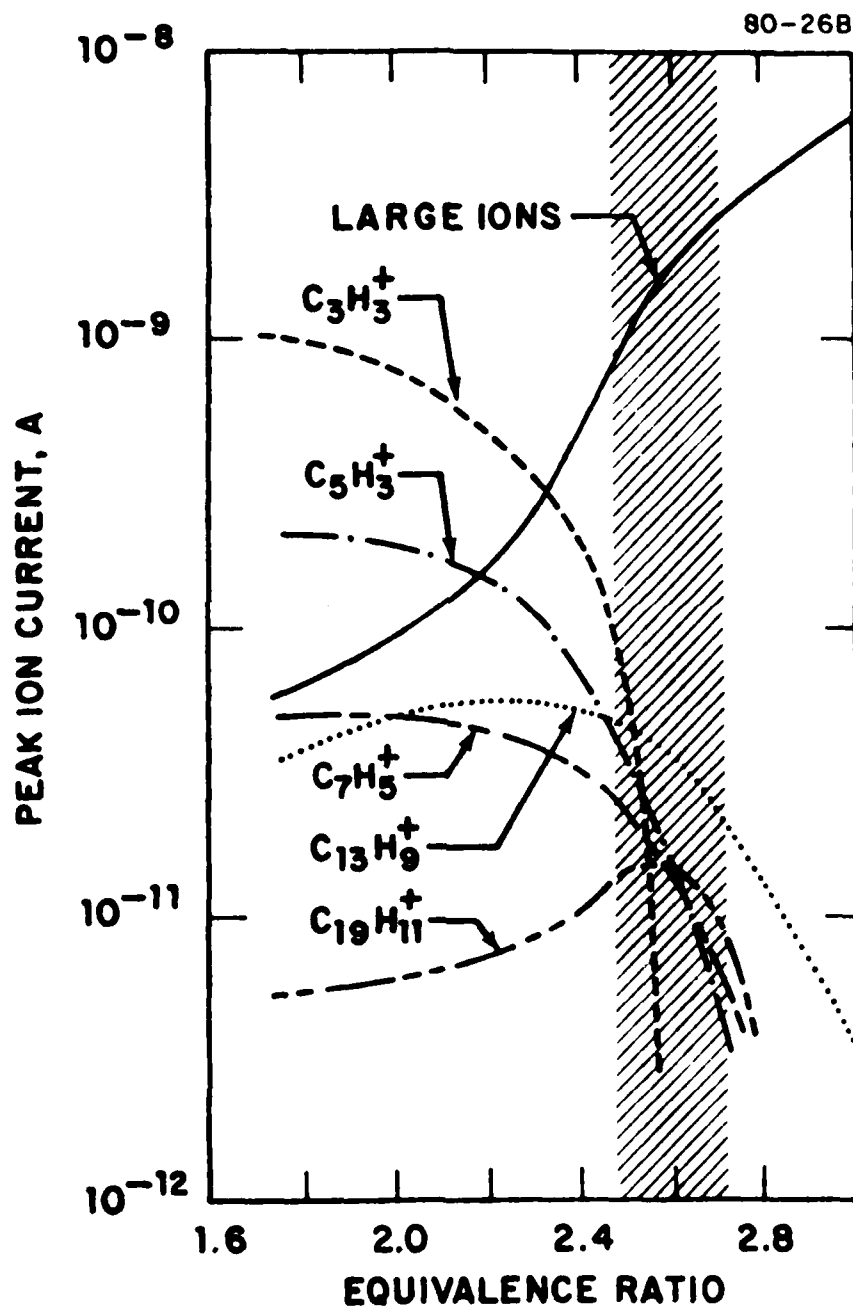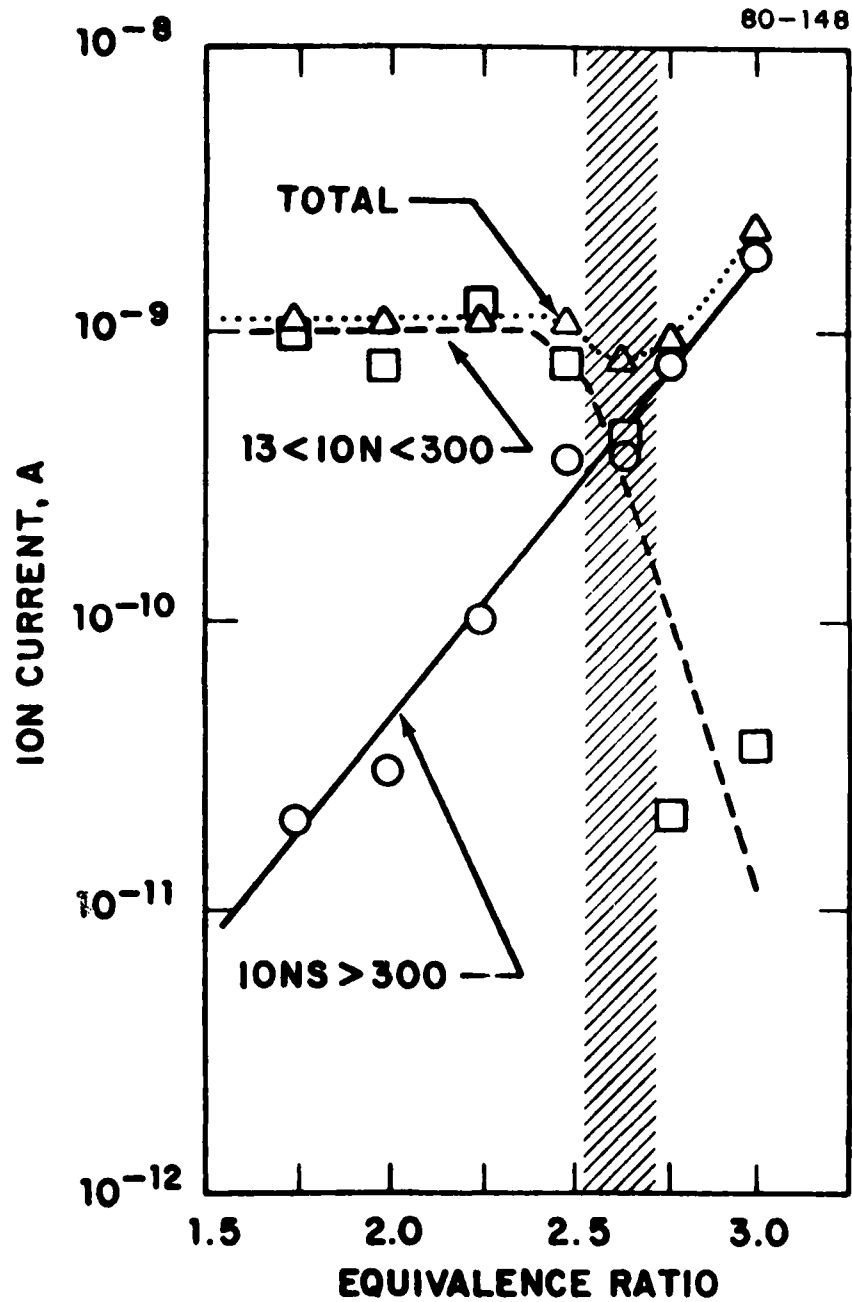
FIGURE 2

FIGURE 3

33
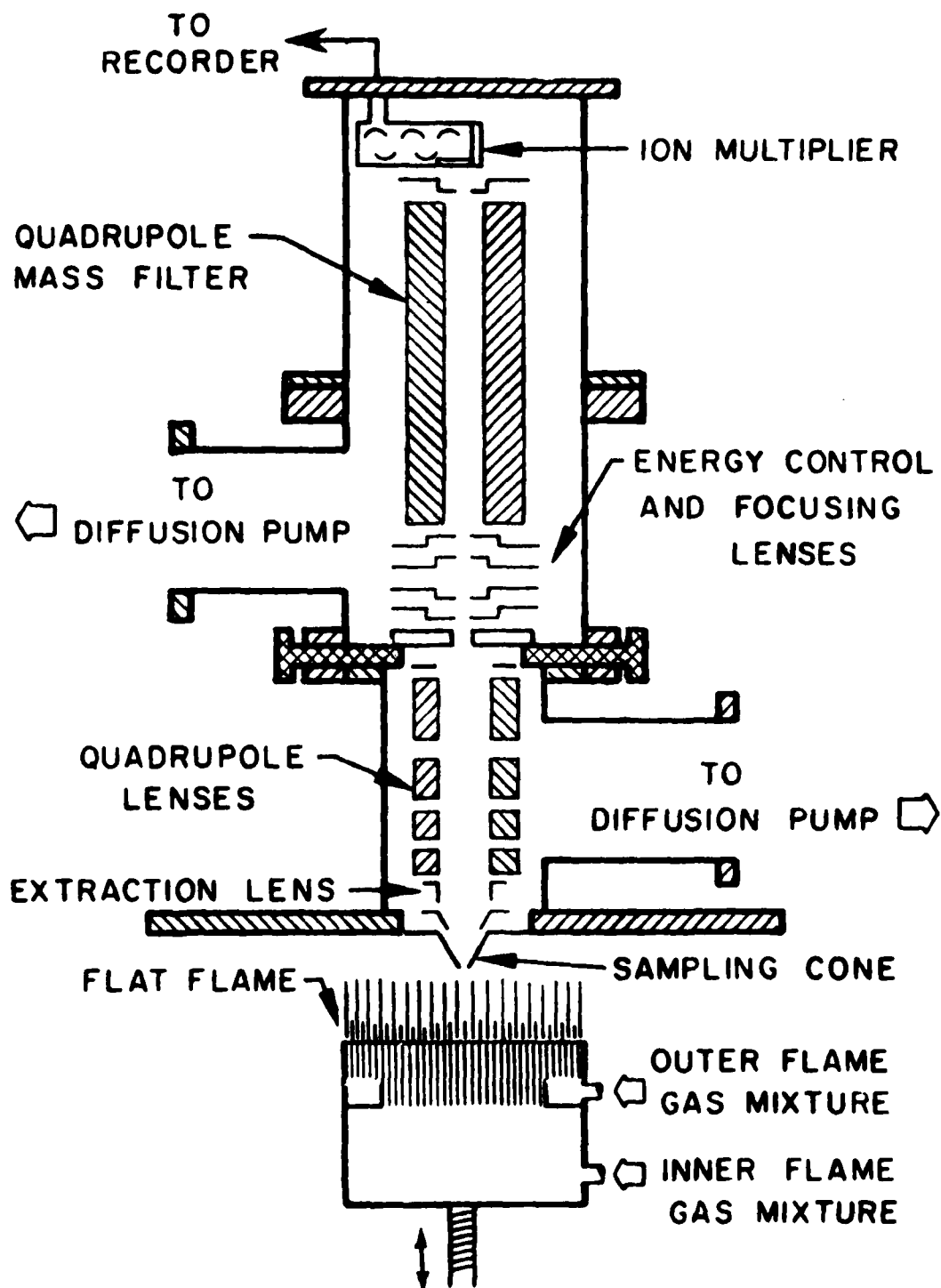
FIGURE 4

FIGURE 5

FIGURE 6
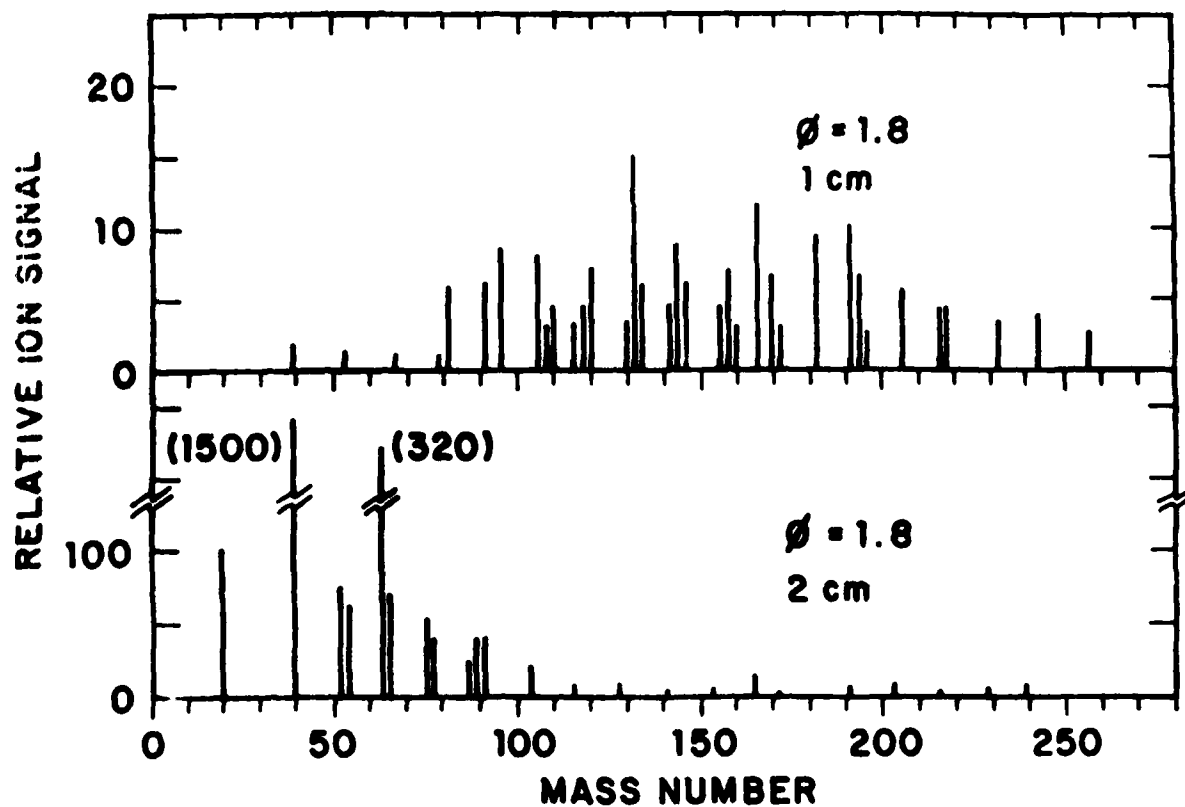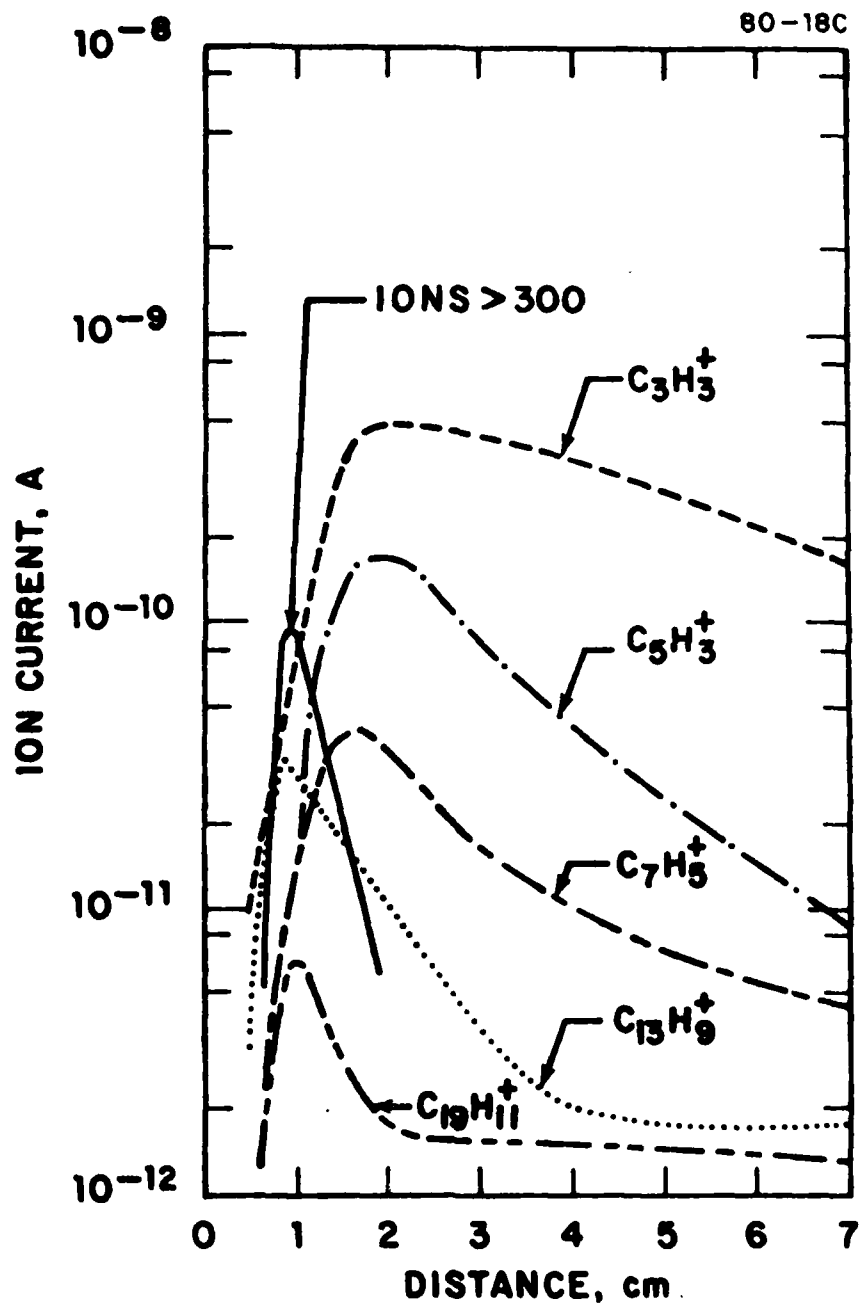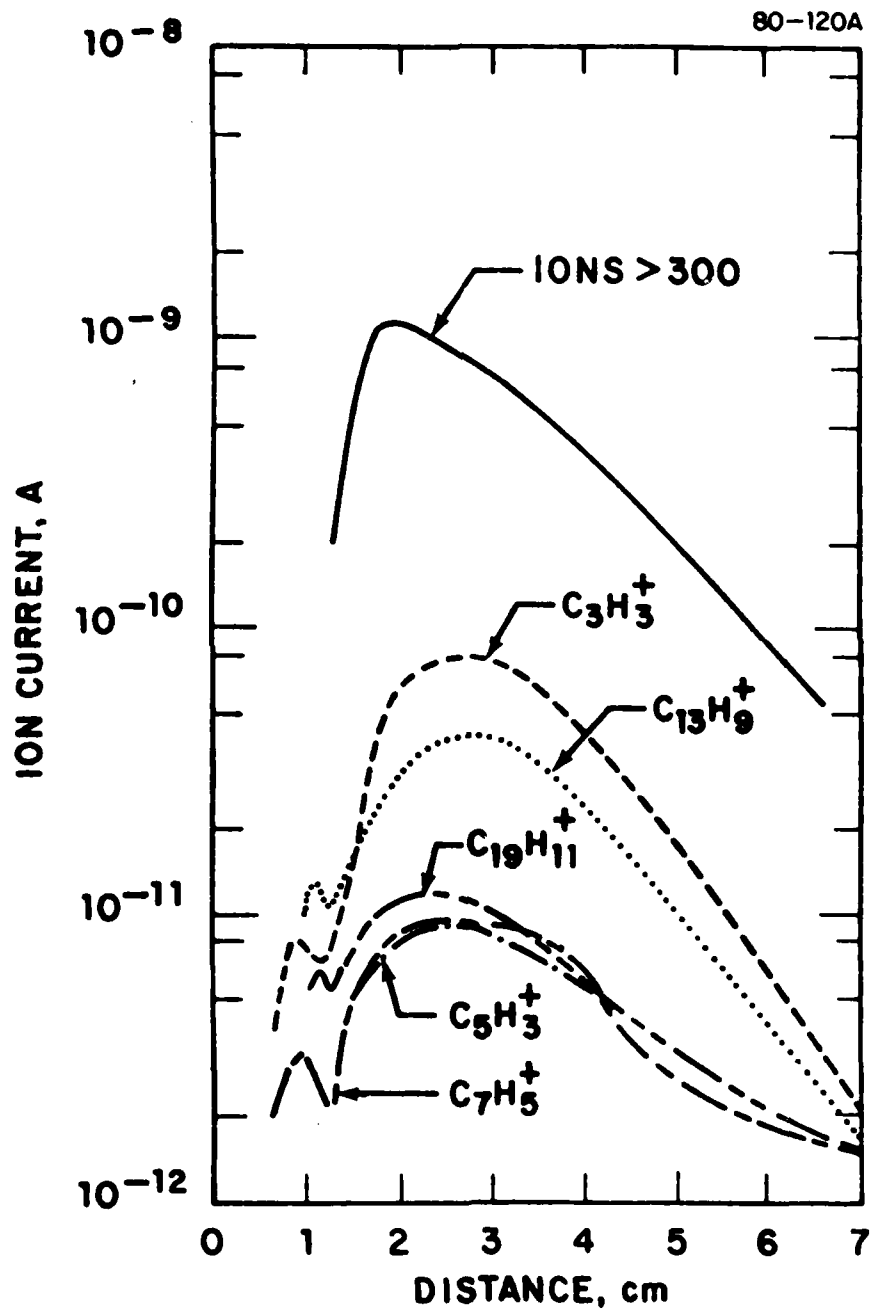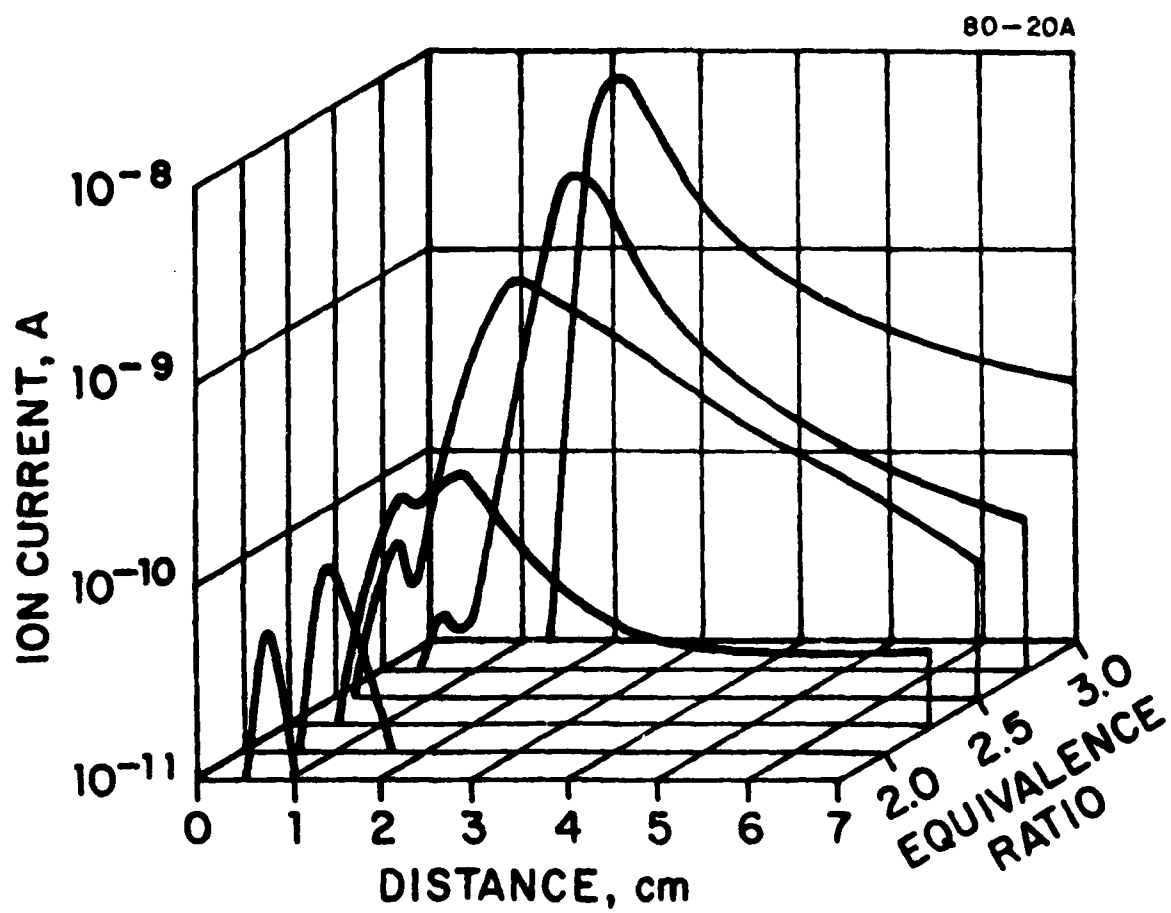
FIGURE 7

FIGURE 8

38

FIGURE 9

39

FIGURE 10

40

FIGURE 11

41

FIGURE 12

80 – 110A

FIGURE 13

43

APPENDIX   D
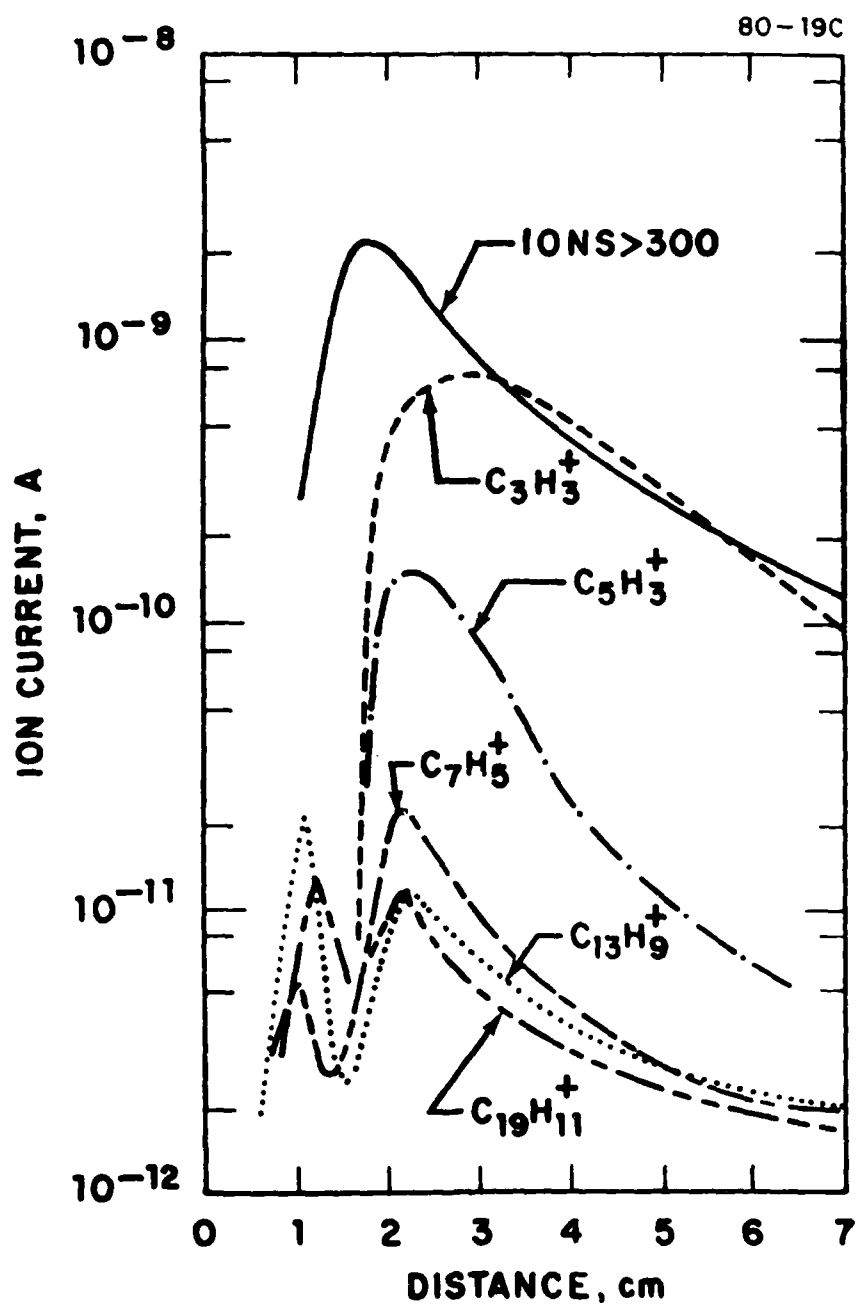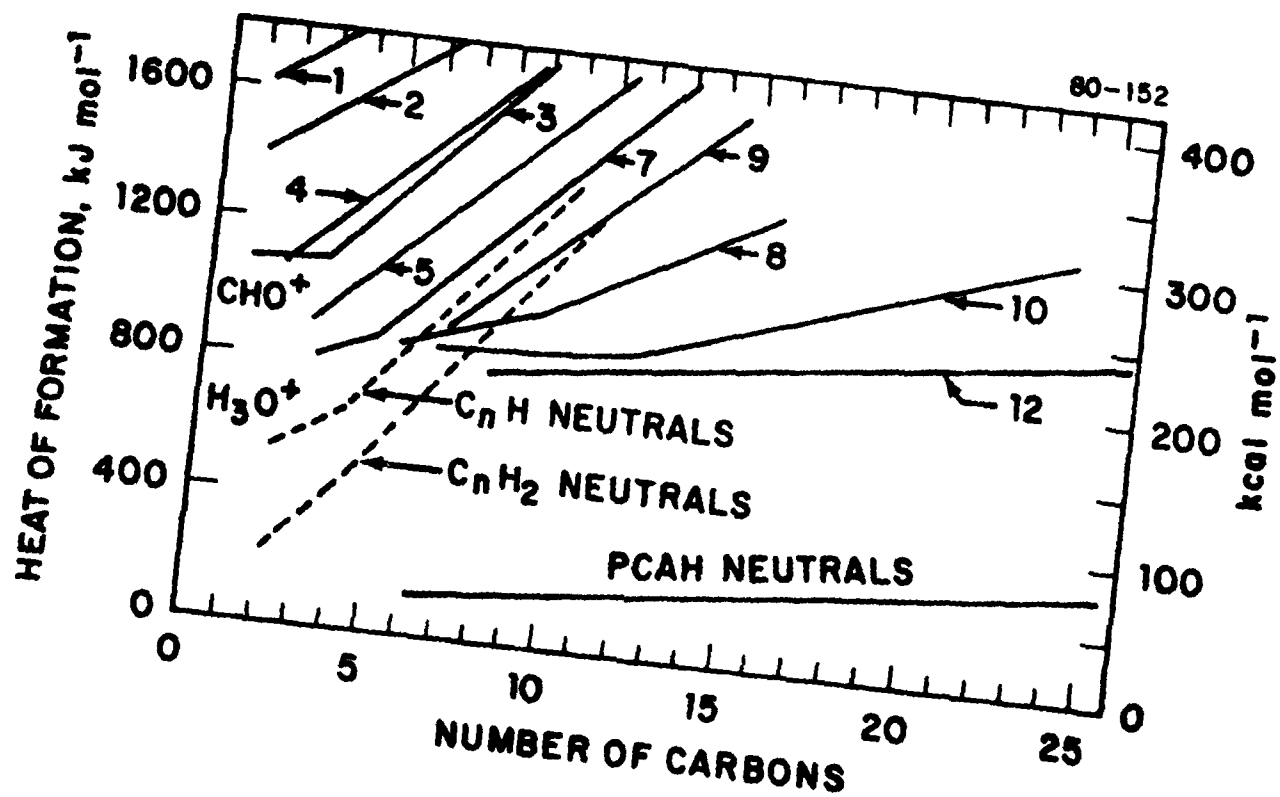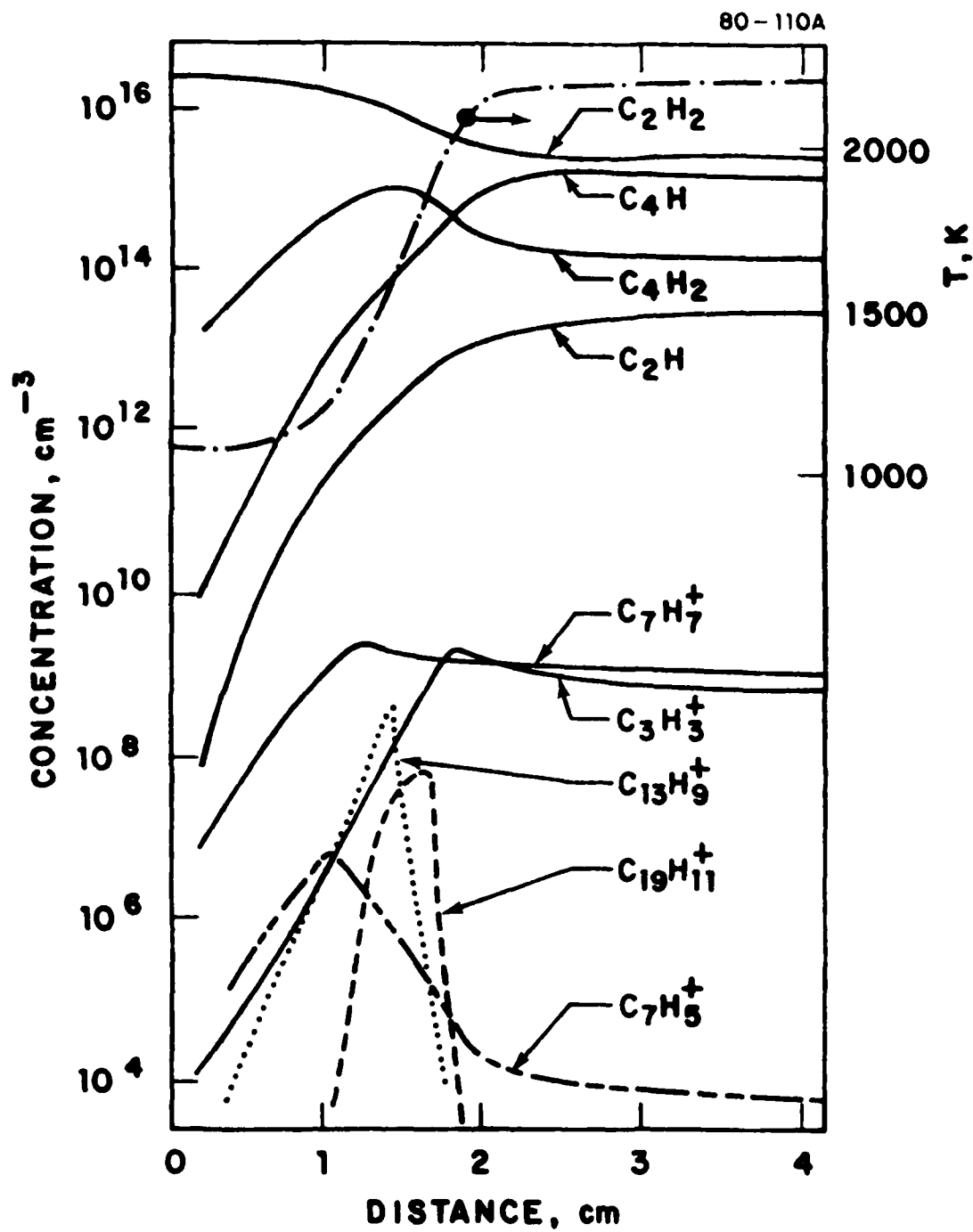
Effect of Molecular Structure on
Incipient Soot Formation

H.F. CALCOTE and D.M. MANOS*

AeroChem Research Laboratories, Inc.
P.O. Box 12, Princeton, New Jersey 08540

ABSTRACT

By defining a rational threshold soot index, TSI, varying from
0 to 100 to measure the onset of soot formation in both premixed and
diffusion flames, it is shown that all of the data in the literature
on premixed and diffusion flames, taken by many techniques, are con-
sistent with respect to molecular structure for the two types of
flames. There is a closer similarity between the effect of molecular
structure on soot formation in premixed and diffusion flames than pre-
viously thought. The use of TSI permits one to use all of the litera-
ture data to interpret molecular structure effects and thus arrive at
rules for predicting the effect of molecular structure for compounds
which have not yet been measured or to convert the results from one
experimental system to another. If a correlation can be demonstrated
between the effect of molecular structure on soot formation in the
laboratory and in practical systems, the TSI's will be important to
the synfuels program in defining the desired fuels to be prepared
from a given feed stock.

---

* Present address: Plasma Physics Laboratory, Princeton University,
  Princeton, NJ.

INTRODUCTION

As synfuels play a greater role in meeting future energy demands, a better

understanding of the factors governing their propensity to form soot is required.

Quantitative prediction of the soot forming characteristics of new fuels can

best be achieved from an understanding of the quantitative behavior of their

individual hydrocarbon constituents.

There are two distinct facets to the consideration of the effects of fuel

molecular structure on sooting. First, as a given premixed fuel/oxidant combina-

tion is made fuel rich (or as the primary aeration of a diffusion flame is

decreased), a rather sharp onset of sooting is observed. This facet of the

tendency to soot is important in practical applications where the total absence

of sooting is desirable. The second facet is that further increasing the fuel

concentration beyond the point of soot onset causes increasingly greater quanti-

ties of soot to form at a rate which depends on fuel structure. In this paper

we concentrate on the specification of the onset of soot formation. Data from

a variety of measurements made in both premixed and diffusion flames have been

gathered from the literature and correlated on this aspect of sooting. The

objective was to determine the degree of consistency, or inconsistency, of the

data in the literature on the effect of molecular structure on soot formation

in both premixed and diffusion flames, and the relationship, if any, between

the two types of flames. Assuming a consistency is established for the data,

then the objective would be to deduce an empirical description of how molecular

structure controls the onset of soot. Other people have considered the effect

of molecular structure on soot formation but have limited themselves to data

collected in a single type of apparatus where they have been limited by the

number of compounds studied. These studies usually conclude that certain

trends in the effect of molecular structure agree with results of previous

2

work, although significant differences in the actual numerical values occur between different studies. In this study we have made such comparisons quantitative so that separately obtained sets of data can be compared directly and so that all of the available data can be used to deduce molecular structure effects.

We define a "threshold soot index" (TSI) which ranks the fuels from 0 to 100, (0 = least sooty), independent of the particular experimental apparatus in which the data were obtained. A quantitative value for each molecule is thus obtained so that different molecules studied by different investigators (using different experimental apparatus) can be considered in elucidating the effect of molecular structure on soot formation. One of the first objectives will be to demonstrate the validity of the assumption of consistency underlying this statement.

This kind of information should be of great value in attempts to understand the relationship between laboratory data and engine data. Such correlations, if they could be demonstrated, would reduce the number of engine tests required to establish the effect of molecular structure on engine performance. The real impact should be on the synfuels engineer in determining the type of molecules to strive for in the refining processes. The situation is analogous to the empirical understanding of the relationship between octane or cetane number and molecular structure and the objectives of petroleum engineers in structuring the products of petroleum refineries.

SOURCES OF DATA

The data on incipient soot formation are divided into two categories: premixed flames and diffusion flames. Data on premixed flames were taken from Street and Thomas [1], Wright [2], Calcote and Miller [3], Grumer, Harris and Rowe [4], and Blazowski [5]. Data on diffusion flames came from the work of

Minchin [6], Clarke, Hunter, and Garner [7], Hunt [8], Schalla and McDonald [9], Van Treuren [10], and Schug, Manheimer-Timnat, Yaccarino, and Glassman [11]. In addition to measurements on pure hydrocarbons, some of these workers studied fuels consisting of mixtures of hydrocarbons and organic compounds containing heteroatoms (O, N, S, Cl, etc.). Only the reported data on unblended hydrocarbons, C_nH_m, are considered here.

The most extensive data set from premixed flames is that of Street and Thomas [1]. These authors used an apparatus in which a flow of fuel was mixed with air to form either a vapor mixture or fuel mist, according to the compound's vapor pressure. These mixtures were then burned in a shielded flame and the ratio of fuel/air was increased until a yellow tip was first observed. This critical composition was reported. Grumer et al. [4] burned only premixed fuel vapors, reporting fuel-air composition at the yellow-tip limit. Similar measurements on completely vaporized fuels were made by Calcote and Miller [3] with a shielded flame burner. They demonstrated a sensitivity of their results to the unburned mixture flow velocity, although at higher velocity their results were independent of velocity. Wright [2] used a heavily backmixed, jet-stirred combustor from which he reported the critical fuel/air ratio which caused the first visible appearance of soot on a probe filter placed in the reactor outlet. This reactor allowed richer mixtures to burn without sooting; a number of compounds found to soot in other premixed flame studies reached their rich blow-off limit without sooting in this apparatus. Additional studies from the same apparatus have been reported recently by Blazowski [5].

For diffusion flames Minchin [6] made measurements of the (now standard) smoke point employing a wick style burner in which the fuel flow was increased until soot was observed to be liberated from the tip of the flame. The flow

4

was decreased just enough to suppress the liberation of soot and the height of the flame, referred to as the "smoke point", was recorded. Hunt [8] performed the same type of measurement on a very large number of pure compounds, using a burner of different dimensions. Clarke and coworkers [7] also measured flame heights, as described above; however, they burned the liquids as pools in a funnel-shaped burner, rather than on wicks. By elevating the level of the liquid in such a funnel the area of the pool is increased and more fuel is vaporized into the flame. The physical characteristics of a duplicate of this burner were studied by Van Treuren [10] who reported excellent agreement with the values of Clarke et al. Van Treuren showed that the actual numerical results of such measurements depend strongly on the burner temperature and burner and chimney dimensions. Schalla and McDonald [9] used three different burners, one for gases and two for liquids. Liquids were burned either in a wick style lamp or in a burner with prevaporization. Rather than recording the flame height, Schalla and McDonald recorded the volume rate of fuel flow $(cm^3(STP)s^{-1})$ at the point where further increases in fuel flow caused the onset of soot. Glassman and associates [11] used an apparatus similar to that described by Schalla and Hubbard [12] consisting of a 1 cm i.d. central fuel jet and a 10 cm concentric confining tube through which the flow of air was regulated. Both sooting heights and the critical flow velocity were measured.

Because of the various experimental differences between these studies, a direct comparison of the quantitative results is not possible without further processing the data. We will now show how the data were treated to condense all premixed flame data and all diffusion flame data into two internally consistent data sets.

DEFINITIONS AND METHOD OF TREATING DATA

In this section we define a threshold soot index, TSI, which is derivable from measured quantities of both premixed and diffusion flames. This allows one to consider all of the data available in these categories and to quantitatively compare TSI for different types of molecules. Qualitative comparisons of this sort, though common [13,14], can be grossly misleading.

It is generally recognized that substances with lower smoke points are in some sense "sootier" than those with higher smoke points. Minchin defined a parameter called "tendency to smoke" as a constant divided by the smoke point. This definition has been accepted since his 1931 paper. Similarly, it has been recognized that in premixed flames the lower the carbon to oxygen ratio, C/O, or the lower the critical equivalence ratio,[1] ϕ_c, the greater the tendency of the fuel to soot.

In defining TSI it is desirable to define a parameter which reflects the correlation of incipient sooting with molecular structure, i.e., the oxidative chemistry of the fuel, and does not reflect differences in transport properties due to the nature of the measurement apparatus or the quantity of oxygen which must diffuse into the flame front (in the case of diffusion flames).

For a premixed flame, consider two hypothetical hydrocarbon fuels of very different molecular weights or C/H ratios both of which liberate soot when burned in a premixed flame with a stoichiometric amount of oxidizer. It is clear that a definition of TSI as

$$TSI = a - b\,\phi_c \tag{1}$$

---

[1] ϕ_c is defined as the minimum equivalence ratio, ϕ, for sooting where $\phi = $ (fuel flow/oxidizer flow)/(fuel flow/oxidizer flow)$_{stoichiometric}$.

with a and b constants for a given set of data will yield the same value for both of these hypothetical compounds. The use of C/O does not do this. We therefore adopt the definition of Eq. (1) in this work.

Minchin's definition of tendency to soot for diffusion flames as inversely proportional to the height of the flame which would just soot, contains an inherent flaw; it does not account for the increased height of the flame which would be required with increasing fuel molecular weights. An increase in molecular weight requires more oxygen to diffuse into the flame to consume a unit volume of the fuel. This can be accounted for by defining the threshold soot index for diffusion flames as:

$$TSI = a\left(\frac{MW}{h}\right) + b \tag{2}$$

where a and b are constants for any given experimental setup and h is the critical height of the flame for which soot is observed. A better approximation would be to employ the moles of air required for the combustion of one mole of fuel instead of M.W. The accuracy of the data and the arbitrariness of defining the products of combustion are such that the convenience of using the molecular weight is acceptable.

The critical volumetric flow velocity, V, is also used as a measure of the tendency to soot in diffusion flames. According to the Burke and Schuman theory of diffusion flames [15]

$$h = \frac{V}{4\pi C_f D} \tag{3}$$

where C_f is the concentration of fuel and D is an average diffusion coefficient of the system. This equation predicts a linear correlation between the height of a diffusion flame and the volumetric flow rate. This has been confirmed recently by Glassman and associates [11]. Thus we can also define

7

for a diffusion flame

$$TSI = a\left(\frac{MW}{V}\right) + b \qquad (4)$$

where V is the critical volumetric flow rate for production of soot as used by Schalla and McDonald.

To compare the various data sets we adjust the arbitrary proportionality constants, a and b, in Eqs. (1), (2), and (4) for each data set to minimize the error between the values of TSI for compounds which are common to more than one set of data. The resulting merged set of TSI values, spanning the range of hydrocarbons measured by all experimenters, is then linearly scaled so that the compounds have $0 \leq TSI \leq 100$. The calculation was done by picking the two compounds from the largest data set with the highest and the lowest MW/h (for diffusion flames) and solving Eq. (4) for a and b denoted as a_1 and b_1. With these constants the TSI was calculated for each of the compounds in data set 1. For a second data set, two compounds were selected which were in common with the first data set and by assigning them the same TSI values as for the first data set, a_2^o and b_2^o of Eq. (4) were derived and used to calculate a TSI_2^o value for each member of data set 2. Next a least-squares linear correlation of the two sets of data for TSI_1 and TSI_2^o was made using the above derived constants for each set. This yielded m and C in the equation correlating the two sets of data

$$TSI_1 = m \; TSI_2^o + C \qquad (5)$$

The two sets of data can now be considered to have been merged so that $TSI_1 = TSI_2$. Thus the TSI for the second set of data on the same scale as data set 1 is calculated by substituting TSI_2^o in the form of Eq. (4) in Eq. (5), yielding:

$$TSI_1 = TSI_2 = ma_2^o\left(\frac{MW}{h}\right) + mb_2^o + C \qquad (6)$$

where $a_2 = ma_2^o$, $b_2 = mb_2^o + C$ in Eq. (4) for data set 2. With the values of a_2

and b_2 the TSI values were calculated by Eq. (4) for all of the data in the second set. This process was repeated for each data set, yielding constants which minimize the differences between the various sets of data. For those compounds which occurred in more than one data set, the TSI's were averaged to give a mean value. Then to fix the TSI scale range from 0 to 100 the TSI of the lowest value in the total of all the data sets was set equal to 0 and the highest value equal to 100 [TSI (ethane) = 0, TSI (naphthalene) = 100]; the original values had deviated from these values in the averaging process. This linear adjustment of the TSI_{0-100} was accomplished as follows:

$$TSI_{0-100} = (TSI - X) \left(\frac{100}{Y - X} \right) \tag{7}$$

where: TSI = TSI value being corrected

   X = TSI of ethane on old scale

   Y = TSI of naphthalene on old scale

The constants a and b reported in Table 1 are thus given by combining Eqs. (7) and (4).

$$TSI_{0-100} = \frac{100}{Y - X} \left(a_1 \left(\frac{MW}{h} \right) + b_1 - X \right) \tag{8}$$

or $a = \left(\frac{100}{Y - X} \right) a_1$ $b = \frac{100}{Y - X} \left(b_1 - X \right)$

This process can clearly be iterated for any new data set, adjusting the total scale, or the new data set may be fit into the total data base by calculation of a and b for the new data through the least-squares linear correlation.

   The data for premixed flames can be treated similarly.

   The constants, a and b, for each data set are given in Table 1. These allow translation of the TSI for any fuel to the conditions of a particular experiment, even though that substance may not have been investigated under those conditions.

9

The consistency of the resulting data sets shown in Tables 2 and 3 may be judged by comparing the deviations in values for those compounds common to two or more data sets. In spite of the very different nature of premixed measurements and the uncertainties that are associated with each of them, it is clear from Table 2 that they are fairly consistent. When the data are averaged for these compounds the mean scatter introduced is less than ± 10%; only one data point in the total of 63 was excluded for reasons of gross disagreement. The above deviation is probably not more than the absolute error associated with the individual members of the set; some results are given to only one significant figure. Table 2 includes not only Bunsen burner type data but the data by Wright and Blazowski in a backmixed jet stirred reactor. The rationale for taking data in a jet stirred reactor was that the aerodynamics more closely duplicates that occurring in actual hardware, especially gas turbines. The correlation in Table 2 strongly indicates that chemistry, not aerodynamics, is controlling the critical composition for soot formation.

The mean scatter from averaging the diffusion flame data, Table 3, is less than ± 15%; if propane and propylene are excluded the mean scatter is less than ± 10%. Seven data points out of 146, or 5% of the data points were excluded. A data point was excluded only when three or more measurements were available for the same substance and one of them was obviously out of line—see the bracketed numbers in Table 3. Again the agreement between different investigators using different techniques emphasizes the importance of chemistry in determining the critical composition for soot formation.

RESULTS AND DISCUSSION

It was demonstrated in the previous section that measurements of the threshold for soot formation for either premixed or diffusion flames made by many different investigators using different methods are consistent when the sets of data are appropriately treated using two constants to normalize each data set. This implies that chemistry is the controlling process in soot formation in both premixed and diffusion flames.

Before discussing the question of a correlation between the premixed data and the diffusion data, the effect of molecular structures on premixed and diffusion flames will be discussed separately.

Premixed Flames

Most of the TSI data in Table 2 are plotted against the number of carbon atoms in the molecule in Fig. 1. To simplify the figure, smooth curves have been drawn through the n-alkane and n-alkene data. Isomers have been left off because inspection of Table 2 shows that they generally produce only a slightly higher TSI. The most striking feature of Fig. 1 is that most of the data fall roughly in a band, with TSI increasing with number of carbon atoms; the slope is about 7 TSI units per carbon atom. Exceptions are acetylene, 1,3-butadiene, and the higher molecular weight alkanes and alkenes. When TSI is plotted against the C/H ratio, Fig. 2, butadiene is no longer out of order. It is also interesting that butadiene (as does acetylene) attains its maximum burning velocity [16] and minimum ignition energy [17] in very rich mixtures compared to other hydrocarbons. For example, butadiene has a maximum burning velocity of 57 cm s^{-1} at ϕ = 1.23 while butene has a maximum burning velocity of 45 cm s^{-1} at ϕ = 1.08. Most hydrocarbons reach their maximum burning velocity between ϕ = 1.0 and 1.1.

11

The adiabatic flame temperature of acetylene is considerably greater than that of the other species; this may tend to mask the effect of molecular structure. It is clear, however, that the temperature is not the controlling factor in the tendency of a fuel to soot (cf. Refs. 18 and 19); for Bunsen burner flames the calculated adiabatic flame temperatures at the incipient soot point for acetylene, benzene, and n-hexane are 2380, 2200, and 1850 K, respectively, which bears very little relationship to their position on Fig. 1. Blazowski reports measured temperatures in a stirred reactor at the incipient soot limit for ethylene, 1-methyl naphthalene, and toluene of 1550, 1905, and 1951 K, respectively, which again bears little relationship to their position in Fig. 1.

It is also clear from Fig. 1 that increasing aromatic character increases the tendency to soot; compare, e.g., cyclohexane to benzene (TSI = 56 to 80), and decalin to tetralin (TSI = 85 to 98).

Based only on their results, Street and Thomas [1] reported the following (frequently quoted [13,14]) qualitative, relative ordering for the tendency to soot of hydrocarbons in premixed flames:

acetylene < alkenes < iso-alkanes < n-alkanes < monocyclic aromatic hydro-

carbons < naphthalenes

As shown in Fig. 1 these are rather poor summaries of the actual situation. Consideration of the <u>quantitative</u> ordering demonstrates that the reported trend is misleading. Further, it is clear that the effect of increasing the number of carbons within a family is sometimes much greater than changing families at fixed carbon number. As an illustration, consider the relatively small differences between hexane (TSI = 64) and hexene (TSI = 58 interpolated) compared to changing from ethylene (TSI = 30) to heptene (TSI = 60), or ethane (TSI = 35) to pentane (TSI = 63).

Another frequently reported qualitative trend is the increase in tendency
to soot with increasing C/H ratio [20,21]. The results in Table 2 plotted in
Fig. 2 against C/H ratio, show that while there is a general increase in
tendency to soot with increasing C/H ratio, the trend is weak and thus of
limited predictive value. All of the alkenes at fixed C/H should be equal but
have TSI values from 30 to 65, and acetylene with one of the highest C/H
ratios has (TSI = 0) the lowest value of any compound measured; further, acet-
ylene and benzene have the same C/H but TSI = 0 and 80, respectively.

Street and Thomas suggested that the somewhat higher TSI of aromatics in
premixed flames may be caused by the ability of the benzene ring to resist
oxidation and survive into the burnt gas zone. Fenimore, Jones, and Moore [22]
subsequently studied the onset of soot in premixed flames as a function of
various species concentrations in the burnt gas zone. They found that the
correlation between sooting and the survival of benzene into this zone was
quite strong. In a recent review summarizing the role of aromatics in soot
formation, Bittner and Howard [23] confirm this observation, but suggest that
more information on the role of intact aromatics will be required to clarify
the reasons for this large apparent enhancement.

Clearly more data are required on the effect of molecular structure on
soot formation in premixed flames and that data should include the effect of
temperature.

Diffusion Flames

Much of the data in Table 3 have been plotted in Figs. 3 and 4. Smooth
curves have been drawn through the n-alkanes, n-alkenes, and n-alkynes.
Isomers and cyclic structures for these substances have been deleted because
they differ little from the normal compound and the tendency to soot of the
alkanes and alkenes is small compared to other structures. The effect of

13

isomeric structure is demonstrated by examining the octanes in Table 3. This table demonstrates what Clarke et al. [7] recognized, that the more compact the molecular structure the greater the tendency to soot.

The most striking feature of Fig. 3 is that most of the data, with the exception of the alkanes and alkenes, but including the alkynes, fall in a band with TSI increasing with number of carbon atoms, with slope varying from about 6 to 12 per carbon atom. This is better demonstrated when all of the data in Table 3 except that for the alkanes and alkenes, are plotted on a single graph. Only typical molecules are plotted in Fig. 3 because the displayed structures would overlap; the molecules with greatest deviation from the rest of the data have been included however. Butadiene again stands out as having a greater tendency to soot than any other small molecule; unfortunately, there are no other examples of conjugated systems. Glassman [11,19] interprets this observation as indicating that butadiene may be a major "precursor element in soot nucleation". Again, however, when TSI is plotted against C/H, Fig. 4, butadiene falls in with all the other fuels. Styrene with its conjugated double bond is also an outstanding sooter in Fig. 3 but falls within the other fuels in Fig. 4 when TSI is plotted against C/H.

The second most notable feature of Fig. 3 is the very low tendency of the alkanes and alkenes to soot and the major importance of aromatic character on the tendency to soot.

The failure of C/H to correlate the data is vividly clear in Fig. 4 in the comparison of acetylene and benzene, both having C/H = 1.0 but TSI of 3.9 and 31, respectively, or the trend from acetylene to hexyne with C/H from 1.0 to 0.6 and TSI from 3.9 to 20. We note that it has erroneously been reported [24] that the incipient sooting tendency decreases with increasing size for all compounds except paraffins. These conclusions were based on Fig. 6 of

Minchin [6] which has been interpreted as summarizing his experimental data. In fact the credit for this data is usually given to Clarke, Hunter, and Garner [7] who simply redrew Minchin's curves. Minchin's Fig. 6 is actually the result of a hypothetical calculation based on only a few data points. The relationship used in that calculation is not in agreement with the extensive data subsequently collected by other workers.

It is sometimes stated that in diffusion flames soot formation increases in the order [14]

paraffins < mono-olefins < di-olefins < acetylenes < benzenes < naphthalenes

Reference to Fig. 3 demonstrates how misleading this qualitative statement is when compared with quantitative data.

Comparison between Premixed and Diffusion Flames

It is classical mythology to recognize the different tendency to soot of premixed and diffusion flames [13,14]. Comparison of Figs. 1 and 3 show some differences and much in common. The most striking difference is the relative position of the alkenes and alkanes on the two figures; this is determined by the relative position of acetylene with respect to these two groups of compounds. In premixed flames acetylene has a much lower tendency to soot than the alkanes and alkenes but in diffusion flames it has a greater tendency to soot. In addition, the tendency to soot for the alkanes and alkenes is reversed in the two flames. Nevertheless, the tendency to soot increases with increasing molecular weight (increasing number of carbon atoms) in both flames for both classes of compounds, and the tendency to soot increases with isomerization (increasing molecular compactness) in both flames--see Tables 2 and 3. Both Figs. 1 and 3 show major overall trends in common when the total range of fuels is considered. At the extremes in both flames are acetylene

15

and the naphthalenes. Further, it is apparent that aromatic character plays a dominant role in both flame types and 1,3-butadiene has a greater tendency to soot in both flames than the corresponding alkane or alkene when TSI is plotted against numbers of carbon atoms but not when plotted against C/H.

The fuels in common between the two flames are compared in Fig. 5. All of the alkanes and alkenes fall in the cross-hatched area. The correlation, although not linear, between the premixed and diffusion flames is surprisingly good. In diffusion flames differences between molecular structure of alkanes and alkenes cause only a small change in TSI while in premixed flames the change is more dramatic; on the other hand, for mono- and di-cyclic compounds large changes are noted for diffusion flames and small changes for premixed flames. It is obvious that more data on premixed flames are required; these are being collected in our laboratory.

The choice of definitions for TSI was somewhat arbitrary; a different choice should be possible to force the points in Fig. 5 to fall more nearly on a 45° line. It should also be pointed out that the manner of presentation of the data as TSI for the whole range of fuels appears to suppress the differences, especially in diffusion flames, between the alkanes, alkenes, and alkynes, although on a percentage basis the differences between these may be quite large. Another caveat is in order--the data reported here should not be interpreted as applying to practical systems such as turbojets, diesels, or power plants until a correlation between the laboratory system and the practical system has been demonstrated. The early examination of such correlations is of great importance to the synfuels program.

SUMMARY

By defining a rational threshold soot index, TSI, varying from 0 to 100 to measure the onset of soot formation in premixed and diffusion flames, it is shown that all of the data in the literature on premixed and diffusion flames, taken by many techniques, can be succesfully correlated with respect to molecular structure. The differences in effect of molecular structure between premixed and diffusion flames are less than previously thought. The major differences between premixed and diffusion flames are the relative order of alkanes, alkenes, and alkynes; the relative importance of aromatic structure, isomerization, or increasing molecular size is the same. The role of C/H, often taken as important in determining the effect of molecular structure, is of very little value in correlating data from laboratory systems.

For premixed flames, the effect of molecular structure on the onset of soot formation as measured by the TSI can be tentatively summarized, until more data are available, in approximately decreasing order of importance:

1. TSI is strongly influenced by the number of carbon atoms in the molecule, about 7 TSI per carbon atom. Two exceptions to the rule are acetylene with a TSI of 0, about 30 TSI below any other molecule, and butadiene, 20 TSI greater than n-butane.

2. Aromatic character increases the tendency to soot. TSI is increased 15 to 25 units on converting a saturated ring to an aromatic ring. (The change from tetralin to methyl naphthalene is, however, very small.)

3. n-alkanes and iso-alkanes have essentially the same TSI (iso-alkanes slightly higher) starting at 35, rising to about 65 at pentane and then rising more slowly for larger molecules.

4. Alkenes fall below alkanes by about 10 TSI units for small molecules, decreasing to about 5 TSI units for larger molecules.

5. Adding a side chain to an aromatic molecule increases the TSI; lengthening the side chain decreases the TSI.

For diffusion flames the effect of molecular structure on the onset of soot formation can be summarized, in approximately decreasing order of importance:

1. TSI, with the exception of alkanes, and alkenes, but including the alkynes, is strongly influenced by the number of carbon atoms in the molecule, 6 to 12 TSI per carbon atom. Two major exceptions to the rule are 1,3-butadiene and styrene which are about 15 and 20 TSI, respectively, above the average curve.

2. Aromatic character greatly increases the tendency to soot; TSI is increased for changing a saturated ring to an aromatic ring by from 25 to 60.

3. Alkanes and alkenes have very low tendencies to soot, TSI < 7, with alkenes having TSI from 2 to 6 above alkanes.

4. Isomeric or cyclic structures for alkanes or alkenes do not compare in increasing the tendency to soot with increasing aromatic character; however, making an alkene or alkane more compact generally increases the tendency to soot by as much as 80%.

5. Multi-ring structures including saturated rings increase the tendency to soot.

6. The addition of a side chain to an aromatic molecule has complex effects, generally increasing TSI but for long side chains decreasing TSI.

ACKNOWLEDGMENT

REFERENCES

[1] Street, J.C. and Thomas, A., Fuel 34: 4 (1955).

[2] Wright, F.J., Twelfth Symposium (International) on Combustion, The
     Combustion Institute, Pittsburgh, 1969, p. 867.

[3] Calcote, H.F. and Miller, W.J., "Ionic Mechanisms of Carbon Formation in
     Flames," TP-371, AeroChem Research Laboratories, Inc. (May 1978); Fall
     Technical Meeting, Eastern Section: The Combustion Institute, 10-11
     November 1977.

[4] Grumer, J., Harris, M.E., and Rowe, V.R., "Fundamental Flashback, Blow-
     off, and Yello-tip Limits of Fuel Gas-air Mixtures," Bureau of Mines,
     Rep. of Investigations 5225 (1956).

[5] Blazowski, W.S., Combust. Sci. Technol. 21: 87 (1980).

[6] Minchin, S.T., J. Inst. Petrol. 17: 102 (1931).

[7] Clarke, A.E., Hunter, T.G., and Garner, F.H., J. Inst. Petrol. 32:627 (1946).

[8] Hunt, R.A. Ind. Eng. Chem. 45: 602 (1953).

[9] Schalla, R.L. and McDonald, G.E., Ind. Eng. Chem. 45: 1497 (1953)

[10] Van Treuren, K.S., "Sooting Characteristics of Liquid Pool Diffusion
     Flames," M.S. Thesis, Princeton Univ., Dept. Mech and Aero. Eng. (July
     1978).

[11] Schug, K.P., Manheimer-Timnat, Y., Yaccarino, P., and Glassman, I.,
     Combust. Sci. Technol. 22: 235 (1980).

[12] Schalla, R.L. and Hubbard, R.R., "Formation and Combustion of Smoke in
     Flames, in Basic Consideration of Hydrocarbon Combustion," NACA Report
     1300, Chap. IX (1959).

[13] Gaydon, A.G. and Wolfhard, H.G., Flames. Their Structure, Radiation and
     Temperature, Chapman and Hall, London, 4th ed., 1978, Chap. VIII.

[14] Glassman, I., Combustion, Academic Press, New York, 1973, p. 246.

[15] Lewis, B. and Von Elbe, G., Combustion, Flames and Explosions of Gases,
      Academic Press, New York, 2nd ed., 1961, p. 479.

[16] Gibbs, G.J. and Calcote, H.F., J. Chem. Eng. Data 4: 226 (1959).

[17] Calcote, H.F., Gregory, C.A., Jr., Barnett, C.M., and Gilmer, R.B.
      Ind. Eng. Chem. 44: 2656 (1952).

[18] Glassman, I. and Yaccarino, P., "The Temperature Effect in Sooting
      Diffusion Flames," to be published in proceedings of The Eighteenth
      Symposium (International) on Combustion.

[19] Glassman, I., "Phenomenological Models of Soot Processes in Combustion
      Systems," Princeton Univ. Dept. Mech. and Aero. Eng. Report 1450, AFOSR
      TR 79-1147 (July 1979).

[20] Longwell, J.P., in Alternative Hydrocarbon Fuels: Combustion and Chemical
      Kinetics (C.T. Bowman and J. Birkeland, Eds.) Progress in Astronautics
      and Aeronautics, AIAA, New York, 1978, Vol. 62, p. 3.

[21] Blazowski, W.S. and Maggitti, L., ibid., p. 21.

[22] Fenimore, C.P., Jones, G.W., and Moore, G.E., Sixth Symposium (Interna-
      tional) on Combustion, Butterworths, London, 1956, p. 140.

[23] Bittner, J.D. and Howard, J.B., in Alternative Hydrocarbon Fuels: Combus-
      tion and Chemical Kinetics (C.T. Bowman and J. Birkeland, Eds.) Progress
      in Astronautics and Aeronautics, AIAA, New York, 1978, Vol. 62, p. 335.

[24] See e.g., Fig. 4 of Ref. 7; Fig. 10 of Ref. 14; Fig. 8.1 of Ref. 13; or
      Fig. 5.1 of Palmer, H.B. and Cullis, C.F., in Chemistry and Physics of
      Carbon (P.L. Walker, Jr., Ed.) Marcel Dekker, Inc., New York, 1965.

TABLE 1

Constants for Calculation of TSI from Original Data

Source Premixed Flames	Original Data Form	a	b
Street and Thomas [1]	ϕ_c	219	101
Grumer, Harris, and Rowe [4]	ϕ_c	181	81.6
Wright [2]	ϕ_c	204	78.1
Calcote and Miller [3]	ϕ_c	303	147
Blazowski [5]	ϕ_c	227	101
Diffusion Flames			
Minchen [6]	h	0.178	-15.7
Clarke, Hunter, and Garner [7]	h	0.381	-0.76
Hunt [8]	h	3.10	1.13
Schalla and McDonald [9]	v	0.322	0.85
Van Treuren [10]	h	0.594	-1.16
Schug, Manheimer-Timnat, Yaccarino, and Glassman [11]	v	0.144	-1.55

TABLE 2

Threshold Soot Index for Compounds Measured in Premixed Flames

Data source indicated in brackets

Formula	Name	Mol. Wt.	C/H	Threshold Soot Index TSI
CH_4	methane	16	0.250	34[4]
C_2H_6	ethane	30	0.333	42[1] 28[4] 35 ± 7
C_3H_8	propane	44	0.375	53[1] 47[3] 49[4] 50 ± 2
C_4H_{10}	n-butane	58	0.400	61[1] 53[4] 57 ± 4
C_5H_{12}	n-pentane	72	0.417	63[1]
C_5H_{12}	isopentane	72	0.417	61[1]
C_6H_{14}	n-hexane	86	0.429	65[1] 63[3] 64 ± 1
C_6H_{14}	2-methyl pentane	86	0.429	65[1]
C_6H_{12}	cyclohexane	84	0.500	58[1] 53[3] 56 ± 3
C_8H_{18}	n-octane	114	0.444	72[1] 52[3] 62 ± 10
C_8H_{18}	isooctane	114	0.444	65[1]
$C_{10}H_{18}$	decalin[a]	138	0.556	85[1]
$C_{12}H_{26}$	isododecane	170	0.462	70[1]
$C_{16}H_{34}$	n-cetane	226	0.471	76[1]
C_2H_4	ethylene	28	0.500	26[1] 33[3] 41[2] 24[5] 27[4] 30 ± 5
C_3H_6	propylene	42	0.500	42[1] 37[2] {63[37]}[b] 40 ± 2
C_4H_8	n-butene	56	0.500	53[1] 46[2] 50 ± 4
C_4H_8	isobutene	56	0.500	62[2] 67[4] 64 ± 3
C_5H_{10}	n-pentene	70	0.500	56[1]
C_7H_{14}	n-heptene	98	0.500	65[1] 55[3] 60 ± 5
C_4H_6	1,3-butadiene	54	0.667	77[2]
C_2H_2	acetylene	26	1.00	-1.5[1] 1.6[3] 0.00 ± 1.5
C_6H_6	benzene	78	1.00	68[1] 75[3] 93[2] 85[4] 80 ± 9
C_7H_8	toluene	92	0.875	78[1] 93[3] 87[2] 86[5] 72[4] 83 ± 7
C_8H_{10}	xylenes	106	0.800	85[1] 93[3] 90[2] 95[5] 91 ± 3
C_9H_{12}	cumene[c]	120	0.750	83[1] 74[3] 79[2] 85[5] 80 ± 4
$C_{10}H_{10}$	dicyclopentadiene[d]	130	1.00	85[2] 86[5] 86 ± 0
$C_{10}H_{12}$	tetralin[e]	132	0.833	108[1] 92[2] 94[5] 98 ± 6

TABLE 2 (continued)

Formula	Name	Mol. Wt.	C/H	Threshold Soot Index TSI			
$C_{11}H_{10}$	1-methyl naphthalene[f]	142	1.10	110[1] 86[2] 104[5] 100 ± 9			
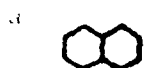
[b] { } Included in determining fit but excluded from average when plotting
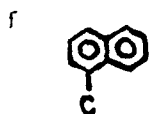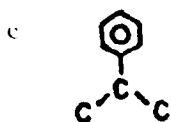
TABLE 3

Threshold Soot Index for Compounds Measured in Diffusion Flames

Data source indicated in brackets

Formula	Name	Mol. Wt.	C/H	Threshold Soot Index TSI			
C_2H_6	ethane	30	0.333	1.2[9]	-1.3[11]		0.0 ± 1.2
C_3H_8	propane	44	0.375	1.3[9]	-0.07[11]		0.7 ± 0.7
C_3H_6	cyclopropane	42	0.500	3.2[9]			
C_4H_{10}	n-butane	58	0.400	1.6[9]	1.2[11]		1.4 ± 0.2
C_4H_{10}	isobutane	58	0.400	2.2[9]			
C_5H_{12}	n-pentane	72	0.417	1.0[7]	1.3[8]	1.7[9]	1.3 ± 0.2
C_5H_{12}	isopentane	72	0.417	1.6[7]			
C_5H_{12}	2,2-dimethyl propane	72	0.417	2.7[8]	3.8[9]		3.3 ± 0.5
C_5H_{10}	cyclopentane	70	0.500	3.5[8]	3.0[7]	3.5[9]	3.3 ± 0.3
C_6H_{14}	n-hexane	86	0.429	2.7[8]	2.3[9]		2.5 ± 0.2
C_6H_{14}	2-methyl pentane	86	0.429	2.9[8]	2.9[10]		2.9 ± 0
C_6H_{14}	3-methyl pentane	86	0.429	2.9[8]	2.6[9]		2.8 ± 0.1
C_6H_{14}	2,2-dimethyl butane	86	0.429	3.3[8]	4.0[7]		3.6 ± 0.4
C_6H_{14}	2,3-dimethyl butane	86	0.429	3.2[8]			
C_6H_{12}	methyl cyclopentane	84	0.500	5.0[8]	4.8[9]		4.9 ± 0.1
C_6H_{12}	cyclohexane	84	0.500	3.2[8]	3.4[7]	3.0[9]	3.2 ± 0.1
C_7H_{16}	n-heptane	100	0.438	3.0[8]	2.5[10]	2.6[9]	2.7 ± 0.2
C_7H_{16}	2-methyl hexane	100	0.438	3.2[8]			
C_7H_{16}	3-methyl hexane	100	0.438	3.2[8]			
C_7H_{16}	2,3-dimethyl pentane	100	0.438	3.5[8]			
C_7H_{16}	2,4-dimethyl pentane	100	0.438	3.6[8]			
C_7H_{14}	methyl cyclohexane	98	0.500	4.2[8]	4.6[7]		4.4 ± 0.2
C_8H_{18}	n-octane	114	0.444	3.3[8]	3.2[10]	3.2[9]	3.2 ± 0.1
C_8H_{18}	2-methyl heptane	114	0.444	3.5[8]			
C_8H_{18}	3-methyl heptane	114	0.444	3.7[8]			
C_8H_{18}	4-methyl heptane	114	0.444	4.0[8]			
C_8H_{18}	3-ethyl hexane	114	0.444	4.0[8]			
C_8H_{18}	2,2-dimethyl hexane	114	0.444	4.5[8]			
C_8H_{18}	2,3-dimethyl hexane	114	0.444	3.8[8]			
C_8H_{18}	2,2,4-trimethyl pentane	114	0.444	5.0[8]	6.1[7]		5.6 ± 0.5
C_8H_{18}	2,3,4-trimethyl pentane	114	0.444	5.7[7]			

TABLE 3 (continued)

Formula	Name	Mol. Wt.	C/H	Threshold Soot Index TSI
C_8H_{18}	2,3,3-trimethyl pentane	114	0.444	5.7[7]
C_8H_{18}	2-methyl 3-ethyl pentane	114	0.444	4.4[8]
C_8H_{16}	1,3-dimethyl cyclohexane	112	0.500	5.9[8]
C_8H_{16}	ethyl cyclohexane	112	0.500	4.6[8]
C_9H_{20}	nonane	128	0.450	4.1[9]
C_9H_{20}	isononane	128	0.450	5.0[9]
$C_{10}H_{22}$	decane	142	0.485	4.1[8] 4.5[10] 4.3 ± 0.2
$C_{10}H_{18}$	decalin	138	0.556	12[8] 13[7] {3.7[6]}^{a} 13 ± 0.5
$C_{11}H_{24}$	undecane	156	0.458	4.3[8]
$C_{12}H_{26}$	dodecane	170	0.466	4.8[8]
$C_{13}H_{28}$	tridecane	184	0.464	5.2[8]
$C_{14}H_{30}$	tetradecane	198	0.467	5.4[8]
C_2H_4	ethylene	28	0.500	1.3[9] 1.3[11] 1.3 ± 0
C_3H_6	propylene	42	0.500	2.6[9] 6.9[11] 4.7 ± 3.8
C_4H_8	n-butene	56	0.500	4.4[9]
C_4H_8	2-butene	56	0.500	4.3[9]
C_4H_8	isobutene	56	0.500	4.8[9]
C_5H_{10}	1-pentene	70	0.500	4.8[7] 3.5[9] 4.2 ± 0.6
C_5H_8	cyclopentene	68	0.625	15[9]
C_6H_{12}	hexene	84	0.500	3.9[8] 4.9[7] {8.1[10]} 4.4[9] 4.4 ± 0.3
C_6H_{10}	cyclohexene	82	0.600	6.3[8] 5.8[7] 5.0[9] 5.7 ± 0.5
C_7H_{14}	1-heptene	98	0.500	4.1[8] 4.5[7] 5.1[9] 4.6 ± 0.4
C_7H_{14}	2-heptene	98	0.500	4.3[8] 5.3[9] 4.8 ± 0.5
C_8H_{16}	1-octene	112	0.500	4.4[8]
C_8H_{16}	2-octene	112	0.500	4.4[8]
$C_{10}H_{20}$	decene	140	0.570	5.5[8] 6.2[7] 7.6[9] 6.5 ± 0.8
$C_{12}H_{24}$	dodecene	168	0.500	6.4[8]
$C_{12}H_{22}$	dicyclohexyl^b	166	0.545	10[8] 11[7] 10 ± 0.2
$C_{14}H_{28}$	tetradecene	196	0.500	7.6[8]
$C_{16}H_{32}$	hexadecene	224	0.500	8.3[8]
$C_{18}H_{36}$	octadecene	252	0.500	9.2[8]
C_2H_2	acetylene	26	1.00	2.7[9] 4.6[11] 3.9 ± 0.7
C_3H_4	propyne	40	0.750	5.9[9]

TABLE 3 (continued)

Formula	Name	Mol. Wt.	C/H	Threshold Soot Index TSI
C_5H_8	pentyne	68	0.625	15[9]
C_6H_{10}	hexyne	82	0.600	20[9]
C_4H_6	1,3-butadiene	54	0.667	26[9] 24[11] 25 ± 0.9
C_8H_{14}	2,5-dimethyl,1,5-hexadiene	110	0.570	34[9]
C_6H_6	benzene	78	1.00	31[8] 30[7] {24[9]} 31 ± 0.4
C_7H_8	toluene	92	0.875	48[8] {34[7]} 52[6] 48[10] 50[9] 50 ± 2
C_8H_{10}	xylene	106	0.800	63[8] 44[7] 46[10] 51 ± 8
C_8H_{10}	ethyl benzene	106	0.800	56[8] 61[6] {75[9]} 58 ± 3
C_9H_{12}	mesitylene[c]	120	0.750	47[8]
C_9H_{12}	trimethylbenzenes	120	0.750	47[8]
C_9H_{12}	cumene	120	0.750	63[8]
C_9H_{12}	propyl benzene	120	0.750	47[8] {111[9]}
$C_{10}H_{14}$	p-cymene[d]	134	0.714	84[8] 39[7] 61 ± 23
$C_{10}H_{14}$	butyl benzene	134	0.714	70[8]
$C_{10}H_{14}$	sec butyl benzene	134	0.714	60[8]
$C_{10}H_{14}$	tert butyl benzene	134	0.714	84[8]
$C_{10}H_{14}$	diethyl benzene	134	0.714	60[8]
$C_{11}H_{16}$	sec pentyl benzene	148	0.688	58[8]
$C_{11}H_{16}$	tert pentyl benzene	148	0.688	58[8]
$C_{12}H_{18}$	m-di-isopropyl benzene	162	0.667	51[7]
$C_{12}H_{16}$	phenyl cyclohexane	160	0.750	72[8]
$C_{10}H_{12}$	tetralin	132	0.833	69[8] 41[7] 58[6] 56 ± 10
C_9H_8	indene[e]	116	1.125	52[8]
C_8H_8	styrene[f]	104	1.000	81[8]
	pinene[g]	136	0.625	24[7]
	naphthalene	128	1.25	100[8]
	methyl naphthalene	142	1.10	89[8] 89[6] 89 ± 0
	naphthalene	142	1.10	89[8]
	naphthalenes	156	1.00	98[8]

TABLE 3 (continued)

a { } Included in determining fit but excluded from average.

b

c

d

e

f

g
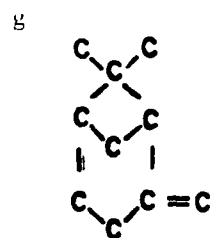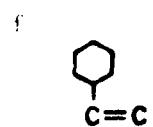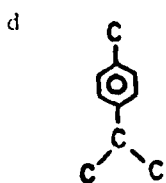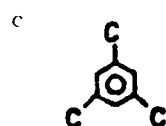
FIGURE CAPTIONS

Fig. 1   Effect of molecular structure on soot formation in premixed flames.

Fig. 2   Effect of molecular structure on soot formation in premixed flames.
Arrows indicate increasing molecular weight.

Fig. 3   Effect of molecular structure on tendency to soot in diffusion flames.

Fig. 4   Effect of molecular structure on tendency to soot in diffusion flames.
Arrows indicate increasing molecular weight.

Fig. 5   Comparison of diffusion and premixed flames.
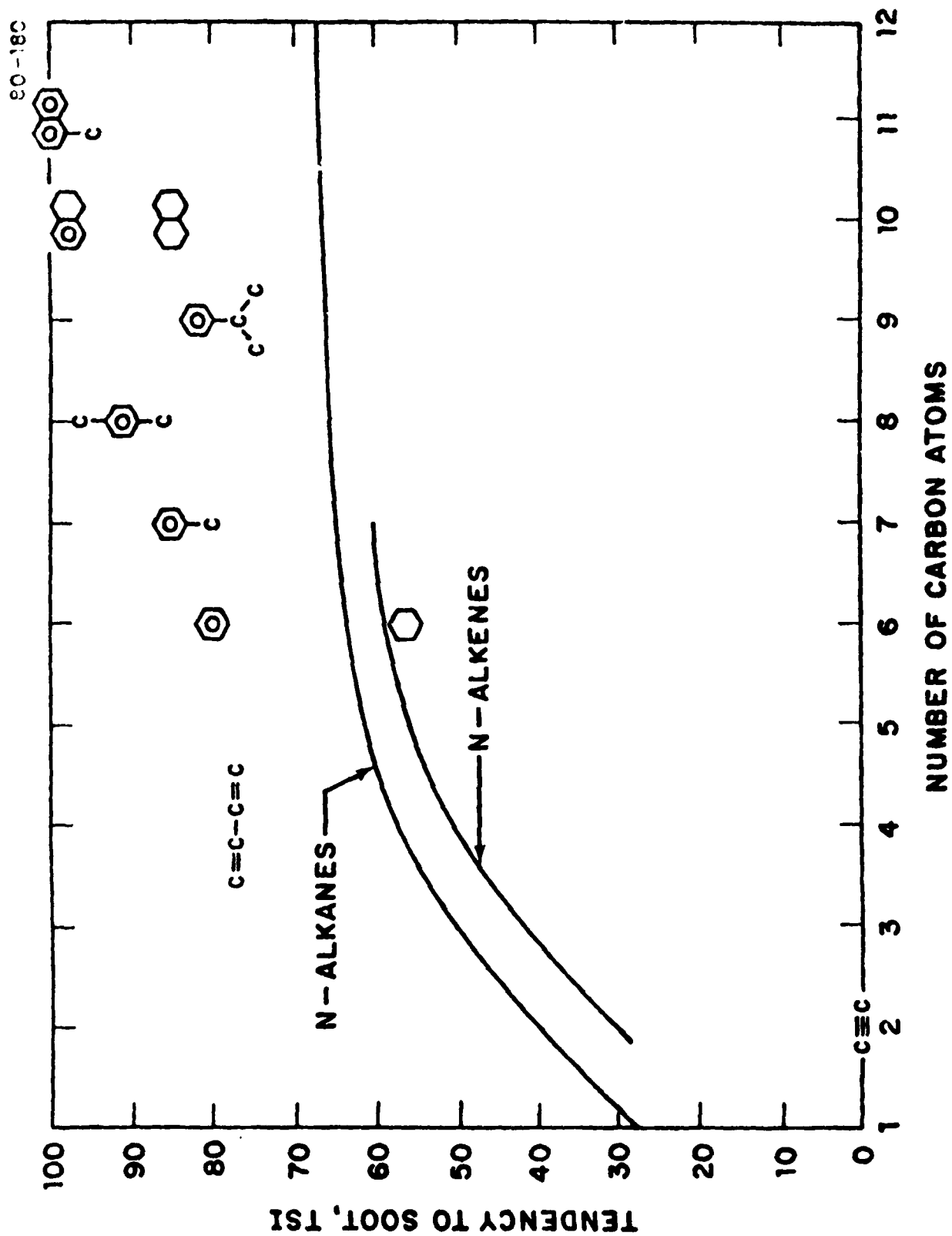
FIGURE 1
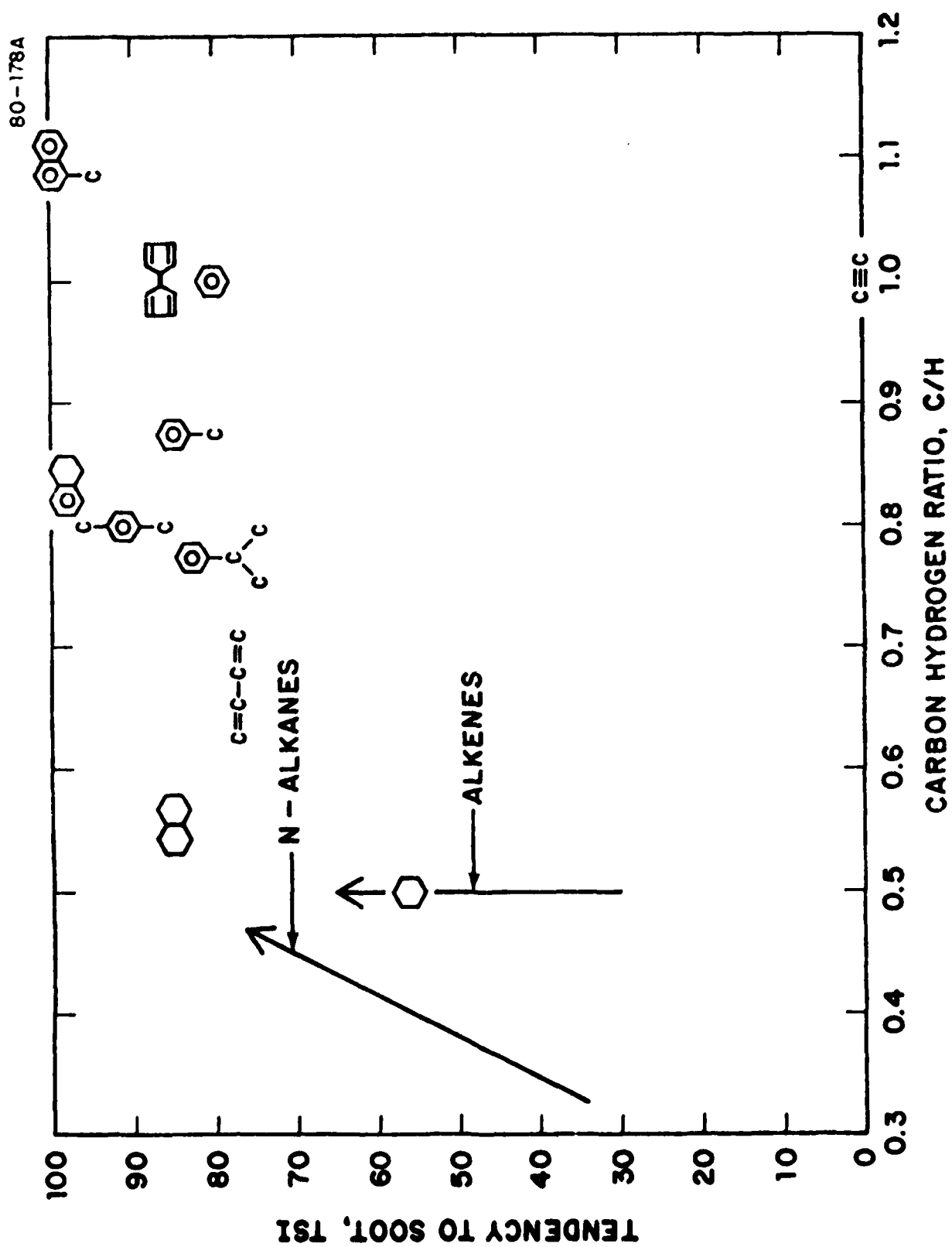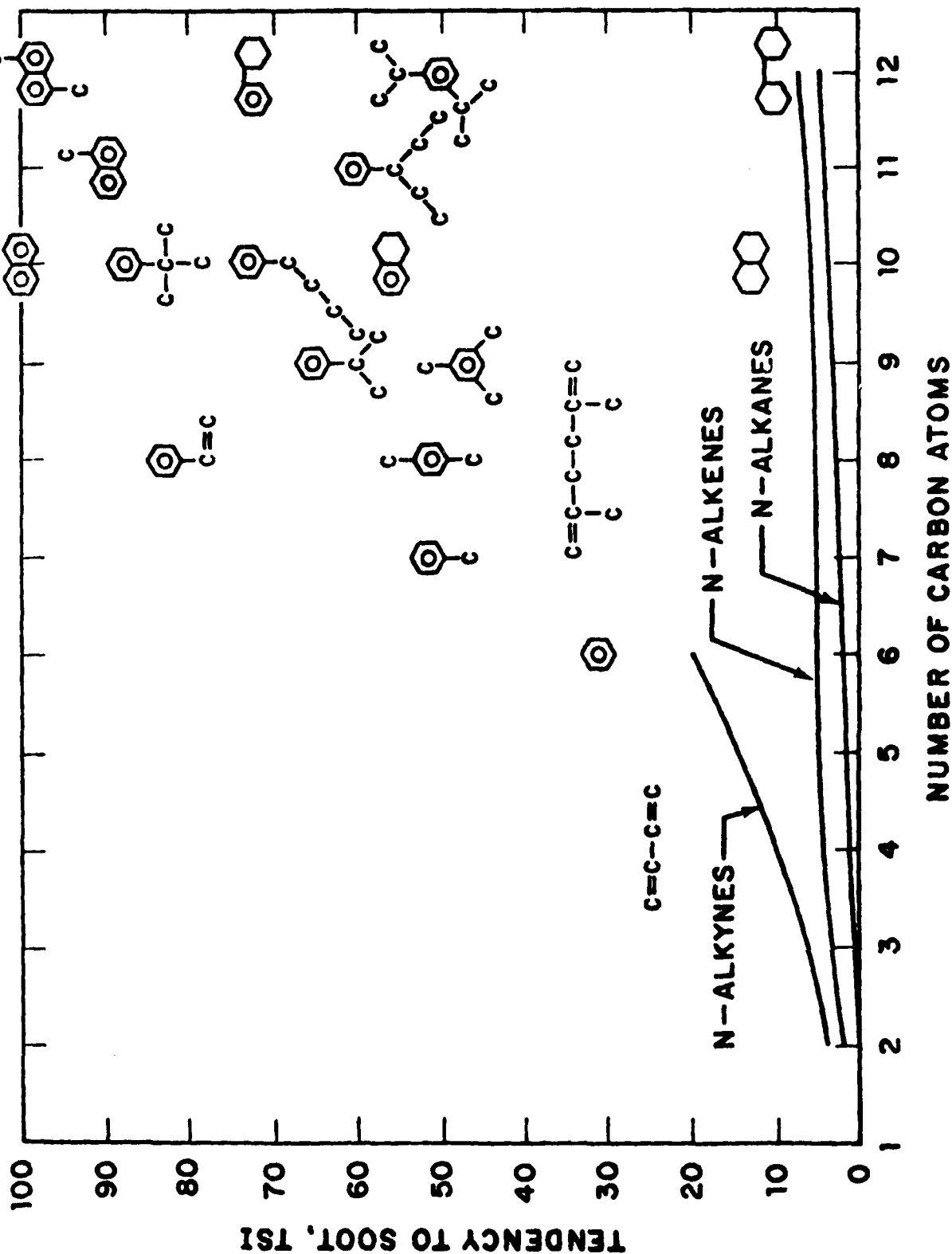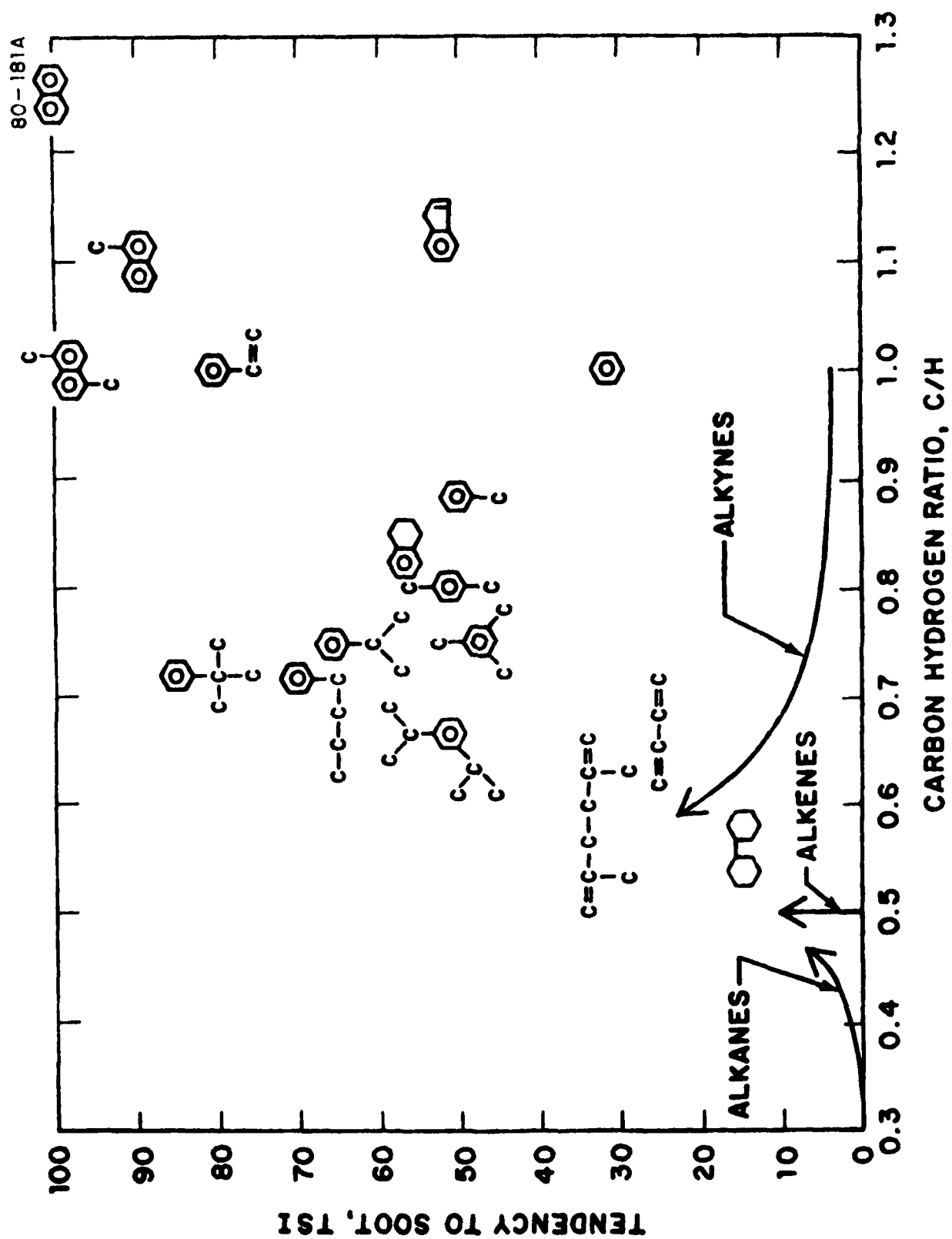
30

FIGURE 2

31

FIGURE 3

32

FIGURE 4

33

FIGURE 5

80-193A

TSI, PREMIXED FLAMES

TSI, DIFFUSION FLAMES

ALKANES
AND ALKENES

C≡C—C≡C

C≡C
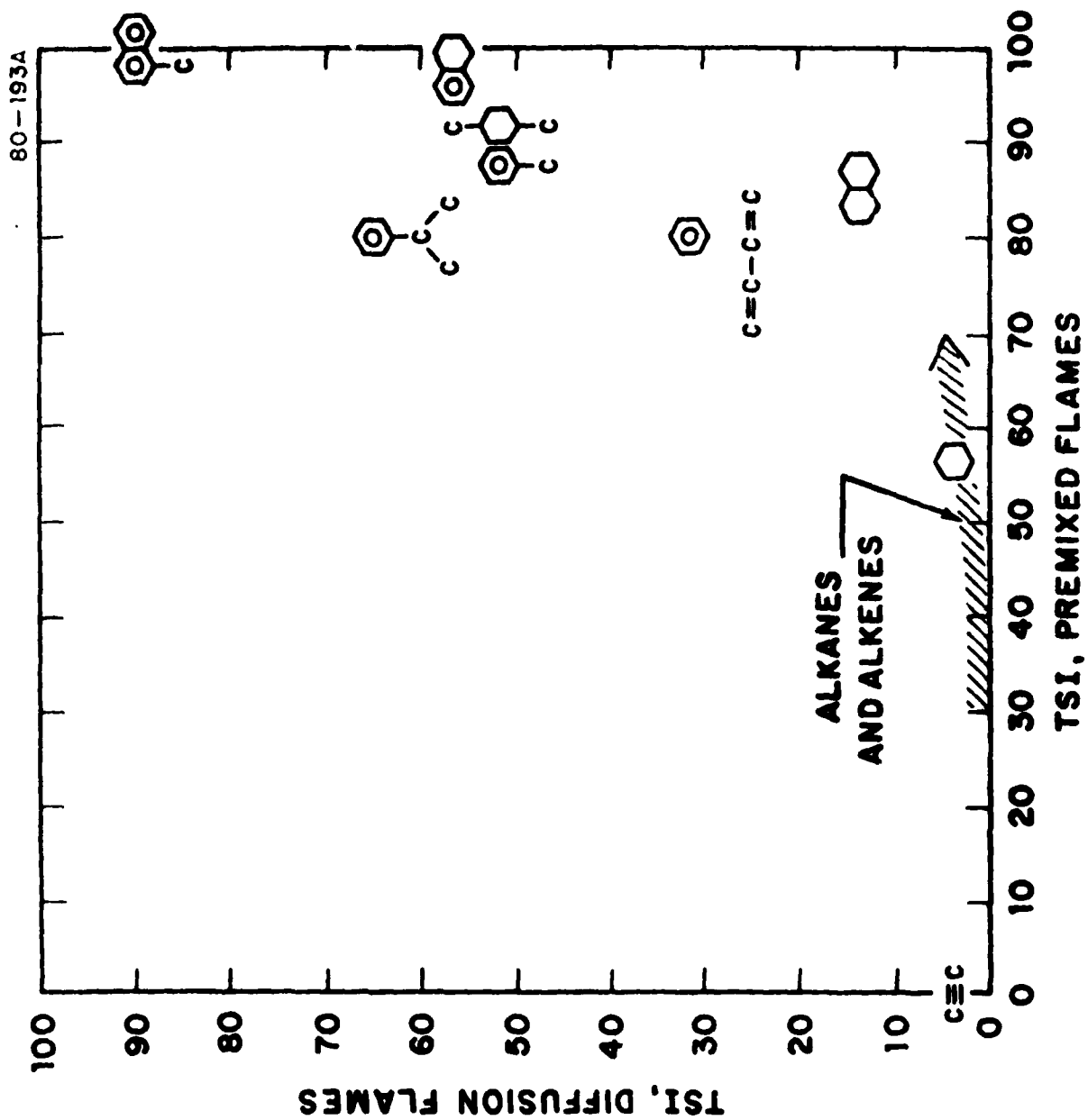
CORRELATION OF SOOT FORMATION IN
TURBOJET ENGINES AND IN
LABORATORY FLAMES

R.K. Gould, D.B. Olson, and H.F. Calcote

AeroChem Research Laboratories, Inc.
P.O. Box 12
Princeton, NJ 08540

February 1981

FINAL REPORT FOR PERIOD: AUGUST-SEPTEMBER 1980

Prepared for

AF ENVIRONICS DIVISION, ENGINEERING AND SERVICE LABORATORY
TYNDALL AFB, FLORIDA 32403

AIR FORCE OFFICE OF SCIENTIFIC RESEARCH
BOLLING AIR FORCE BASE
WASHINGTON, DC 20332

SECURITY CLASSIFICATION OF THIS PAGE *(When Data Entered)*

REPORT DOCUMENTATION PAGE		READ INSTRUCTIONS BEFORE COMPLETING FORM
1. REPORT NUMBER ESL-TR-81-09	2. GOVT ACCESSION NO.	3. RECIPIENT'S CATALOG NUMBER
4. TITLE *(and Subtitle)* CORRELATION OF SOOT FORMATION IN TURBOJET ENGINES AND IN LABORATORY FLAMES		5. TYPE OF REPORT & PERIOD COVERED Final Report August–September 1980
		6. PERFORMING ORG. REPORT NUMBER AeroChem TP-407
7. AUTHOR(s) Robert K. Gould Douglas B. Olson Hartwell F. Calcote		8. CONTRACT OR GRANT NUMBER(s) F449620-77-C-0029
9. PERFORMING ORGANIZATION NAME AND ADDRESS AeroChem Research Laboratories, Inc. P.O. Box 12 Princeton, New Jersey 08540		10. PROGRAM ELEMENT, PROJECT, TASK AREA & WORK UNIT NUMBERS PE: 62601F JON: 1900-20-51
11. CONTROLLING OFFICE NAME AND ADDRESS Engineering and Service Laboratory Air Force Engineering and Services Center Tyndall Air Force Base, Florida 32403		12. REPORT DATE February 1981
		13. NUMBER OF PAGES 64
14. MONITORING AGENCY NAME & ADDRESS*(if different from Controlling Office)* Air Force Office of Scientific Research Bolling Air Force Base Washington, DC 20332		15. SECURITY CLASS. *(of this report)* UNCLASSIFIED
		15a. DECLASSIFICATION/DOWNGRADING SCHEDULE

16. DISTRIBUTION STATEMENT *(of this Report)*

Approved for Public Release; Distribution Unlimited

17. DISTRIBUTION STATEMENT *(of the abstract entered in Block 20, if different from Report)*

18. SUPPLEMENTARY NOTES

19. KEY WORDS *(Continue on reverse side if necessary and identify by block number)*

Jet Fuels
Soot Formation
Fuel Structure
Smoke Point

20. ABSTRACT *(Continue on reverse side if necessary and identify by block number)*

Data obtained from aviation gas turbine combustor tests have been examined to determine the effects of fuel properties on soot-related measurements such as engine smoke number, combustor flame radiation, and/or combustor liner temperature. Some tests of smaller laboratory combustors used to simulate these large combustors were also examined. From the existing data it is clear that soot production is a strong function of the fuel chemical composition. Variations in the physical properties of the fuel do not correlate well with soot-related effects. In studies in which a broad range of fuel properties was examined,

DD FORM 1 JAN 73 **1473** EDITION OF 1 NOV 65 IS OBSOLETE

SECURITY CLASSIFICATION OF THIS PAGE *(When Data Entered)*

20. (CONCLUDED)

correlation of soot-related effects with basic fuel compositional parameters including (1) the hydrogen content of the fuel, (2) the aromatic content of the fuel, and (3) the amount of multiple-ring aromatics in the fuel show that typically only the first of these correlates well. However, it has also been shown that fuel compositions can be chosen for which this correlating parameter fails.

In addition to examining the ability of basic compositional information to correlate with soot-related effects, the correlation of these effects with the reciprocal of the fuel smoke point was examined. The correlation of this simple empirical laboratory measurement with sooting was typically similar to that obtained with hydrogen content although in some cases where the hydrogen content did poorly, the reciprocal smoke point did well.

To reduce small-scale laboratory flame data on soot thresholds (including ASTM smoke point measurements) to a form which allows measurements taken on various laboratory apparatus to be compared with one another and with engine test results, a threshold soot index (TSI) based on smoke point data for pure compounds is defined and described. Once defined for pure compounds, TSI's can be calculated for fuel mixtures by using weighted sums of the TSI's of the fuel components if sufficient compositional information is available. Although only crude estimates of fuel TSI's can be made for the fuels used in most of the tests surveyed, correlations of these estimated fuel TSI's with soot data indicate that even crudely calculated TSI's do as well as other correlating parameters used to predict sooting behavior of fuels. Laboratory and large-scale experiments are needed to determine if accurate fuel TSI's can provide much improved predictions of the soot production from highly aromatic, out-of-specification fuels.

Correlation parameters of reciprocal smoke point or fuel TSI with soot-related effects were found to be > 0.9 in several tests. However, in several recent studies which appear to be quite extensive, these fuel parameters as well as hydrogen content all produced correlations of < 0.8. The reasons for such poor correlations are unclear. Recommendations are made for tests to further examine this lack of consistency.

PREFACE

The work reported herein represented a special study undertaken in conjunction with our laboratory study of the mechanism of soot nucleation in flames which is supported by the Air Force Office of Scientific Research (AFOSR). Additional funds to cover this work during the period 1 August through 30 September 1980 were provided by Tyndall Air Force Base. The program manager representing Tyndall Air Force Base was Captain Harvey J. Clewell, and the program manager representing AFOSR was Bernard T. Wolfson.

This report has been reviewed by the Public Affairs Office (PA) and is releasable to the National Technical Information Service (NTIS). At NTIS it will be available to the general public, including foreign nations.

(The reverse of this page is blank.)

TABLE OF CONTENTS

LIST OF FIGURES

LIST OF TABLES

LIST OF TABLES (CONCLUDED)

AD-A102 411   AEROCHEM RESEARCH LABS INC PRINCETON NJ   F/G 21/2
                IONIC MECHANISMS OF CARBON FORMATION IN FLAMES.(U)
                MAY 81   H F CALCOTE, D B OLSON   F49620-77-C-0029
UNCLASSIFIED   AEROCHEM-TP-413   AFOSR-TR-81-0611   NL

3 OF 3
AD A
10 24 11

END
DATE
FILMED
8 -81
DTIC

SECTION 1

INTRODUCTION

Economic and availability factors are forcing a trend toward increased use of out-of-specification jet fuels. In particular, increased use of petroleum fractions with high aromatic contents is likely, and the prospect exists of substantial reliance on shale, tar sand, and coal derived fuels in the future. The tendency of these fuels to increase exhaust emissions and reduce engine performance and reliability has been the subject of increasing interest (References 1 to 11) over the last twenty years. Several reviews of the subject have recently been published (References 12 to 15).

In this work the literature describing several investigations of fuel effects on the performance of jet aircraft combustors (References 1 to 11) and on smaller stirred reactor combustors used to simulate these systems (References 1, 10, 16 to 19) has been examined. The goal of this review is to learn which fundamental fuel properties determine, or at least correlate well with, the tendency of highly aromatic fuels to form soot. Of course, the workers responsible for the cited efforts have attempted to do precisely this for their own results and have, in the process, focused attention on several fuel properties which appear to be important in soot production and emission. What is hoped for here is that by examining a broad range of tests and experiments from a variety of sources it will be possible to:

(1)   Select more universal criteria for predicting the extent of sooting from out-of-specification fuels.

(2)   Point the way to what additional work would be useful in refining these criteria or developing better ones.

The approach in this study has been to be selective rather than exhaustive, and it should be pointed out that time and money restrictions precluded consideration of all available studies. Much of the relevant work is in the report literature and therefore is not immediately accessible on a short time scale. Examination of a large volume of literature relating to fuel effects on gas turbines has focused, in this effort, on those papers which include a detailed examination of the physical and chemical properties (the independent variables) of the fuels used and measurements of either smoke emission or

1

related phenomena such as flame radiation or combustor liner temperatures (the dependent variables) (References 1 to 11, 16 to 19). Further concentration was made in this examination on those studies which tested a large enough variety of fuels to yield reasonable statistics. As a result of this selection process, the reports described in Table 1 have been closely examined. The first of these tabulated data sources is a study by Schirmer, McReynolds, and Daley (Reference 1) using a J57 can-type combustor. In this study an aromatic-free JP-5 was used as the base fuel with triethyl benzene (single-ring aromatic) and methyl naphthalene (double-ring aromatic) additions of up to 1% (volume). In addition, decalin (a double-ring saturated compound), tetralin (a double-ring partially saturated compound), iso-octane, n-heptane, and JP-4 were tested. The measured dependent variables were the flame radiation in the primary combustion zone and the combustor liner temperature.

Naegeli and Moses (Reference 10) measured flame radiation, smoke number, and liner temperature in a T63 can combustor using JP-5 as a base fuel to which aromatics were added. Also a Jet A, synthetic JP-5's from shale, coal, and tar sands, and marine diesel fuel were tested. In another paper (Reference 19), these authors described a smaller set of experiments in which Jet A was blended with xylenes, decalin, methyl naphthalene, tetralin, and anthracene to produce a series of fuels all with a hydrogen content of 12.8% (wt). These experiments were performed in a small 2-inch Phillips Combustor where flame radiation was measured. Although the number of fuels tested is not as large in this study as in others, the constraint on H content makes this study notable.

Two reports by Gleason et al. (References 6, 7) and a similar report by Vogel et al. (Reference 8) describe a series of tests for a J79 combustor (Reference 6), a F101 combustor (Reference 7), and a TF41 combustor (Reference 8). The base fuel in these studies was JP-4 to which xylenes, naphthalenes, and mineral oil were added. A very similar series of fuels was used for all of the tests in these three combustors. A variety of independent variables was measured including smoke number, smoke emission (g/kg), and liner temperature. The reports extensively analyze the results to determine how well these soot-related quantities correlate with numerous fuel properties over a wide range of operating conditions.

2

TABLE 1. SELECTED REPORTS DESCRIBING EFFECTS OF FUEL ON SOOT
PRODUCTION IN JET ENGINE COMBUSTORS

Ref.	Combustor	Soot-Related Measurements	Inlet Pressure Range, atm	Description of Fuels
1	J57	Flame radiation, liner temperature	5.0-15.0	Twelve fuels including aromatic-free JP-5, JP-5 blended with triethyl benzene and methyl naphthalene, JP-4, decalin, tetralin, iso-octane, n-heptane, kerosene.
10	T63	Flame radiation, liner temperature	2.3-4.7	Eighteen fuels including Jet A, JP-5, JP-5 blended with monocyclic and dicyclic aromatics, synthetic JP-5's, JP-5 blended with diesel fuel, JP-5 blended with decalin, diesel fuel, leaded gasoline. (Data using leaded gasoline were excluded from this report.)
19	2-inch combustor	Flame radiation	5.0-10.5	Eight fuels including Jet A, Jet A blended with xylenes, decalin, methyl naphthalene, anthracene, tetralin.
6	J79	Flame radiation, liner temperature, smoke number, smoke emission	2.4-12.4	Thirteen fuels including JP-4, JP-8, and blends of these with xylenes, and naphthalenes and mineral oil, diesel fuel.
7	F101	Flame radiation, liner temperature, smoke number, smoke emission	3.9-12.4	
8	TF41	Flame radiation, liner temperature smoke number, smoke emission	2.9-18.5	

3

All these reports demonstrate clearly that the physical properties (viscosity, density, surface tension, vapor pressure, boiling points) of the fuels have, at most, secondary effects on sooting behavior. Therefore, these workers have concentrated their efforts on examining soot production (or a related quantity such as flame radiation or smoke number) as it varies with chemical properties of the fuel. In particular, attention was concentrated on the following chemical properties of the fuels as measured by the report authors: (1) hydrogen content, (2) aromatic content, and (3) amount of multiple-ring aromatics. A fourth fuel property, the fuel smoke point,* also was considered. The first of these independent variables has been demonstrated to often correlate very well with soot-related combustor measurements (References 4, 5, 10). Indeed, hydrogen content is most commonly judged the fundamental property of choice in predicting the tendency of a fuel to produce soot. It is striking that such a crude measure of the chemical makeup of the fuel does so well as an indicator of the propensity of a fuel to form soot.

Aromatic content has long been known to be a cause of soot formation. For typical fuel blends, it often correlates with hydrogen content, of course, but typically it is found to correlate less well with soot production than does hydrogen content (see, e.g., References 6, 7, and 8 and the following section). In Reference 1 it is shown that increasing the multiple-ring aromatic content of a fuel is very effective in producing a large increase in flame radiation (beyond that observed with an equivalent amount of a single-ring aromatic). This is examined more closely below.

Finally, the importance of fuel smoke point as a means of predicting sooting behavior has been examined. Although it has not been widely noted, when this is done it is found that the reciprocal of the smoke point is typically as good and, in some cases, a considerably better predictor of sooting than the hydrogen content. The objection is sometimes made that, whereas the first three variables listed above are fundamental properties of a fuel capable of being predicted or unambiguously measured in repeatable, standardized ways, the smoke point of a fuel is an empirical quantity, which although a

---

* The smoke point of a fuel is the minimum height of a small laboratory diffusion flame, burning the fuel in air, at which luminosity at the flame tip from soot formation is observed. The standardized apparatus and procedure are described in Reference 20.

4

standardized ASTM test is defined (Reference 20), is nonetheless ambiguous in
the sense that it has historically been dependent on the type of burner employed
in the test (see, e.g., References 1 and 21). It will be shown here that this
objection can be removed by defining an index based on the smoke point which
unambiguously defines the sooting tendency of a fuel regardless of which sort
of diffusion flame burner is used to measure the smoke point. An objection can
also be made to using a smoke point defined by using small laboratory diffusion
flames to indicate the sooting tendency of fuels in highly turbulent combustors
which are generally treated as well-stirred combustors in which premixed flames
are burning. However, in the context of soot production, the extent to which
engine combustion chambers can be considered well stirred is questionable in
view of the very low overall fuel/air ratios which yield soot in these systems.
Fuel-rich flamelets which produce soot unquestionably *occupy some fraction of*
the combustor dome and primary combustion volumes and to this extent diffusion
flame-derived quantities such as the smoke point might, and indeed do, correlate
well with soot production in these practical systems. Furthermore, a conceptual
problem in the relating of smoke point and sooting in large combustors is that
measurement of smoke point is a measurement of the threshold at which sooting
commences. On the other hand, in large combustors, the soot yield or a quantity
dependent on yield is measured. That a good correlation exists between these
two quantities is a reflection of the tendency of fuels which have low thresh-
olds to produce more soot at a given equivalence ratio than fuels with high
thresholds (Reference 22). It may also be due to the fact that in a large com-
bustor one is dealing with a large ensemble of small partially mixed diffusion
flamelets of various sizes for which, at any given moment, a fraction will be
of small enough scale or at low enough equivalence ratio to be below soot
threshold. The soot yield will then vary with the fraction which burns beyond
threshold and thus the correlation is established.

In the sections which follow, first the pertinent data from the selected
references will be examined. Then laboratory data on small sooting flames will
be described from which the tendency to soot based on the smoke point measure-
ment will be quantified and shown to be an unambiguous property of the fuel or
compound measured. In the last sections the implications of the comparison of
full-scale and laboratory smoke measurements will be discussed and recommenda-
tions made for further work.

SECTION II

REVIEW AND ANALYSES OF THE DEPENDENCE OF GAS TURBINE
COMBUSTOR SOOT PRODUCTION ON FUEL PROPERTIES

As can be seen from selected reports of Table 1, a wide variety of avia-
tion gas turbine combustion systems has been tested. Most of the selected
studies have been extensive, involving more than ten fuel blends, a large range
of operating conditions, and a wide variety of measurements which include, in
addition to soot-related quantities, determination of NO_x, CO, and unburned
hydrocarbon emission, combustion efficiency, relight tests, and other perfor-
mance parameters which might be a function of fuel properties. The reader is
directed to the cited reports for details on measurement techniques and results.

Analyses of the data in the selected reports has generally led to the con-
clusion that fuel hydrogen content (H%) and smoke points (SP) of the fuels (as
measured by the report authors using ASTM procedures) are the best indicators
of soot production in both large-and small-scale combustors. Table 2 lists
the correlations* between soot-related variables, flame radiation, or smoke num-
ber, and these two fuel properties at high operating power levels for the
selected studies. The correlation between the H content, H%, and the recipro-
cal of the smoke point, $(SP)^{-1}$, is also given, as well as the ranges for these
fuel variables and the engine operating conditions (the fuel/air weight ratio
and the burner inlet pressure). From the data of Table 2, it would appear that,
at most, only slightly better correlations occur between the soot-related quan-
tity and $(SP)^{-1}$ as opposed to H%. However, for all but the data from References
10 and 19, there is no firm statistical criterion for choosing between these

---

* The correlation between two ordered sets of numbers $\{y_i\}$ and $\{x_i\}$ is a mea-
  sure of the degree to which one variable appears to vary with or depend on
  the other. The correlation, r, is given by

$$r = \left\{ \frac{\overline{xy} - \overline{x}\,\overline{y}}{\sigma(x)\sigma(y)} \right\}^{1/2}$$

  where σ is a standard deviation and bars over a variable indicates an average
  value. If a plot of points (y_i, x_i) all lie on a straight line, $r = +1$ or -1.
  Scatter about a best fit line results in $|r| < 1$. The smaller $|r|$ is the
  greater the scatter.

TABLE 2. CORRELATIONS OF SOOT-RELATED MEASUREMENTS WITH HYDROGEN CONTENT AND RECIPROCAL SMOKE POINT

HIGH POWER CONDITIONS

Reference/ Combustor	Dependent Variable	Fuel Property/ Dependent Variable[a] Correlations		Correlation between H% and $(SP)^{-1}$	Ranges of Fuel Properties		Operating Conditions		
		H%	$(SP)^{-1}$		H%	$(SP)^{-1}$	F/A g/kg	pb, atm	Description
1/J57	Flame radiation at dome	- 0.98	0.98	- 0.96	9.1-14.0	< 0.02-0.17	15	15	High power
10/T63	Flame radiation at dome	- 0.91	0.94	- 0.88	12.0-14.3	0.039-0.084	20	4.7	Full power
19/2-inch combustor	Radiation index[c]	- 0.81	0.95	- 0.86	12.8-14.2	0.042-0.080	8-24	5-15	Data averaged over range
6/J79	Smoke number[d]	- 0.65	0.72	- 0.97	12.0-14.5	0.031-0.083	20	12.4	Sea-level takeoff
7/F101	Smoke number	- 0.71	0.70	- 0.97	12.0-14.5	0.031-0.083	29	12.4	Sea-level takeoff
8/TF41	Smoke number	- 0.73	0.73	- 0.97	11.9-14.4	0.026-0.083	21	18.5	Sea-level takeoff

a Independent variables are hydrogen content, H%, and the inverse of the reciprocal smoke point for the fuels, $(SP)^{-1}$, mm^{-1}.

b Burner inlet pressure.

c This index with ratio of combustor radiation for the test fuels relative to that observed using a Jet A base fuel.

d SAE smoke number, see Reference 23.

7

two fuel properties since they correlate so well with one another. The fuels studied in Moses and Naegeli's work were such that the $H\%/(SP)^{-1}$ correlation is less good (in Reference 19 this was done purposely by choosing fuels of fixed $H\%$ but varying SP) and in these tests the correlation of soot with inverse smoke point is clearly superior. In Figures 1 and 2, comparisons between $H\%$ and $(SP)^{-1}$ are shown graphically for the data of References 1 and 10. These figures were prepared by performing best fits of the independent variables $H\%$ or $(SP)^{-1}$ to the dependent soot related, measured variables of Table 2. These best fit functions are then used to obtain the predicted values of the dependent variable which are compared to observed values in these figures.

It is disturbing that in the very complete series of tests of References 6, 7, and 8 all the correlations are relatively poor. Figure 3 (made using the TF41 data) makes this point very clear when compared to Figures 1 and 2. The engines tested in these three studies range from the older, sooting J79 through the more modern, but still relatively sooty TF41 to the modern, very clean burning F101. Despite the fact that the F101 burns very cleanly, the predicted decrease in liner life of this engine from the use of high aromatic fuels is almost as severe as that predicted for the J79. Thus, the impact of new fuels on liner life and reliability remains an important consideration and low correlations of fuel properties with sooting behavior are a matter of concern because of their implications with regard to the predictability of fuel property effects.

In Table 3 data from the same studies (using the same sets of fuels) under low power (idle) conditions are analyzed. The correlations tend to be slightly better under these operating conditions than those obtained at high power. There is, however, no difference apparent in the data between the H content and reciprocal smoke point as a correlating parameter. The fact that for the J79 and F101 systems the correlations are improved under idle conditions is not of much comfort since in these situations liner life is of little concern.

Table 4 shows the correlations of soot-related quantities measured under high power conditions (as tabulated above in Table 2) with aromatics and multiple-ring aromatics as the fuel-related variables. As can be seen by comparison with Table 2, neither of these fuel properties correlates as well with sooting behavior as do H content or reciprocal smoke points except in the instance of Reference 6 where the correlation of aromatics with smoke

8
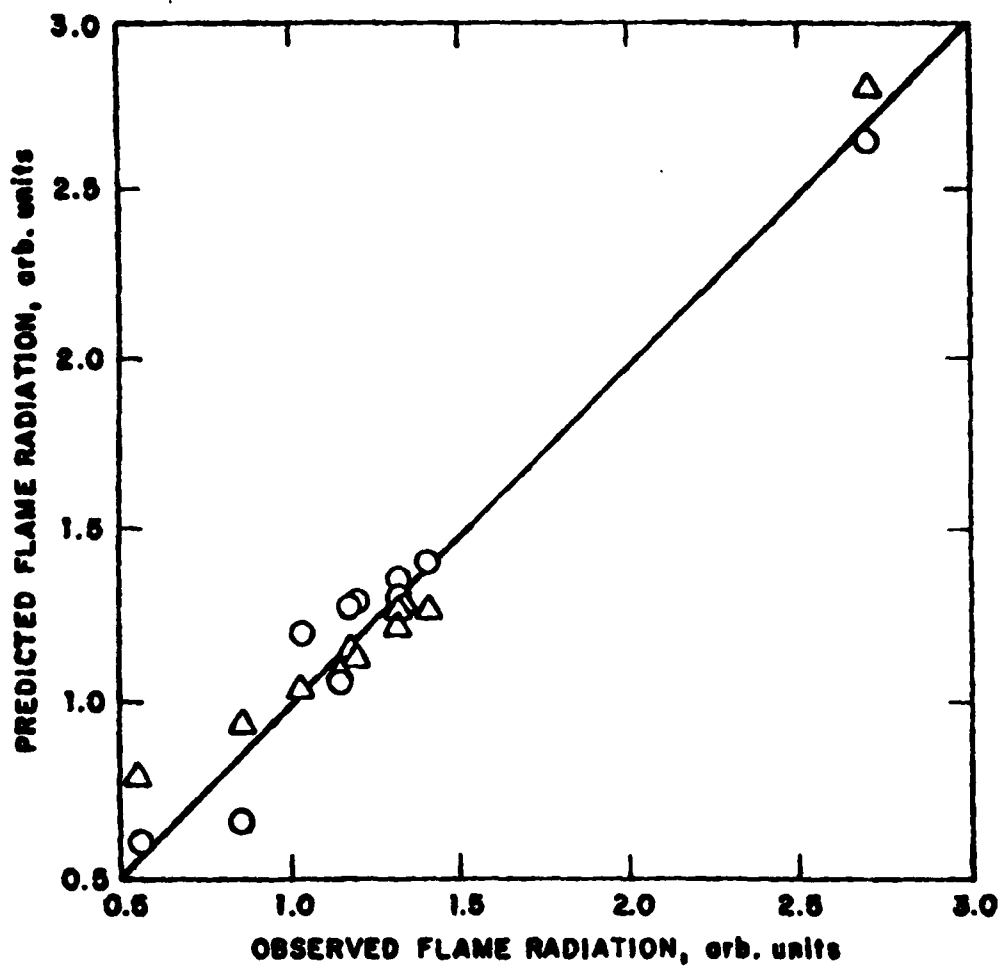
Figure 1. Comparison of Fuel Hydrogen Content and Reciprocal
Smoke Point as a Soot Predictor for the J57 Combustor
(Reference 1)

O - Correlation using H%, r = - 0.98
△ - Correlation using (SP)$^{-1}$, r = 0.98
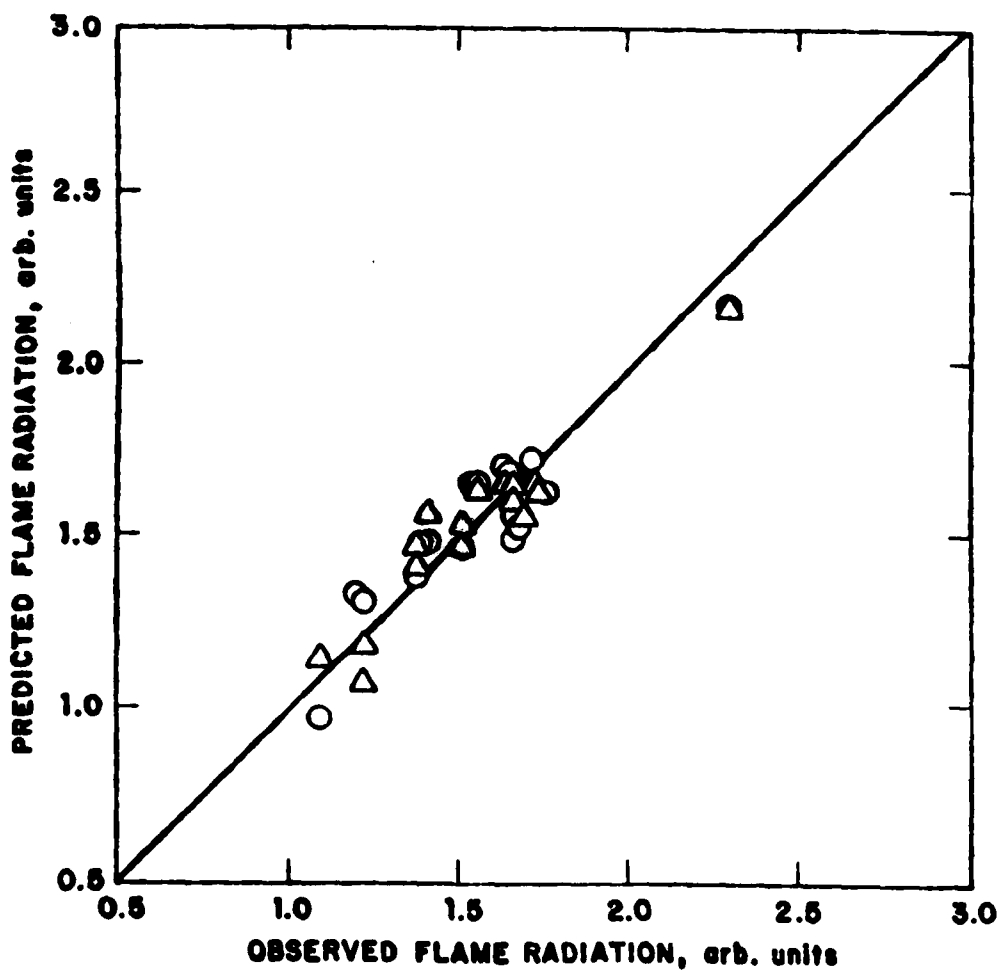
Figure 2. Comparison of Fuel Hydrogen Content and Reciprocal
Smoke Point as a Soot Predictor for the T63 Combustor
(Reference 10)

O - Correlation using H%, $r = -0.91$
△ - Correlation using $(SP)^{-1}$, $r = 0.94$
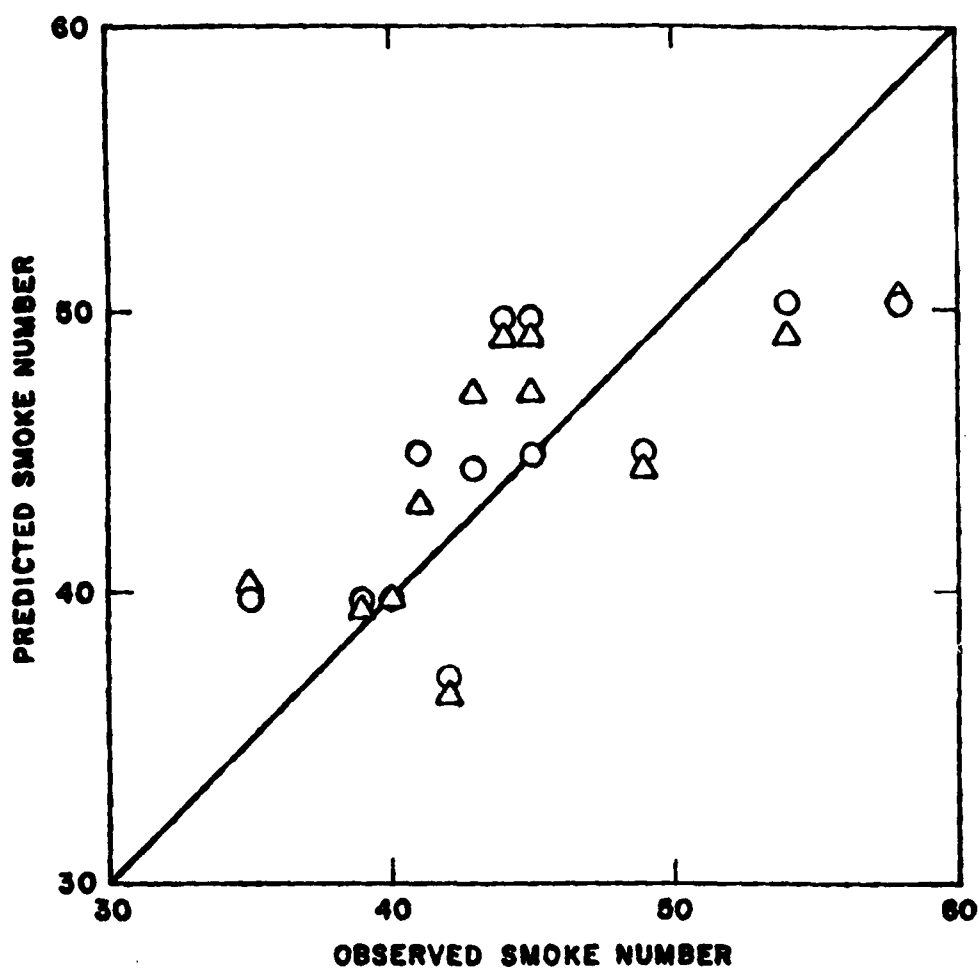
Figure 3. Comparison of Fuel Hydrogen Content and Reciprocal
Smoke Point as a Soot Predictor for the TF41 Combustor
(Reference 8)

O - Correlation using H%, r = - 0.73
△ - Correlation using (SP)$^{-1}$, r = 0.73

11

TABLE 3. CORRELATIONS OF SOOT-RELATED MEASUREMENTS WITH FUEL H CONTENT AND RECIPROCAL SMOKE POINT

LOW POWER CONDITIONS

Reference/ stor	Dependent Variable	Fuel Property/ Dependent Variable Correlations		Correlation between $H\%$ and $(SP)^{-1}$	Ranges of Fuel Properties		Operating Conditions		
		$H\%$	$(SP)^{-1}$		$H\%$	$(SP)^{-2}$	F/A g/kg	P, atm	Description
1/J57	Flame radiation at dome	− 0.98	0.99	− 0.96	9.1−14.0	0.02−0.17	10	5	Low power
10/T63	Flame radiation at dome	− 0.89	0.90	− 0.88	12.0−14.3	0.039−0.083	12	2.8	25% of full power
6/J79	Smoke number	− 0.95	0.92	− 0.97	12.0−14.5	0.039−0.083	9.4	2.4	Idle
7/F1..	Smoke number	− 0.84	− 0.77	− 0.97	12.0−14.5	0.031−0.083	14	3.9	Idle
8/TF41	Smoke number	− 0.88	0.86	− 0.97	11.9−14.4	0.026−0.083	14	2.9	Idle

TABLE 4. CORRELATIONS OF SOOT-RELATED MEASUREMENTS WITH FUEL AROMATICS AND MULTIPLE-RING CONTENTS UNDER HIGH POWER CONDITIONS

Reference/ Combustor	Dependent Variable	Fuel Property/ Dependent Variable Correlations		Correlation between Ar and M-R Ar	Ranges of Fuel Properties		Operating Conditions		
		Ar, %	M-R Ar, %		Ar, %	M-R Ar %	F/A g/kg	P, atm	Description
1/J57	Flame radiation at dome	0.93	0.069	-0.11	0-94[a]	0-8.5[a]	15	15	High power
10/T63	Flame radiation at dome	0.89	0.83	0.79	8.1-37.8[b]	0-9.4[b]	20	4.7	Full power
19/2-inch combustor	Radiation index	0.70	0.74	0.30	8.1-33.8[b]	1.3-20.1[b]	8-24	5-15	Data averaged over range
6/J79	Smoke number	0.42	0.79	0.17	12.2-63.4[a]	0.6-24.6[a]	20	12.4	Sea-level takeoff
7/F101	Smoke number	0.59	0.56	0.17	12.2-63.4[a]	0.6-24.6[a]	29	12.4	Sea-level takeoff
8/TF41	Smoke number	0.70	0.36	0.22	11.4-59.1[a]	0.6-24.8[a]	21	18.5	Sea-level takeoff

[a] Volume %

[b] Weight %

number is greater than that of any of the other fuel properties. This exception is in all likelihood accidental, however, and its value, 0.79, is not large in any case. Data on aromatic content and soot taken under low power conditions show these correlations to also be lower than those found using H content and reciprocal smoke point.

As noted above, for most combustors the increase in liner temperature which accompanies soot radiation is a cause for concern. The question thus arises of how well the liner temperature correlates with the four fuel properties selected for examination and how well liner temperature correlates with the other soot-related properties of Tables 2 to 4. These correlations are given in Table 5 for the combustors of References 1, 6, 7, and 8 at the high power levels of Tables 2 and 4. From Table 5, it is clear that the H content is a slightly better correlating parameter than the other fuel properties examined. Reciprocal smoke point is better than aromatic content. Multiple-ring aromatics seem to play little role. Again for the J79, F101, and TF41 studies (References 6, 7, and 8), none of the parameters are exceptionally good. Furthermore, the correlation of peak liner temperature with smoke number is low in these last three studies. In short, in these studies, not only do none of the fuel properties correlate exceptionally well with soot-related measurements, but the soot-related quantities (e.g., combustor liner temperature, engine smoke number) do not correlate well with one another. To further emphasize this point, examination of data taken under engine idle conditions shows the correlations corresponding to those of Table 5 to be even weaker. As a flagrant example, one finds from Reference 7 that the correlation of smoke number to peak liner temperature is -0.43 for the F101 engine under idle conditions apparently indicating that in this case the role of soot radiation in determining liner temperature is minimal for this engine under idle conditions.

An additional way of examining the data involves determining whether a particular set of fuels used in different engines soots in a consistent way. That is, does the amount of soot produced in one engine by a fuel correlate well with the amount of soot that fuel produces in another engine operating under comparable conditions, relative to that produced in the engines by some reference fuel? References 6, 7, and 8 allow this hypothesis to be checked. These studies used nearly identical series of fuels. One fuel (Fuel No. 4, a JP-8, xylenes blend) used in the Reference 8 study (which corresponds to

Fuel No. 10 of References 6 and 7) seems way out of line and has been excluded. In Table 6, the correlation of smoke numbers measured using this series of fuels is shown, and in Figure 4 an example of the comparison between the J79 and TF41 data is shown. As can be seen from Figure 4, a lot of scatter exists. Thus, the correlations are not strikingly large, but are possibly significant in view of the low correlation found between all the measurements of soot in these studies.

TABLE 5. CORRELATIONS OF LINER TEMPERATURE WITH FUEL PROPERTIES HIGH POWER CONDITIONS[a]

Reference/ Combustor	Correlations of Liner Temperature with Fuel Properties[b]				Correlation between Liner Temperature and Radiation Smoke Number[c]
	H%	$(SP)^{-1}$	Ar, %	M-R Ar,	
1/J57	- 0.98	0.92	0.85	0.12	0.97
6/J79	- 0.89	0.83	0.83	0.44	0.42
7/F101	- 0.65	0.59	0.59	0.43	0.64
8/TF41	- 0.69	0.64	0.61	0.46	0.62

[a] See Table 2 or 4 for fuel air ratio and inlet pressures. Liner temperatures are the temperature differences between the inlet and peak liner temperatures observed.

[b] See Tables 2 and 4 for ranges of fuel properties.

[c] Radiation or smoke number volume are those used to obtain correlation.

TABLE 6. CORRELATIONS OF SMOKE NUMBERS MEASURED IN DIFFERENT COMBUSTORS FOR A SET OF FUELS[a]

Ranges of Smoke Numbers			Correlations between Combustors		
J79	F101	TF41	J79/F101	J79/TF41	F101/TF41
55.2-88.9	2.6-4.7	35-57	0.68	0.56	0.60

[a] From References 6, 7, and 8. All at sea-level takeoff operating condition.
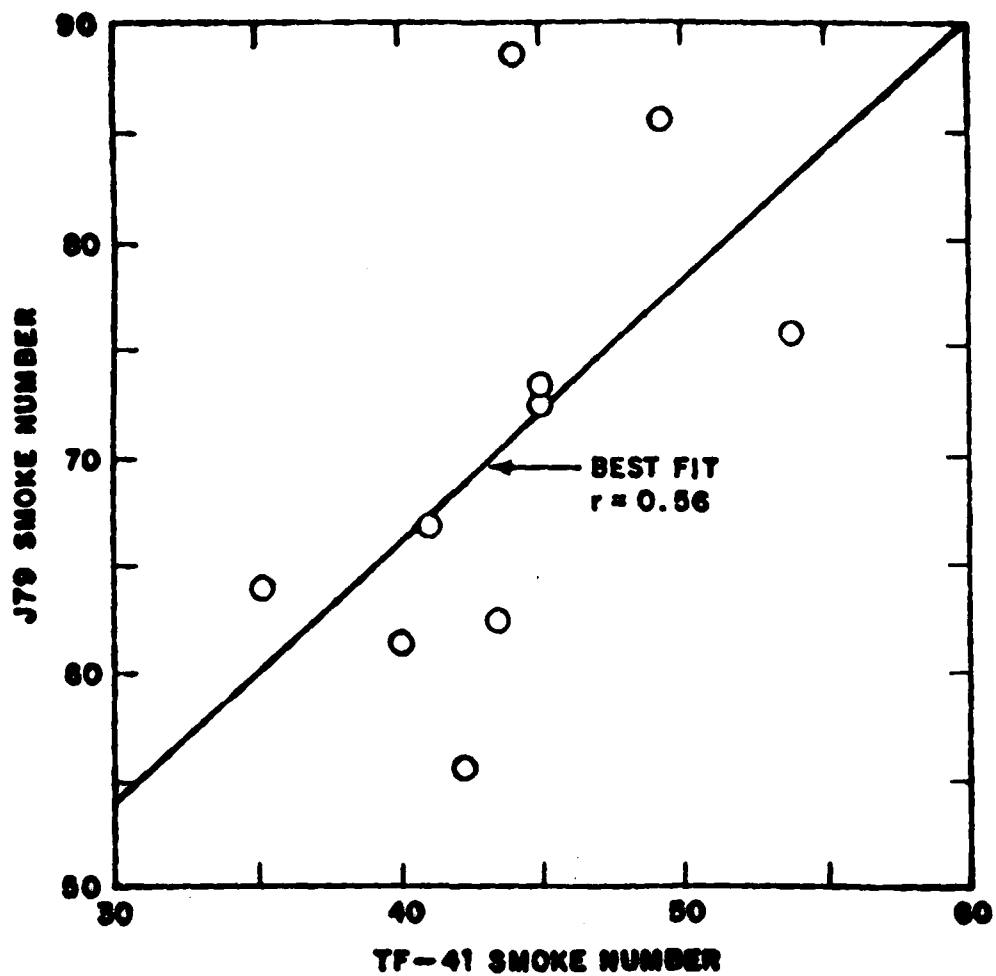
15

Figure 4. Comparison of Smoke Numbers Produced in Two Engines
Using Similar Series of Fuels

In a final attempt to find improved correlating parameters, it was deemed worthwhile to examine multiple variable linear regressions in which two or more fuel properties are used in linear combination to produce best fits to the soot data. Since multiple-ring aromatics are known to increase soot formation dramatically in laboratory flames (see below) and in large combustors (see Reference 1), the data of the selected reports were fit with multiple variable linear regressions using the pairs of independent variables (H content, multiple-ring aromatic content and inverse smoke point, multiple-ring aromatic content). The correlations achieved by fitting multiple-variable linear equations of the forms

$$\text{soot-related quantity} = a_0 + a_1(H\%) + a_2(M\text{-}R \text{ Ar}, \%)$$

or $$\text{soot-related quantity} = b_0 + b_1(SP)^{-1} + b_2(M\text{-}R \text{ Ar}, \%)$$

to the data are shown and compared to single variable correlations in Table 7. Table 7 shows that, in most cases, little is gained by this multiple-variable approach. (In the study described in Reference 8 a more extensive attempt at applying multiple-variable regressions to the data set led to the same conclusion.) Only in the case of the J79 data (Reference 6) is a dramatic increase in the quality of the fit noted. The failure of the multiple-variable approach to help significantly in most cases is twofold. First multiple-ring aromaticity in these studies often does not correlate very well with sooting and, secondly, where it does, it also correlates well with H% and $(SP)^{-1}$. Thus, its inclusion is not very helpful.

Similar efforts in which other combinations of fuel properties are tried generally do less well than the combinations of Table 7. Of course, increasing the number of independent variables which are simultaneously fit tends to increase the correlation coefficient simply by decreasing the statistical degrees of freedom. More sophisticated statistical tests (the F-test) are then needed to determine whether the better correlation obtained using more than one variable is a true improvement or simply a mathematical artifact. Such an examination is not included, but it seems likely that only in the case of the J79 data is a true improvement to be made by correlating more than one variable. Even in this case use of three or four of the fuel properties simultaneously provided no significant further advantage, e.g., a correlation of only 0.84 is achieved by using all four fuel properties in a multiple linear regression fit to these data.

TABLE 7. MULTIPLE VARIABLE REGRESSION FITS TO SOOT DATA
UNDER HIGH POWER CONDITIONS

Reference/	Single-Variable Correlations			Multiple-Variable Correlations	
Combustor	H%	$(SP)^{-1}$	M-R Ar, %	H%/M-R Ar%	$(SP)^{-1}$/M-R Ar%
1/J57	- 0.98	0.98	0.07	0.98	0.99
10/T63	- 0.81	0.95	0.74	0.96	0.95
19/2-inch combustor	- 0.91	0.94	0.83	0.93	0.96
6/J79	- 0.65	0.72	0.79	0.84	0.84
7/F101	- 0.71	0.70	0.56	0.75	0.72
8/TF41	- 0.73	0.73	0.36	0.73	0.73

SECTION III

LABORATORY STUDIES OF SOOTING FLAMES

Laboratory studies of soot thresholds in small premixed and diffusion flames have traditionally suffered from the lack of a method of comparing results of one study with those of other studies. The standardization of laboratory diffusion flame measurements (Reference 20) to allow smoke points to be obtained in a repeatable way is an attempt to get around this problem. However, what has been needed is a means of reducing or removing altogether the influences of geometry and fluid mechanical processes occurring in these small flames so that soot threshold for a fuel can be assigned based only on the chemical structure of that fuel. Such a method is presented in Appendix A. In the paper presented in Appendix A, it is shown that data from laboratory studies can be compared in such a way that fuel compounds can be assigned a number which specifies the sooting tendency of that compound. This threshold soot index (TSI) appears to be assignable to a wide variety of compounds with an accuracy of $\pm$ 10%.

For premixed flames, the TSI is directly proportional to the minimum equivalence ratio at which sooting occurs, ϕ_c

$$TSI = a - b \, \phi_c$$

For diffusion flames, the TSI is inversely proportional to the smoke point,

$$TSI = a'(MW) (SP)^{-1} + b'$$

where MW is the molecular weight of the fuel. The constants a and b and a' and b' are specific to the measurement apparatus and must be determined by calibration of each apparatus with at least two fuels having known TSI's. Tables of TSI's for a variety of pure fuel compounds are given in Appendix A.

Jet fuels are, of course, mixtures containing large numbers of compounds. Measurement of the diffusion flame smoke point in the laboratory, as indicated in the previous section, produces results which often correlate well with large scale engine results. However, as noted earlier, one objection to relying on fuel smoke point as an indicator of sooting tendency is that it is not a fundamental fuel property as are, for instance, the aromatic or hydrogen contents of the fuel. A major step toward making soot threshold information

19

reflect the chemical composition of the fuel and thus a fundamental, predict-able property of the fuel is to define a fuel TSI based on the TSI's of the compounds making up the fuels. This can be done using either diffusion flame or premixed flame TSI's. The simplest approach is to make the fuel TSI a linear, weighted sum of the TSI's of the fuel constituents,

$$\text{Fuel TSI} = \sum_i x_i \, TSI_i$$

where x_i is either the weight, volume, or mole fraction of the ith constituent having TSI_i. This procedure has some basis in experimental work performed on sooting thresholds in the past. Minchin (Reference 24) examined a series of kerosenes having varying amounts of aromatics or naphthalenes and found that plots of the reciprocal smoke points of these kerosenes against the aromatic or naphthenic volume fraction produced straight lines. Thus, fuel TSI's calculated for these kerosenes could be used to predict their smoke points. The generality of the procedure and whether weight or mole fractions would produce better smoke point predictions need to be examined further. How well fuel TSI's calculated in this manner work in correlating sooting in engine combustors is examined below.

SECTION IV

RELATIONSHIP BETWEEN LABORATORY STUDIES OF SOOT AND LARGER SCALE TESTS

As detailed in Appendix A, it is possible to calibrate a wide variety of
laboratory-scale diffusion or premixed flame burners so that if soot thresh-
olds for a particular compound are obtained on a particular apparatus, the
threshold for that compound on other apparatus is predictable. In other words,
it is possible to calibrate out the fluid mechanical and geometric factors
which affect the smoke point or onset equivalence ratio measurement and obtain
a TSI for a compound which is dependent only on its chemical structure. Having
obtained a useful definition for the TSI of a particular compound, it is natu-
ral to see if this can be used to form an index for fuels which correlates with
smoke emissions observed in large scale tests.

Effective TSI values were computed for the fuels tested in References 1,
6, 7, 8, 10, and 19 for correlation with smoke number and flame radiation
results. To do this one must first select whether premixed or diffusion flame
TSI's are most applicable. Diffusion flame TSI's were selected since the spray
fueled combustors all burn with many fuel-rich regions which must be diffusion-
controlled. (Also, data on premixed flames are less complete and hence can be
used with less certainty. This point should be examined in the future when a
more complete data base is available, however.) Next TSI values must be as-
signed for base fuels and some of the hydrocarbon mixtures used in these
studies. For example, in Reference 19, where pure components were used to
adjust fuel properties, we must also consider Jet A and DFM. This procedure
was accomplished using Reference 10 data which gives smoke points of several
pure components along with JP-5, JP-4, and kerosene. For a first approximation,
the variation in average molecular weights among the jet fuels was ignored and
a linear least-squares fit of TSI's was performed for n-heptane, decalin, and
tetralin to the Reference 10 smoke points. (This essentially calibrates the
smoke point apparatus used.) Then using this fit, TSI's were estimated for jet
fuels from smoke points. For most of the engine tests, fuel compositions were
not known; only simplified analytical results on the concentration of single-
ringed, double-ringed aromatic species, etc. were known. Average TSI values were
assigned to these component classifications by referring to Table 3 in Appendix A.

This procedure is not at all unique and time restraints prevented more detailed, and possibly much better, TSI assignments.

It should be noted that, in cases of pure compounds, soot production which correlates well with $(SP)^{-1}$ will automatically correlate well with TSI since the two variables are so closely related. However, fuels are a blend of many compounds and, as noted in Section III, an assumption is being made that the TSI's of fuel blends can be calculated by simply calculating the weighted sums of the TSI's of the compounds or groups of compounds making up the fuel. (For these calculations, weight fractions were used as weighting factors in the summations.)

Results of correlating computed average TSI's against experimental results are given in Table 8 along with summary results from the other correlations. Some average performance numbers are also given in Table 9. Overall the TSI correlation does as well as H% but not quite as well as $(SP)^{-1}$. It correlates flame radiation data better than smoke number values (as do H% and $(SP)^{-1}$). In fairness to TSI efforts we note that only from References 1 and 19 was detailed fuel composition information of the type needed to calculate accurate TSI's available. In the former case, TSI does as well as the other two fuel variables; in the latter case, the TSI correlation does appreciably better than $(SP)^{-1}$ and much better than H%. In the other cases estimates were made of average TSI's for broad classes of compounds. This may be at least partly responsible for the lack of strong correlation between fuel TSI and sooting in these cases.

TABLE 8. COMPARISON OF HYDROGEN CONTENT, RECIPROCAL SMOKE POINT, AND THRESHOLD SOOT INDEX CORRELATION WITH ENGINE SOOTING

Reference/ Combustor	Soot-Related Variable	Operating Condition	Correlation		
			H%	$(SP)^{-1}$	TSI
1/J57	Flame radiation	High power	− 0.98	0.98	0.98
1/J57	Flame radiation	Low power	− 0.98	0.99	0.99
10/T63	Flame radiation	Full power	− 0.91	0.94	0.88
10/T63	Flame radiation	25% of full power	− 0.89	0.90	0.87
19/2-inch combustor	Radiation index	Averaged over range	− 0.81	0.95	0.98
6/J79	Smoke number	Sea-level takeoff	− 0.65	0.72	0.63
6/J79	Smoke number	Idle	− 0.95	0.92	0.94
7/F101	Smoke number	Sea-level takeoff	− 0.71	0.70	0.57
7/F101	Smoke number	Idle	− 0.84	0.77	0.83
8/TF41	Smoke number	Sea-level takeoff	− 0.73	0.73	0.72
8/TF41	Smoke number	Idle	− 0.88	0.86	0.86

TABLE 9. AVERAGE CORRELATIONS OF HYDROGEN CONTENT, RECIPROCAL SMOKE POINT, AND THRESHOLD SOOT INDEX FOR SELECTED REFERENCES

Category	Average Correlations		
	H%	$(SP)^{-1}$	TSI
High power measurements, References 1, 10, 19, 6, 7, 8. From Tables 2 and 8.	-0.79	0.83	0.79
Low power measurements, References 1, 10, 19, 6, 7, 8. From Tables 3 and 8.	-0.91	0.89	0.90
Flame radiation, References 1, 10, 19. From Tables 2, 3, and 8.	-0.91	0.95	0.94
Smoke number, References 6, 7, and 8. From Tables 2, 3, and 8.	-0.78	0.78	0.76
Overall	-0.84	0.86	0.84

SECTION V

CONCLUSIONS AND RECOMMENDATIONS

A number of data sets obtained on a variety of aircraft gas turbine and laboratory scale combustors have been examined to determine which, if any, chemical properties of jet fuels are reliable predictors of soot formation. For some data sets, certain fuel properties, notably hydrogen content and the reciprocal of the fuel smoke point, correlate very well (>0.9) with the amount of soot or flame radiation observed. In other cases correlations are poor (<0.8). Unfortunately, these latter cases involve tests of widely used and/or quite modern combustor systems [J79 (Reference 6), F101 (Reference 7), TF41 (Reference 8) combustors]. The problem appears serious since, even for combustors such as the F101 which are very "clean", sizable ($\approx 50\%$) decreases in combustor liner lifetime are predicted for the sootier fuels.

A fuel property defined in this report, the threshold soot index or TSI, is based on the smoke points of fuel components. The TSI of a fuel is defined as the sum of the TSI's for the compounds making up the fuel times the weight fraction of that compound in the fuel. For some of the data sets, particularly those where a great deal is known about the specific compounds making up the fuel, the TSI correlation appears to do as well or better than H% of $(SP)^{-1}$. Where both H% and $(SP)^{-1}$ do poorly as predictors, TSI also fails.*

It has been widely noted that the chemical composition, not the physical properties of a fuel, appears to dominate the formation of soot in these combustors (see especially References 5, 10, and 12). However, the results to date do not allow one to pick between fuel properties such as hydrogen content, or reciprocal smoke point as a superior predictor of sooting behavior since typical series of fuels tested were not selected to produce independent variation of these properties. In only two data sets was the correlation between the hydrogen content and $(SP)^{-1}$ below 0.95 (see Table 2). For these two data sets where

---

* This is to be expected since, by its definition, the TSI is very closely related to the reciprocal smoke point. It differs from the reciprocal smoke point mainly in that, like the hydrogen content, it is a property which can be predicted for a fuel (assuming the fuel composition is known) whereas the smoke point must be measured.

the two variables were poorly correlated, $(SP)^{-1}$ was a better predictor of sooting (more precisely, flame radiation). For one of these sets (Reference 19) the fuels were purposely blended to make H% a poor correlator. However, the value of a correlation is to a large extent based on its ability to work in exceptional cases. Based on this, $(SP)^{-1}$ currently appears superior.

TSI has the potential to be a better predictor than H% and is more readily useful than $(SP)^{-1}$, but more precise fuel composition measurement is needed to test this. In References 1 and 19, where pure compounds were used as additives, TSI does better than H%. Its failure to do as well in other tests may well be due to our inability to calculate it correctly since the fuel composition information available is known only with regard to broad classes of compounds which can have widely varying TSI's within themselves. TSI would be expected to be more valuable than $(SP)^{-1}$ because the TSI is a calculable property like H% and can thus be used to design fuels without resorting to laboratory measurements of each possible blend. A useful set of experiments needed to make certain that this last statement is true would be to complement the data of Reference 19 (in which hydrogen content was fixed for all but the base fuel) by testing blends which have differing hydrogen contents but the same TSI's in small scale combustors like the Phillips Combustor and then in larger engine combustors.

The results of References 1, 10, and 19 show that the correlation between soot related effects and fuel composition can be very high. Thus, it is particularly troublesome that the recent series of tests described in References 6, 7, and 8 yielded such poor correlations between fuel composition and soot related effects. These latter experiments should be repeated using fuels with very well defined compositions to see if better predictability can be achieved. Experiments using blends of compounds with an aromatic-free base fuel, as in Reference 1, would be very helpful.

In this report the TSI of a fuel has been defined to be the weighted average of the component TSI's. This definition makes sense if the reciprocal smoke point of a fuel can also be calculated using the TSI's of the fuel components. Reference 24 indicates that this may be the case, but this additivity should be fully tested in the laboratory.

In the same vein, it may well be that computing TSI's of fuel blends using compound mole fractions rather than weight or volume fractions would produce more accurate predictions of blend smoke points and better correlations of TSI with engine soot data. This has not been tested but should be.

The smoke point and TSI of a fuel are based on laboratory measurements of the threshold at which sooting begins to occur. It may well be that a more complete knowledge of not just threshold behavior but soot yield above threshold for pure compounds and blends would lead to a more useful index for predicting soot yields in engines. Very little laboratory scale soot yield data exists, a situation which should be corrected.

If it should be found that, in fact, the TSI rather than the hydrogen content of a fuel is the important parameter, the practical significance is great. To know that fuel blends with olefinic and cyclic hydrocarbons produce less soot and flame radiation than blends of alkanes and aromatics, which have the same hydrogen content, would have obvious important implications for the refiner of jet fuels.

REFERENCES

1. Schirmer, R.M., McReynolds, L.A., and Daley, J.A., "Radiation from Flames in Gas Turbine Combustors," SAE Trans. 68, 554-561 (1960).

2. McClelland, C.C., "Effects of Jet Fuel Constituents on Combustor Durability," Naval Air Propulsion Test Center, NAEC-AEL-1736, May 1963.

3. Butze, H.F. and Ehlers, R.C., "Effect of Fuel Properties on Performance of a Single Aircraft Turbojet Combustor," NASA TMX-71789, October 1975.

4. Butze, H.F. and Smith, A.L., "Effects of Fuel Properties on Performance of Single Aircraft Turbojet Combustor at Simulated Idle, Cruise and Takeoff Conditions," NASA TM-73780, September 1977.

5. Blazowski, W.S. and Jackson, T.A., "Evaluation of Future Jet Fuel Combustion Characteristics," AFAPL-TR-77-93, July 1978.

6. Gleason, C.C., Oller, T.L., Shayeson, M.W., and Bahr, D.W., "Evaluation of Fuel Character Effects on J79 Engine Combustion System," AFAPL-TR-79-2015, General Electric Company, June 1979.

7. Gleason, C.C., Oller, T.L., Shayeson, M.W., and Bahr, D.W., "Evaluation of Fuel Character Effects on the F101 Engine Combustion System," AFAPL-TR-79-2018, General Electric Company, June 1979.

8. Vogel, R.E., Troth, D.L., and Verdouw, A.J., "Fuel Character Effects on Current, High Pressure Ratio, Can-Type Turbine Combustion Systems," AFAPL-TR-79-2072, General Motors Corporation, April 1980.

9. Moses, C.A. and Naegeli, D.W., "Fuel Property Effects on Combustor Performance," MED 114, Southwest Research Institute, March 1980.

10. Moses, C.A. and Naegeli, D.W., "Fuel Property Effects on Combustor Performance," Gas Turbine Combustor Design Problems, Lefebvre, A.H., ed. (Hemisphere Publishing Corp., 1980) pp. 39-69.

11. Gleason, C.C. and Bahr, D.W., "Fuel Property Effects on Life Characteristics of Aircraft Engine Combustors," J. Energy 4, 216-222 (1980).

12. Blazowski, W.S. and Maggiti, L., "Future Fuels in Gas Turbine Engines," Alternative Hydrocarbon Fuels: Combustion and Chemical Kinetics, Bowman, C.T. and Birkeland, J., eds. (American Institute of Aeronautics and Astronautics, New York, 1978) pp. 21-73.

13. Blazowski, W.S., "Future Jet Fuel Combustion Problems and Requirements," Prog. Energy Combust. Sci. 4, 177-199 (1978).

14. Szetela, E.J., Lohmann, R.P., and Smith, A.L., "Impact of Broad Specification Fuels on Aircraft Gas Turbine Combustors," J. Energy 4, 24-31 (1980).

15. Mellor, A.M. "Soot Studies in Gas Turbine Combustors and Other Turbulent Spray Flames," presented at General Motors Research Laboratories Symposium on Particulate Carbon, Formation during Combustion, October 1980 (to be published).

16. Blazowski, W.S., "Dependence of Soot Production on Fuel Blend Characteristics and Combustion Conditions," Gas Turbine Conference and Exhibit and Solar Energy Conference, March 1979. ASME Paper 79-GT-155.

17. Wyatt, W.R., Clark, J.A., Peters, J.E., and Mellor, A.M., "Size Distribution and Surface Area Measurements of Gas Turbine Combustor Smoke," J. Energy $\underline{3}$, 285-290 (1979).

18. Hoult, D.P. and Ekchian, A., "Soot Formation in a Turbulent Swirl Stabilized Laboratory Combustor," 25th International Gas Turbine Conference, March 1980. ASME Paper 80-GT-77.

19. Naegeli, D.W. and Moses, C.A., "Effect of Fuel Molecular Structure on Soot Formation in Gas Turbine Engines," 25th International Gas Turbine Conference, March 1980. ASME Paper 80-GT-62.

20. ASTM Method DI322-75, "Standard Method of Test for Smoke Point Aviation Turbine Fuels," Annual Book of ASTM Standards (American Society for Testing and Materials, Philadelphia, PA, 1975).

21. Van Treuren, K.W., "Sooting Characteristics of Liquid Pool Diffusion Flames," Master's Thesis, Princeton University, AFIT-CI-79-44T, July 1978.

22. Blazowski, W.S., Sarofim, A.F., and Keck, J.C., "The Interrelationship between Soot and Fuel NO_x Control in Gas Turbine Combustors," 25th International Gas Turbine Conference, March 1980. ASME Paper 80-GT-76.

23. Champagne, D.L., "Standard Measurement of Aircraft Gas Turbine Engine Exhaust Smoke," Gas Turbine Conference and Products Show, March 1971. ASME Paper 71-GT-88.

24. Minchin, S.T., "Luminous Stationary Flames: The Quantitive Relationship between Flame Dimensions at the Sooting Point and Chemical Composition, with Special Reference to Petroleum Hydrocarbons," J. Inst. Petrol. $\underline{17}$, 102-120 (1931).

DATE FILMED

-8